UNIVERSITY OF CALIFORNIA,
IRVINE

Comparative Analysis of Primary and Liver Fibroblasts Reveals MET as a Unique Target in Pancreatic Cancer Metastasis

DISSERTATION

submitted in partial satisfaction of the requirements
for the degree of

DOCTOR OF PHILOSOPHY

in Biological Sciences

by

Rima Singh

Dissertation Committee:
Assistant Professor Christopher J. Halbrook, Chair
Associate Professor Roberto Tinoco
Assistant Professor Dequina Nicholas
Associate Professor Marcus Seldin

2025

TABLE OF CONTENTS

LIST OF FIGURES

LIST OF TABLES

ACKNOWLEDGMENTS

I was once told that “PhD is a marathon, and not a sprint.” It requires years of consistent efforts, hard work, resilience, and an attitude to show up no matter what. There have been good days and bad days. However, as I look back at these 5 years, I see how much I have grown as a scientist and a person over the course of time. As I finish this chapter of my life and reflect on every individual who has played a pivotal role in this journey, I realize how immensely lucky I have been to meet so many amazing people along the way.

First and foremost, I would like to thank my PI Dr. Christopher Halbrook for his constant support and guidance. I was his first graduate student, and I am thankful for the faith he showed in me. He has groomed me into becoming a better scientist, writer, and presenter. This journey would not have been as fulfilling without his efforts and time that he invested in mentoring me. I would also like to thank my committee members- Dr. Marcus Seldin, Dr. Roberto Tinoco, and Dr. Dequina Nicholas. They applauded my good work and provided critical feedback on the areas that needed improvement. I also want to thank them for bringing their respective expertise that played a crucial role in shaping my project. Dr. Seldin has been a wonderful mentor and has also provided me with important resources to navigate the challenges I faced while performing computational analyses on my data.

I would also like to thank Dr. Nina Steele from the University of Cincinnati for all her mentorship, training, and help in analyzing the single cell RNA sequencing dataset. She has also been very motivational as a mentor and never missed any opportunity in appreciating my hard

work and dedication as a PhD student. Her ideologies as a scientist and mentor have greatly inspired me and I will always hold these values close to my heart.

I would like to acknowledge the Halbrook lab- Cecily Anaraki, Walker Allen, Sabrina Calderon, Taryn Morningstar, Austin Silva, Cavina Lee, Mariam Mohagheghi, Sophia Estrada, and Anai Campos. I would also like to thank former Halbrook lab members- Natalie Yousefian and Alica Buetel. My journey in this lab has been extremely fulfilling, and these individuals have played a key role in shaping it. They have been my source of strength and encouragement in times of despair and failures. They have also been my biggest cheerleaders and applauded my small and big achievements along the way. They did not shy away from helping in experiments, reading manuscript drafts, giving me feedback during practice talks, and providing great company during lunch and coffee breaks. I have looked forward to coming to lab almost every day of my past 5 years because of their radiant energy and great lab atmosphere. I am thankful for their friendship and support, and I would not have wanted it any other way.

I want to thank my family members- my parents and my sister Savita. My parents have supported me through thick and thin. They have always motivated me to chase my dreams while they provided full emotional and financial support. My childhood and adulthood were full of love and good memories that I created with my parents and my sister. My father has been a big source of inspiration for pursuing my dreams. I see him learn new skills like excel, PowerPoint, working on his presentation skills, reading books and it taught me that there’s no age to learn something new. My mother never fails to check on me no matter how busy she is. Her words of motivation helped me get through the setbacks that I faced during my PhD. She tries her best to

make my life easier in any which way she can whether it's sending me huge amount of food every time I visit her or handing me money to treat myself every now and then. My sister is my number one cheerleader from day one. She has always praised and encouraged my hard work, and I am thankful to have an extremely loving and supportive older sister. Her regular phone calls and daily messages remind me of the unwavering love and unconditional support I have been blessed with.

Lastly, I want to thank my best friend, my biggest supporter, my harshest critic, and my go to person for everything, my husband- Himanshu. Himanshu and I met at a dance class in 2019 and have been inseparable since then. From helping me during PhD application process by reading my personal statements and prepping for interviews to proofreading my dissertation- life has come to a full circle. He is my biggest blessing, and I thank my lucky stars every day that I have him by my side in this journey of life. His coding experience as a software developer made the learning curve less steep for me when I first started learning computational analyses for my project. He has a fantastic sense of humor that has picked me up and kept me going when an experiment or technique didn't work. I thank him for his time, motivation, support, and love through every stage of my PhD and beyond. I love you till eternity and a little longer after that, Himanshu!

NOTE: The text of this dissertation is a reprint of the material as it appears in (1). The co-authors listed in this publication are Natalie Yousefian, Walker Allen, Cecily Anaraki, Alica Beutel, Sabrina Calderon, Ian Loveless, Oliver Mcdonald, Jennifer Morton, David Imagawa, Zeljka Jutric, Thomas Martinez, Nina Steele, and Christopher Halbrook.

VITA

Rima Singh

EDUCATION

Ph.D., Biological Sciences, UC Irvine 2025

M.S., Cellular and molecular biology, SF State University 2019

B.S., (Cum Laude) Human Physiology, SF State University 2016

RESEARCH EXPERIENCE

Graduate Student in Cancer Biology- University of California, Irvine 2020-2025

Study the role of distinct stromal and immune cell populations in metastatic PDAC

In vivo study assessing effect of MET inhibition in PDAC

Advisor: Dr. Christopher Halbrook

Master's Research- San Francisco State University, San Francisco 2017-2019

Evaluate the impact of x-ray irradiation on the immune cells in tobacco hornworm

Advisor: Dr. Megumi Fuse

Research Associate- Atreca, FACS department, Redwood City 2019-2020

Assisted in generating tumor cell binding antibodies derived from plasmablasts

PUBLICATIONS

1. Caudill, V. R., Qin, S., Winstead, R., Kaur, J., Tisthammer, K., Pineda, E. G., Solis, C., Cobey, S., Bedford, T., Carja, O., Eggo, R. M., Koelle, K., Lythgoe, K., Regoes, R., Roy, S., Allen, Singh, R., N., Aviles, M., Baker, B. A., Bauer, W., … Pennings, P. S. (2020). CpG-creating mutations are costly in many human viruses. *Evolutionary Ecology*, *34*(3), 339–359. https://doi.org/10.1007/s10682-020-10039-z

2. Boyer, S., Lee, H.-J., Steele, N., Zhang, L., Sajjakulnukit, P., Andren, A., Ward, M. H., Singh, R., Basrur, V., Zhang, Y., Nesvizhskii, A. I., Pasca di Magliano, M., Halbrook, C. J., & Lyssiotis, C. A. (2022). Multiomic characterization of pancreatic cancer-associated macrophage polarization reveals deregulated metabolic programs driven by the GM-CSF–PI3K pathway. *ELife,* 11, e73796. https://doi.org/10.7554/eLife.73796

3. Halbrook CJ, Thurston G, Boyer S, Anaraki C, Jiménez JA, McCarthy A, Steele NG, Kerk SA, Hong HS, Lin L, Law F, Felton C, Scipioni L, Sajjakulnukit P, Andren A, Beutel A, Singh R, Nelson BS, Van Den Bergh F, Krall AS, Mullen PJ, Zhang L, Batra S, Morton JP, Stanger BZ, Christofk HR, Digman M, Beard DA, Viale A, Zhang J, Crawford HC, Pasca di Magliano M, Jorgensen C, Lyssiotis CA (2022). Clonal Heterogeneity Supports Mitochondrial Metabolism in Pancreatic Cancer. *Nat Cancer* 3, 1386–1403 (2022). https://doi.org/10.1038/s43018-022-00463-1

4. Geels, S. N., Moshensky, A., Sousa, R. S., Murat, C., Bustos, M. A., Walker, B. L., Singh, R., Harbour, S. N., Gutierrez, G., Hwang, M., Mempel, T. R., Weaver, C. T., Nie, Q., Hoon, D. S. B., Ganesan, A. K., Othy, S., & Marangoni, F. (2024). Interruption of the intratumor $CD8^+$ T cell:Treg crosstalk improves the efficacy of PD-1 immunotherapy. *Cancer cell*, *42*(6), 1051–1066.e7. https://doi.org/10.1016/j.ccell.2024.05.013

AWARDS, HONORS, AND GRANTS

Graduate Assistance in Areas of National Need (GAANN) Fellowship, UCI — Summer 2022

Best Poster Award, Chao Family Comprehensive Cancer Care Consortium, UCI 2024

PRESENTATIONS

1. Poster, Grad Show Case, San Francisco State University, San Francisco, CA (2019)
2. Poster, CoSE, San Francisco State University, San Francisco, CA (2019)
3. Poster, AACR Pancreatic Cancer, Boston, CA (Sep 2022)
4. Talk, SoCal Metabolism, Sanford Burnham Prebys, San Diego, CA (March 2023)
5. Poster, Chao Family Comprehensive Cancer Care Sci Retreat, Huntington Beach (Sep 2023)
6. Poster, AACR Pancreatic Cancer, Boston (Sep 2023).
7. Poster, University of California Pancreatic Cancer Consortium, Irvine (Dec 15, 2023)
8. Poster, Chao Family Comprehensive Cancer Care Consortium, Huntington (2024)
9. Flash talk, University of California Pancreatic Cancer Consortium (UCSF, January 2025)

ABSTRACT OF THE DISSERTATION

Comparative Analysis of Primary and Liver Fibroblasts Reveals MET as a Unique Target in Pancreatic Cancer Metastasis

by

Rima Singh

Doctor of Philosophy in Biological Sciences

University of California, Irvine, 2025

Associate Professor Christopher J. Halbrook, Chair

Pancreatic ductal adenocarcinoma (PDAC) is a deadly disease with a dismal 5-year survival of only 13.4%. PDAC is expected to become the second leading cause of cancer-related deaths by the end of 2030 in the US. Chemotherapy remains standard of care with most patients developing resistance during the course of treatment. The challenge in treating PDAC lies in the complex physiology of the tumor which is characterized by highly dense stroma and infiltration of heterogeneous stromal and immune cell populations. These populations engage in extensive crosstalk and support tumor growth, immune evasion, and ultimately drive resistance to treatments. Accordingly, immense efforts have been made in the field to understand the biology of PDAC tumors and the tumor microenvironment (TME), mostly focused on the primary tumor.

However, the deadliness of PDAC is attributed to its metastatic nature with a worrisome 3.2% 5-year survival after the tumor cells disseminate to a distant organ. This contrasts with the survival rate of more than 40% for patients diagnosed at earlier stage which often makes them eligible for surgical resection. Liver remains the most common organ of metastasis in PDAC. This study

aims to compare and characterize the distinct stromal and immune cell populations that exist within liver metastatic PDAC. This study shows that a distinct fibroblast population in the liver or liver CAFs exists in this metastatic niche while not observed in primary tumors. This project also looks at the metabolic heterogeneity displayed by PDAC cells. My data suggest that PDAC cells incline toward redox metabolism while establishing a niche in the liver possibly due to higher nutrient availability as compared to hypoxic and nutrient poor pancreas. Next, analysis of intercellular communication using CellChat shows an upregulation of the HGF-MET signaling axis, specifically in the liver and not in the pancreas. Further investigation shows disruption of downstream signaling including MAPK, AKT, and STAT3 upon MET inhibition.

Pharmacological and genetic inhibition of MET in cancer cells lead to reduced tumor growth and increased survival in mice. Lastly, this project also encompasses some key observations in immune cell compartments including T cells and myeloid cells suggesting alternative mechanisms of immune surveillance in the liver vs pancreas. Overall, this study suggests tailored treatment strategies to target metastatic PDAC.

CHAPTER 1: INTRODUCTION

1.1 Pancreatic Ductal Adenocarcinoma (PDAC) overview

Pancreatic Ductal Adenocarcinoma (PDAC) is an aggressive cancer of the exocrine pancreas with a dismal 5-year survival rate of 13.4%. It has recently surpassed breast cancer to become the third leading cause of cancer related deaths in the United States (2,3). PDAC cases are on the rise in the US (4), yet there has been limited advancement in therapeutic strategies. High lethality in PDAC is mostly attributed to the late diagnosis of the disease due to lack of specific symptoms (5). Most patients are diagnosed when the disease has progressed to distant metastasis, most frequently to the liver. In addition, no major risk factors have been conclusively identified in PDAC apart from germline mutations in DNA repair genes *BRCA1* and *BRCA2* (6). However, PDAC cases with *BRCA* mutations make up a minority of the overall PDAC diagnosed cases (7). Further complicating this complex disease is the heterogeneity of tumor cells and tumor microenvironment (TME) created from oncogenic signaling and consists of stromal and immune cells (8). Collectively, cancer cell heterogeneity and the various TME components work together to create tumor progressing environment which is hard to target clinically.

1.1.1 Initiation of PDAC

Similar to other cancers, PDAC progression is accompanied by accumulation of mutations in oncogenic and tumor suppressive genes (9). The exocrine pancreas consists of a system of acinar

and ductal cells. Here, acinar cells produce and secrete digestive enzymes which are transported to the main pancreatic duct via a network of ductal cells (10). Both acinar and ductal cells have been shown to harbor the potential to be the cells of origin in PDAC (11–13). Mutation in oncogenic *KRAS* is thought to be the driver of tumor formation in ~90% of PDAC cases (14). Activation in *KRAS* usually leads to two types of precursor lesions: 1) pancreatic intraductal epithelial neoplasia (PanIN) and cystic lesions 2) intraductal papillary mucinous neoplasm (IPMN) (7,15,16). The mutations commonly associated with these two types of precursor lesions are discussed in detail below.

1.1.2 Genetic drivers of PDAC

Germline mutations in *BRCA1/2* genes are found in a minority of PDAC cases (17). However, majority of PDAC patients have somatic mutation in the oncogene *KRAS* (v-Ki-ras2 Kirsten rat sarcoma viral oncogene homolog). *KRAS* is often considered the driving mutation in PDAC as it often leads to formation of the two precursor lesions mentioned above- PanINs and IPMNs (5,18,19). PanINs are microscopic lesions found in most PDAC patients. Thus, by definition these lesions cannot be detected in abdominal imaging making early diagnosis of this aggressive disease difficult. Initially it was thought that multiple low-grade PanINs start to develop in about 20% adults in their 50s where it can take an average of 35 years to progress to malignancy (20).

However, recent studies have shown that PanIN lesions with KRAS mutations occur in more than half of healthy adults in their 30s (21). IPMNs, on the other hand, are macroscopic precursor lesions that can arise within the main pancreatic duct or in the branches. Most of the early diagnosis of PDAC are attributed to patients with IPMNs which are visible in imaging

scans and often diagnosed accidentally in imaging for unrelated conditions. IPMNs, in addition to activation in KRAS, also experience loss of function in tumor suppressor gene RING type E3 ubiquitin ligase (*RNF43*) and gain of function mutation in G-protein alpha subunit Gαs (*GNAS*) (22–24). Both PanINs and IPMNs undergo low grade to high grade transformation in a series of mutation accumulation including *CKN2A*, and *SWI/SNF* (25–28). Finally, mutations in other tumor suppressor genes like *SMAD4* and *TP53* result in progression of high-grade lesions to malignant PDAC (29–31). Multiple studies suggest that mutations in *SMAD4* and *TP53* are usually only found in high grade lesions or PDAC suggesting late onset of these mutations (9,32).

1.1.3 Current therapeutic options

Most PDAC patients are diagnosed at a metastatic stage when malignant cells have colonized other parts of the body including liver, lungs, and peritoneum (33). Patients who are diagnosed early (around 15-20%) remain the best candidates for surgical resection followed by adjuvant chemotherapy. However, majority of PDAC patients are diagnosed at the metastatic stage with systemic chemotherapy as the sole standard of care treatment (34,35). It is important to note that surgical resection of PDAC tumors is often accompanied by removal of parts of pancreas along with the duodenum (36,37). This results in significant side-effects and compromised metabolism in most patients. Therefore, younger patients with robust health are often considered the best candidates for surgical resection with routine monitoring. Regardless of eligibility to surgical resection, all patients diagnose with PDAC undergo systemic chemotherapy treatment regimens. Gemcitabine and FOLFIRINOX (38) are the two most common chemotherapy treatments used in the US. FOLFIRINOX is a combination of 5-fluorouracil, leucovorin, irinotecan, and oxaliplatin.

In addition to gemcitabine and FOLFIRINOX, other options for PDAC treatment include gemcitabine + erlotinib (39) and gemcitabine + nab-paclitaxel (40). It is important to note that the choice of chemotherapy regimen depends on many factors including patient's age and comorbidities (41), but remain largely at the discretion of the oncologist with no biomarker based selection tools available. Regardless of first line therapy, the majority of these patients end up developing resistance to these treatment regimens. Sadly, there is no standard second line of treatment for PDAC. Further treatment options involve symptom management, targeted therapies, and eligibility of patients to any ongoing clinical trials. Patients with germline BRCA1/2 mutation have been shown to benefit from poly (ADP-ribose) polymerase (PARP) inhibitors (42). Mutations in mismatch repair genes or high microsatellite instability can be targeted by immune checkpoint inhibitors (43). Additionally, there has been extensive research to identify new actionable drug targets. These targets have included both mutations in cancerous cells and/or tumor supporting components of PDAC TME. It is impossible to understand the challenges in treating PDAC without understanding the individual components of the PDAC TME. Some of these populations that are known to play a vital role in PDAC are discussed in detail below.

1.2 PDAC TME

The PDAC TME is characterized by abundant stromal and immune cells that surround the malignant cells. It has been shown that some patient tumor samples consist of 90% stroma and only around ~10% cancerous PDAC cells (44). Therefore, there has been an extensive effort to study the tumor microenvironment of PDAC in a comprehensive manner. Phenotypically, the PDAC tumors are highly fibrotic due to the presence of vast number of fibroblasts, also called

cancer associated fibroblasts (CAFs) (45). Conversely, myeloid cells, macrophages in particular, are the most abundant immune cell type present (46). Most of these macrophages have been described and shown to have pro-tumorigenic role in PDAC. In addition, the PDAC tumors exhibit collapsed vasculature due to high interstitial pressure (47). Lastly, there is a wide range of intratumoral heterogeneity described within the PDAC cells (48–52). The PDAC TME is discussed below in detail.

1.2.1 Cancer cell heterogeneity

Many other tumors have presented with subtypes that can be used to inform clinical treatment strategies. Efforts to understand the transcriptional state of PDACs cells led to classification of PDAC cell subtypes. One of the first major characterization of PDAC cells was done by Collisson et al., where they utilized primary PDAC patient samples along with human and murine PDAC cell lines to identify molecular sub-types. Their analyses yielded 3 major subtypes- classical, quasimesenchymal, and exocrine-like, with each subtype harboring distinct gene signature (48). These subtypes also had varied response to therapeutic treatments. It is important to note that PDAC tumors are often characterized by heavy stromal and immune involvement, therefore, making genetic characterization of only the cancer cells difficult (30,53). This issue was resolved by Moffit and colleague where they used a virtual microdissection strategy, applied blind source separation to PDAC microarray data, and separated tumor cells from other stromal components. This study led to classification of PDAC cells to 2 main sub-groups- “classical” and “basal” (49). They further characterized these sub-types to predict patient outcomes. Their data showed higher disease progression and poor overall survival in patients with basal sub-type with only 11 months of median survival as compared to 19-month survival in

patients with classical-like tumors. In alignment with the Moffit et al., classification of classical and basal, Maurer et al., used micro dissected epithelial tissues and found similar sub-type and gene signatures (51). A further comprehensive study used laser captured microdissection of PDAC tumors and performed whole genome sequencing and transcriptomic sequencing (52). Their characterization showed 5 major sub-types: “classical-A”, “classical-B”, “hybrid”, “basal-A”, and “basal-B.” Overall, these studies showed the wide range of heterogeneity in PDAC tumors between patients and within the same patient tumor highlighting one of the many challenges in treating this devastating disease.

1.2.2 Cancer-associated fibroblasts

Cancer-associated fibroblasts (CAFs) represent the most abundant stromal cell population within the (PDAC) tumor microenvironment. CAFs are the most significant contributor to the desmoplasia frequently found in PDAC tumors (45). This desmoplasia is characterized by extensive deposition of extracellular matrix components such as collagen and fibronectin, ultimately leading to the pronounced fibrotic nature of these tumors (54). Beyond their structural role, multiple studies have shown that CAFs actively participate in dynamic and reciprocal crosstalk with malignant epithelial cells as well as various immune cell subsets within the tumor stroma (55–57). These interactions have been shown to promote tumor progression, immune evasion, and therapy resistance **(Fig.1.1)** (58–61). Notably, PDAC cells can engage in metabolic coupling with CAFs, wherein CAFs supply critical nutrients such as proline, alanine, GlcNAc and many other metabolites and amino acids that support cancer cell survival and proliferation under nutrient-deprived conditions of the pancreas (62–64). Given their multifaceted roles, CAFs have emerged as a major focus of investigation in PDAC research. Similar to tumor cells, CAFs

exhibit significant heterogeneity and phenotypic plasticity, with the capacity to transition between distinct subtypes in response to TME cues (65–67). This complexity underscores the necessity of delineating CAF subpopulations and their context-dependent functions to inform the development of more targeted therapeutic strategies. Accordingly, multiple efforts have been made to target these stromal cells in an effort to make PDAC tumors more accessible to therapeutic agents. Unfortunately, these efforts have failed miserably at pre-clinical or clinical levels (68–72). Below we discuss the origin of CAFs and some of the prominent CAF sub-types that have been described in the field.

Origin of CAFs

The origin of CAFs in PDAC has remained a pressing question that researchers have spent many years trying to answer. The normal pancreas is known to house multiple fibroblast populations with distinct functions. These include pancreatic stellate cells (PSCs) which have been described to have similar roles as the hepatic stellate cells in the liver (73,74). These PSCs are lipid droplets that can be rich sources of vitamin A (75,76). Other stromal populations in pancreas include perivascular and parenchymal fibroblasts (77). Previously, stellate cells were considered the only source of abundant CAFs present in PDAC (78). However, research advances and mouse models showed that stellate cells give rise to a minor, but important, subset of CAFs in PDAC (79). This was shown by the Sherman group where they performed lineage tracing on Fabp4+ stellate cells and showed that these stellate cells make up minority of CAF sub-population in PDAC. It is also now known that perivascular fibroblasts expressing Gli1 give rise to 30-50% of CAFs in both PanINs and PDAC in murine models. In contrast, parenchymal fibroblasts marked with expression of Hoxb6 do not play a significant role in tumorigenesis (80).

In addition, these fibroblasts do not have a well-defined role in adult pancreas even though this is a crucial population in embryonic pancreas development. Lastly, WT1 (Wilms tumor 1) expressing mesothelial cells have also been shown to contribute to a specific CAF sub-type with an immune-suppressive phenotype (81). Using other techniques like bone marrow transplantation has revealed that there is no significant contribution of bone marrow progenitors to the CAF populations (82).

Inflammatory CAF (iCAF)

Inflammatory or iCAFs, along with myofibroblast CAFs, were the first sub-type of CAFs identified and characterized in PDAC by Ohlund and colleagues (83). Using three-dimensional co-culture system, they showed quiescent PSCs can give rise to iCAFs. Transcriptionally, these CAFs upregulate expression and release of cytokines such as IL6 and IL11 which can have immunosuppressive roles in cancer (84–86). These anti-inflammatory cytokines result in the polarization of myeloid derived suppressor cells (MDSCs) that further impair anti-tumor immunity by inhibiting cytotoxic T cells (CTLs). Spatially, these CAFs reside on the periphery of tumors between cancer cell islands (83). This enables iCAFs to remain in close proximity to CTLs and block them from interacting with malignant cells. iCAFs release of IL6 can also facilitate cancer cell progression. IL6 binds to receptor IL6RA which results in the dimerization of GP130 signaling complex. Phosphorylation of GP130 results in the activation of janus kinase-signal transducer and activator of transcription (JAK-STAT) pathway (87). Activation of this pathway results in cell growth and proliferation.

Myofibroblast CAFs (myCAFs)

myCAFs are the most abundant CAF subtype present in PDAC TME. They are transcriptionally described by increased expression of α-SMA (83,88). Additionally, when first described, myCAFs were found to be present in close proximity to neoplastic cells surrounding the cancer organoids. myCAFs are essentially involved in producing extensive amount of extracellular matrix which primarily consists of collagen and hyaluronic acid (HA) (89–91). HA is a glycosaminoglycan with main characteristic to retain water molecules (92). This leads to increased interstitial fluid pressure and collapsed blood vessels. This is further accompanied by poor vasculature, reduced nutrient supply and over all a hypoxic environment. Conversely, cancer cells engage in crosstalk with myCAFs through hedgehog (Hh) signaling pathway and facilitate the deposition of dense extracellular matrix (93–97). Further, this desmoplasia also creates a physical barrier around the tumor cells and can prevent infiltration of therapeutic drugs from entering the tumor vicinity. Drug delivery has been a major challenge in PDAC due to the substantial fibrotic nature of this tumor (34). Early research suggested that targeting PDAC stroma by inhibiting Hh signaling can result in reduced tumor proliferation (98). However, subsequent studies showed that stromal ablation leads to worse overall survival due to increased angiogenesis and easier access to metastasize by PDAC cells (99–102) .

Antigen presenting CAF (apCAF)

A distinct subtype of cancer-associated fibroblasts (CAFs), termed antigen-presenting CAFs (apCAFs), exhibits a transcriptional profile that partially overlaps with that of mesothelial cells, suggesting a potential mesothelial lineage origin. While the precise functional roles of apCAFs within the pancreatic ductal adenocarcinoma (PDAC) tumor microenvironment remain incompletely understood, these cells are characterized by the expression of genes associated with

antigen presentation, including major histocompatibility complex class II (MHC-II) molecules (103,104). The immunological implications of this phenotype are still under investigation; however, emerging evidence indicates that apCAFs are capable of inducing the polarization of naïve $CD4^+$ T cells toward an immunosuppressive regulatory T cell (Treg) phenotype. Their data suggest that mesothelial cells turn off mesothelial genes and in turn, upregulate fibroblastic features in response to cytokines such as interleukin-1 (IL-1) and transforming growth factor (TGF-β) (81). These Tregs, in turn, contribute to tumor progression by dampening cytotoxic T lymphocyte (CTL)-mediated anti-tumor responses, thereby fostering an immune-privileged environment conducive to cancer growth and therapy resistance.

1.2.3 Immune cells

Immune cells within the tumor microenvironment represent a critical component of the host defense mechanism against malignancies. However, PDAC is characterized by an exceptionally immunosuppressive TME, with notably low infiltration of effector immune cells. Paradoxically, despite the paucity of cytotoxic lymphocytes, PDAC harbors a substantial population of immune cells that instead facilitate tumor progression and immune evasion (105).

Among these, myeloid-derived cells—including tumor-associated macrophages (TAMs), myeloid-derived suppressor cells (MDSCs), and dendritic cell subsets—constitute the most abundant immune cell population in PDAC, playing a pivotal role in promoting tumorigenesis, remodeling the extracellular matrix, and suppressing adaptive immune responses (5). The frequency of cytotoxic $CD8^+$ T lymphocytes is markedly reduced, further impairing antitumor

immunity, and contributing to the poor clinical efficacy of immune checkpoint inhibitors in PDAC.

While there are few T cells present in the PDAC TME, the T-cell compartment is largely dominated by immunosuppressive Tregs, which inhibit effector T-cell activation through direct cell–cell interactions and secretion of inhibitory cytokines such as IL-10 and TGF-β (106). This skewing toward an immunoregulatory phenotype establishes a profoundly tolerogenic environment that limits the potential for effective immune-mediated tumor clearance.

The subsequent sections provide a detailed characterization of the immune cell subsets present in the PDAC TME, their phenotypic profiles, and their mechanistic roles in driving disease progression and therapeutic resistance.

Macrophages

Myeloid cells constitute the most prevalent immune cell population within the tumor microenvironment of PDAC. A substantial body of evidence has demonstrated their predominantly pro-tumorigenic functions in this malignancy. Oncogenic KRAS—a hallmark genetic alteration in PDAC—drives the secretion of granulocyte–macrophage colony-stimulating factor (GM-CSF), which in turn recruits myeloid-derived suppressor cells (MDSCs) to the TME (107,108). These MDSCs exert potent immunosuppressive effects, notably through the inhibition of cytotoxic $CD8^+$ T lymphocytes, thereby impairing antitumor immune surveillance. Myeloid cells can differentiate into macrophages, which under physiological conditions play essential roles in innate immunity, pathogen clearance, antigen presentation, tissue repair, and maintenance of homeostasis. In the context of PDAC, these macrophages—termed tumor-associated macrophages (TAMs)—exhibit marked phenotypic heterogeneity. Two primary TAM

polarization states have been characterized: the classically activated, pro-inflammatory M1 phenotype and the alternatively activated, immunosuppressive M2 phenotype (109,110).

M1 macrophages, typically marked by high inducible nitric oxide synthase (iNOS) expression, produce inflammatory cytokines and reactive nitrogen species that can restrict tumor growth. Conversely, M2 macrophages promote tumor progression by facilitating immune evasion, angiogenesis, and extracellular matrix remodeling, while expressing high levels of immunosuppressive and pro-tumor markers such as arginase-1 (ARG1), CD204, and CD206. Notably, the hypoxic microenvironment of PDAC has been implicated in skewing TAM polarization toward the M2-like phenotype (111). Furthermore, phenotypic plasticity enables TAMs to transition between M1 and M2 states in response to dynamic microenvironmental cues (105). Specifically, pathways like Notch signaling, JAK/STAT, phosphatidylinositol 3-kinase (PI3K-AKT), nuclear factor kappa b (NF-κb), and Hh signaling pathway have been shown to play critical role in the polarization of TAMs (112).

Clinically, a high TAM density correlates with poor overall survival in PDAC patients (113). Preclinical studies have shown that depletion of myeloid cells can significantly reduce tumor burden in murine models, underscoring their functional relevance in disease maintenance (114–117). Beyond their immunomodulatory roles, myeloid cells also contribute to therapeutic resistance. Specifically, they secrete deoxycytidine, which competes with the anti-metabolite gemcitabine—the current standard chemotherapeutic agent for PDAC—for cellular uptake and metabolic activation, thereby diminishing its cytotoxic efficacy (118).

As previously discussed, cancer cells in PDAC are vastly outnumbered by other types of stromal and immune cells. PDAC cells also experience a highly nutrient deficient environment due to lack of proper vasculature. To maintain a symbiotic relationship with cancer cells, TAMs can also fuel their metabolism by releasing numerous pyrimidines (111).

Collectively, these findings highlight the multifaceted role of myeloid cells in PDAC pathogenesis, immune evasion, and treatment resistance, positioning them as promising targets for therapeutic intervention.

T cells

PDAC is broadly characterized by poor infiltration of cytotoxic $CD8^+$ T lymphocytes, a feature that contributes significantly to its profoundly immunosuppressive TME. However, considerable heterogeneity exists in T-cell abundance across PDAC tumors, reflecting inter- and intra-tumoral variability in immune composition. Instead of robust cytotoxic infiltration, the PDAC TME is typically enriched in immunosuppressive T-cell subsets, particularly Tregs, as well as other pro-tumorigenic populations such as Th17 and Th22 cells (119–122).

Several therapeutic strategies have been developed to selectively target immunosuppressive T-cell subsets, most notably Tregs, in an attempt to restore antitumor immunity. Unfortunately, these approaches have generally yielded disappointing results. The depletion of Tregs has been shown to trigger compensatory mechanisms, particularly the recruitment and expansion of immunosuppressive myeloid cells, thereby sustaining the overall immunosuppressive niche (123). Furthermore, Tregs serve as an important source of transforming growth factor-β (TGF-β), a cytokine essential for the activation and maintenance of myCAFs. Elimination of Tregs

inadvertently disrupts this stromal support, dismantling the physical barrier provided by myCAFs, which paradoxically can enhance tumor progression. These findings underscore the intricate interdependence between immune and stromal compartments in PDAC and highlight the inherent challenges in therapeutically targeting individual immune populations in isolation.

Despite the general scarcity of $CD8^+$ T cells within PDAC tumors, their presence is strongly associated with improved clinical outcomes. Preclinical evidence from Li et al. demonstrated this principle using autochthonous KPC mouse models of PDAC. By stratifying tumors based on T-cell abundance, they identified “T cell–high” and “T cell–low” groups. Mice harboring “T cell–high” tumors exhibited a reduced metastatic burden and displayed significantly enhanced responses to immunotherapy, including immune checkpoint blockade (124). These findings suggest that although $CD8^+$ T-cell infiltration is limited in most PDAC tumors, when present at sufficient levels, it can profoundly influence disease progression and therapeutic efficacy.

Taken together, these observations highlight the dual nature of T-cell biology in PDAC—where suppressive subsets foster tumor progression and immune evasion, whereas cytotoxic $CD8^+$ T cells, though rare, are key determinants of favorable prognosis and treatment responsiveness. This dichotomy reflects the complexity of immune regulation in PDAC and emphasizes the need for integrated therapeutic strategies that can both enhance effector T-cell function and modulate immunosuppressive networks within the TME.

B cells

Most immunotherapeutic strategies in cancer have historically focused on T cell–mediated antitumor immunity, particularly through the enhancement of cytotoxic $CD8^+$ T-cell function and checkpoint blockade therapies. However, emerging evidence has begun to highlight the critical yet underappreciated role of B cells within the TME (125–128).

B cells, traditionally regarded for their capacity to generate humoral immune responses, have been shown to exhibit remarkable phenotypic and functional heterogeneity in the context of cancer. On one hand, the differentiation of B cells into plasma cells and subsequent antibody production has been correlated with favorable prognosis and improved therapeutic response in several malignancies, including PDAC. These antibodies can facilitate antitumor immunity through mechanisms such as antibody-dependent cellular cytotoxicity and opsonization, thereby complementing T cell–driven immune responses (129).

Conversely, B cells can also adopt immunoregulatory roles that suppress antitumor immunity. Certain B-cell subsets are capable of secreting immunosuppressive cytokines, such as IL-10 and TGF-β, which inhibit effector T-cell responses and foster a tolerogenic environment. Regulatory B cells (Bregs), in particular, share functional similarities with regulatory T cells, exerting broad immune-suppressive effects that promote tumor progression (130).

In the specific context of PDAC, transcriptional reprogramming of B cells has been implicated as a determinant of their functional fate within the TME. Work by Mirlekar et al. demonstrated that IL-35 production by B cells induces a stable immunosuppressive program in naïve B cells

through the upregulation of transcription factors such as BCL6 and PAX5. This transcriptional rewiring favors an immune-suppressive state that limits antitumor immunity. Importantly, targeting BCL6 disrupted this suppressive program, resulting in enhanced infiltration of antibody-secreting plasma cells within the PDAC TME. Such findings suggest that manipulating B-cell plasticity may represent a novel strategy to augment plasma cell–mediated antitumor responses and enhance the efficacy of immunotherapy in PDAC (131).

Collectively, these observations emphasize the multifaceted roles of B cells in PDAC—ranging from tumor-promoting immunoregulators to potent mediators of antitumor immunity. This duality underscores the necessity of broadening the scope of immunotherapy research beyond T cells to include B-cell biology, which may yield new therapeutic opportunities for overcoming immune resistance in PDAC.

1.2.4 Vasculature

PDAC is characterized by a profoundly hypovascular architecture, frequently exhibiting collapsed blood vessels and markedly reduced perfusion. This phenomenon arises largely from the pronounced desmoplastic reaction typical of PDAC, wherein CAFs generate extensive fibrotic stroma. The excessive deposition of ECM components, such as collagen and hyaluronan, leads to substantial accumulation of interstitial fluid within the tumor. This elevated interstitial fluid pressure compresses intratumoral blood vessels, resulting in vascular collapse and severely impaired perfusion (132–135).

One of the major therapeutic challenges in PDAC stems from this compromised vascular network, which significantly limits the delivery and penetration of chemotherapeutic agents. Consequently, poor drug distribution contributes to treatment resistance and suboptimal clinical outcomes.

Recent spatial mapping studies have provided critical insights into the organization of the vascular compartment in PDAC. Notably, researchers have employed imaging mass cytometry on a well-defined cohort of patient tumor samples to investigate the spatial relationships between endothelial cells and other cellular components of the TME. Their findings revealed a negative spatial association between endothelial cells and malignant ductal cells, indicating that tumor cells are frequently located at substantial distances from blood vessels. Moreover, endothelial cells were observed to exhibit spatial avoidance of most cancer cells and immune cell populations (136).

Interestingly, an exception to this pattern was noted in their proximity to $CD44^{high}$ macrophages, suggesting a preferential spatial association. This observation may reflect the immunosuppressive role of certain macrophage subsets in PDAC, which can create a microenvironment conducive to tumor growth while facilitating immune evasion. The close vascular–macrophage relationship could therefore represent a niche that supports tumor progression by balancing nutrient supply with local immunosuppression.

Collectively, these findings underscore the complex interplay between the fibrotic stroma, vascular dynamics, and immune cell spatial organization in PDAC, with important implications for understanding drug delivery barriers and designing stroma-targeted therapeutic strategies.

1.3 HGF-MET signaling axis

The hepatocyte growth factor (HGF)–MET signaling axis plays a pivotal role in regulating diverse cellular processes, including proliferation, motility, invasion, survival, and migration. MET, also known as c-MET, is a receptor tyrosine kinase whose only known ligand is hepatocyte growth factor (HGF). Under physiological conditions, HGF-MET signaling is essential for maintaining tissue homeostasis, regulating embryonic development, organ regeneration, and wound healing (137,138).

Aberrant activation of the HGF-MET pathway, however, has been widely implicated in oncogenesis. Dysregulation of this axis has been reported across a range of malignancies, including thyroid cancer, renal cell carcinoma (RCC), hepatocellular carcinoma (HCC), and pancreatic ductal adenocarcinoma (PDAC) (139–150). Oncogenic MET activation can arise from multiple mechanisms, such as receptor overexpression, gene amplification, mutations, or excessive HGF production within the tumor microenvironment. These alterations drive uncontrolled cellular proliferation, epithelial-to-mesenchymal transition (EMT), angiogenesis, and metastatic dissemination.

The oncogenic potential of the HGF-MET pathway is largely mediated through its ability to engage multiple downstream signaling cascades. Notably, MET activation stimulates the MAPK/ERK pathway, promoting cell cycle progression and proliferation; the PI3K/AKT pathway, enhancing survival and resistance to apoptosis; and the STAT3 pathway, which regulates transcriptional programs associated with immune evasion, angiogenesis, and tumor-

promoting inflammation (151). Together, these pathways form an intricate signaling network that fuels tumor progression and contributes to therapeutic resistance.

Given its central role in tumor biology, the HGF-MET axis has emerged as an attractive therapeutic target. Several classes of inhibitors—including small-molecule tyrosine kinase inhibitors (TKIs), monoclonal antibodies against MET, and HGF-neutralizing agents—are under investigation in preclinical and clinical settings (152). Although challenges such as resistance mechanisms and patient stratification remain, targeting HGF-MET signaling continues to hold promise as a strategy to disrupt oncogenic signaling and improve treatment outcomes across multiple cancers, including PDAC. This section discusses the HGF-MET signaling axis in detail.

1.3.1 Hepatocyte Growth Factor (HGF)

Hepatocyte growth factor (HGF), also referred to as hepatotropin, was first identified in 1984 during investigations aimed at isolating mitogenic factors that could stimulate hepatic regeneration following injury, such as viral hepatitis or partial hepatectomy involving up to 70% liver resection (153). Biochemically, HGF is a heterodimeric protein with a molecular weight of approximately 84 kDa on SDS-PAGE, consisting of an α-chain (69 kDa) and a β-chain (34 kDa) covalently linked by a disulfide bond (154). Structurally and functionally, HGF is classified as a pleiotropic growth factor that exerts diverse biological effects through its exclusive receptor, the c-MET tyrosine kinase (138,155–157).

Physiologically, HGF is indispensable for liver regeneration, where it initiates tightly regulated proliferative signaling cascades in response to hepatic stress or tissue loss. Serum and hepatic

concentrations of HGF rise markedly during episodes of hepatic injury, reflecting its role as an early mediator of regenerative signaling. Although mesenchymal cells represent the principal source of HGF under homeostatic conditions, during acute or chronic hepatic insult, HGF production can also be induced in extrahepatic organs, including the spleen, lungs, and kidneys. This upregulation occurs in response to systemic stress hormones and inflammatory mediators such as norepinephrine and prostaglandins, which facilitate rapid mobilization and delivery of HGF to the injured liver (158).

Beyond its role in hepatic regeneration, HGF has been implicated in tissue protection and repair across multiple organ systems. In the liver, HGF contributes to recovery in the context of chronic injuries such as cirrhosis and viral hepatitis, while in extrahepatic settings it has been associated with pathophysiological processes including pulmonary fibrosis (159) and chronic kidney disease (160–162) . Importantly, HGF also functions as a potent trigger for anti-apoptotic factors, particularly during acute injury states. In fulminant hepatitis, aspiration pneumonia, and acute myocardial infarction, HGF signaling has been shown to limit tissue damage by triggering the release of anti-apoptotic proteins, notably Bcl-xL, thereby preventing cell death and enhancing tissue survival (163).

Together, these findings establish HGF as a multifunctional growth factor with roles extending beyond liver regeneration to encompass tissue protection, repair, and survival across multiple organ systems, highlighting its potential as a therapeutic target in regenerative medicine and disease intervention.

1.3.2 MET

The mesenchymal–epithelial transition factor (MET), also known as c-MET, is a receptor tyrosine kinase and the sole high-affinity receptor for HGF. During embryogenesis, MET is indispensable for processes such as gastrulation, angiogenesis, bone remodeling, and myoblast migration (164). In adults, c-MET expression is particularly enriched in the liver, where it is strongly upregulated during hepatic regeneration, reflecting its role in tissue repair and organ homeostasis (165).

Structurally, MET is a glycosylated heterodimeric protein consisting of an extracellular α-chain and a transmembrane β-chain. Upon HGF binding, MET undergoes dimerization, which promotes autophosphorylation of intracellular tyrosine residues. This conformational shift stabilizes the SEMA domain—the HGF-binding interface—and initiates recruitment of adaptor proteins that propagate multiple downstream signaling cascades (166,167).

To prevent aberrant activity, several negative regulatory mechanisms govern MET signaling. Protein kinase C suppresses phosphorylation in a PLCγ-dependent manner, while tyrosine phosphatases such as density-enhanced phosphatase 1 (DEP1) and leukocyte common antigen-related phosphatase (LAR) dephosphorylate kinase domains. Additionally, activated MET can be targeted for ubiquitination and proteasomal degradation via the E3 ubiquitin ligase Cbl (168,169).

When these regulatory mechanisms are disrupted, MET becomes constitutively active, a phenomenon observed in multiple malignancies, including thyroid carcinoma, renal cell

carcinoma, hepatocellular carcinoma, and pancreatic ductal adenocarcinoma (PDAC). Such aberrant MET activation supports tumorigenesis by promoting sustained proliferation, survival, invasion, and epithelial–mesenchymal transition (EMT) (142). Accordingly, the HGF–MET axis has become a major therapeutic focus, with small-molecule tyrosine kinase inhibitors and neutralizing antibodies under active clinical development.

In PDAC, MET activation has been primarily studied in primary tumors, where it contributes to growth and chemoresistance (170–172). However, the precise function of MET in the metastatic cascade—particularly in dissemination, colonization, and survival in distant organs—remains incompletely understood, representing an important area for ongoing investigation.

1.3.3 Downstream c-MET signaling

As described above, the binding of HGF to its receptor MET leads to dimerization and autophosphorylation of the tyrosine residues in the transmembrane portion of the receptor. This leads to the recruitment of adaptor proteins such as growth factor receptor bound protein-2 (GRB2), Src-homology-2-containing (SHC). This further activates effector molecules such as PI3K and STAT3. Importantly, c-MET can also activate RAS leading to the activation of mitogen activated protein kinase (MAPK) (173). This is particularly interesting in the context of PDAC because of the previously described role of KRAS activation in this specific cancer. This further signals the activation of v-raf murine sarcoma viral oncogene homolog B1 (RAF) kinase leading to the downstream activation of MAPK effector kinase (MEK) and eventually, MAPK which then translocates into the nucleus and starts the transcription of genes responsible for cell proliferation and cell progression. This pathway is well studied and its role in PDAC is well known. In addition to MAPK activation, c-MET can also activate PI3K via GRB2 associated

binding protein 1 (GAB1). This pathway is primarily responsible for promoting cell survival (174,175). Lastly, STAT3 can also directly bind to phosphorylated c-MET which results in the phosphorylation of STAT3 and its translocation to the nucleus (176–178). The involvement of c-MET in activating multiple important cell proliferation pathways simultaneously highlights the significance of this pathway and how its disruption can lead to uncontrolled cell division, malignancy, cell motility, and metastases.

1.3.4 MET Inhibitors in clinic

Due to the well described role of c-MET in malignancies, multiple attempts have been made to inhibit this tyrosine kinase receptor in various cancers either using a small molecule inhibitor approach or a monoclonal antibodies that inhibit the interaction between c-MET and its ligand HGF. This has been particularly useful in cancers where cancer cells experience and rely on *MET* amplification for uncontrolled growth and survival. Conversely, high MET expression is associated with increased metastasis and poor survival (179). Crizotinib and cabozantinib were the first 2 c-MET inhibitors that were approved for advanced RCC and non-small cell lung carcinoma (NSCLC) by the US Food and Drug Administration (FDA) (180). The full list of FDA approved c-MET inhibitors as of 2025 is presented in Table-1. The c-MET inhibitors can be classified into 3 classes- Class I and class II use an adenosine triphosphate (ATP) competitive approach where these inhibitors serve as analogs for ATP which is required for phosphorylation of c-MET. Class I inhibitors are considered for specific to the binding site of c-MET. Class II inhibitors, on the other hand, are less selective and have multiple targets. Lastly, class III inhibitors are non-ATP competitive inhibitors (181). This dissertation specifically focuses on the small molecule inhibitor cabozantinib which is an oral tyrosine kinase inhibitor. For patients, its

approved dosage ranges from 60mg tablet to 140mg capsule taken daily. Cabozantinib can also target other receptor tyrosines such as vascular endothelial growth factor receptor (VEGF), rearranged during transfection (RET), tyrosine-protein kinase receptor UFO (AXL), and KIT (182).

Table 1: Table 1 shows the list of FDA approved c-MET inhibitors as of March 2025. Also listed in the table are the type of drug, the year they were approved in, and the type of cancer they are currently approved and being used for in clinic.

DRUG	TYPE	YEAR OF APPROVAL	TYPE OF CANCER
Crizotinib	Small molecule inhibitor	2011	NSCLC, Anaplastic Large cell lymphoma, Inflammatory myofiborblastic tumors
Cabozantinib	Small molecule inhibitor	2012	Thyroid cancer, RCC, HCC, NET
Capmatinib	Small molecule inhibitor	2020	NSCLC
Amivantamab	Antibody	2021	NSCLC
Tepotinib	Small molecule inhibitor	2021	NSCLC
Telisotuzumab	Antibody drug conjugate	2025	NSCLC

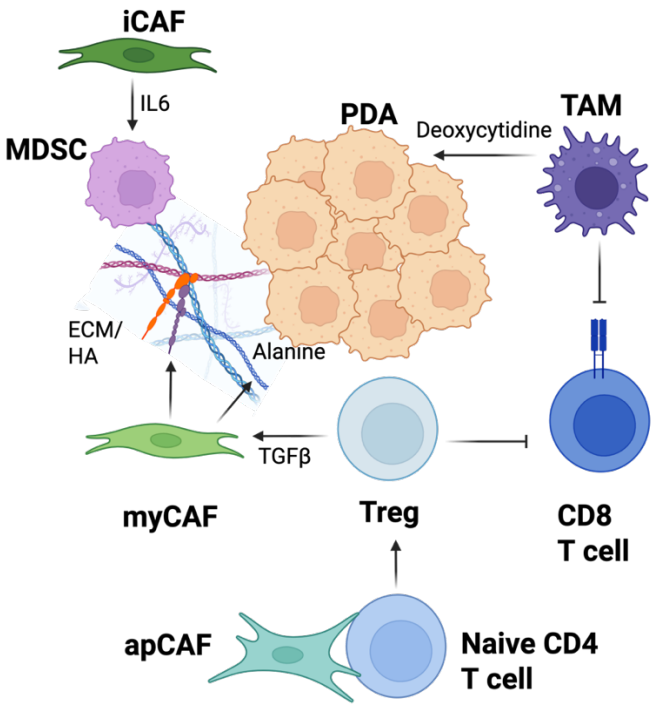

Figure 1.1 CAFs in PDAC: PDAC cells establish a complex niche with multiple types and sub-types of immune and stromal cells. These populations engage in complicated interactions with each other and with the malignant PDAC cells. iCAFs release multiple immune-suppressive cytokines such as IL6 that foster the proliferation of immunosuppressive MDSCs which can inhibit a potential immune response. The excessive amount of extracellular matrix is deposited by myCAFs leading to the collapse of vasculature due to high interstitial pressure. apCAFs can polarize naïve CD4 T cells to exhibit a regulatory phenotype. The most abundant immune cell type present in PDAC are TAMs that can suppress CD8 T cells. The TAMs have also been shown to be the key source of deoxycytidine in the TME that directly contributes to gemcitabine resistance in patients.

CHAPTER 2: MATERIALS AND METHODS

Study approvals: All procedures were performed at the University of California, Irvine in compliance with the Institution Animal Care and Use Committee (AUP-23-084) and the Institutional Biosafety Committees (BUA-R315). Patient specimens were obtained de-identified through UCI 08-70 or the UCI Experimental Tissue Repository.

Cell culture: The KPC-FC1245 cell line was a gift from Dr. David Tuveson (Cold Spring Harbor Laboratory). PATC53 cells were obtained from ATCC. PDAC cells were maintained in high-glucose DMEM (Gibco) supplemented with 10% FBS (Corning). Primary fibroblasts were established by outgrowth from tissue pieces as described (183) and maintained in DMEM with 20% FBS. All cells were routinely tested for mycoplasma contamination using MycoAlert PLUS (Lonza). Cabozantinib was obtained from ChemGood. HGF was obtained from Peprotech.

Orthotopic surgery: Orthotopic transplantation into the pancreas was performed using 50,000 KPC FC1245 cells prepared in a 1:1 ratio with Matrigel and media (DMEM + 10% FBS). Mice were anesthetized with isoflurane and area for surgery was prepared using aseptic techniques. A 2-inch incision was made subcutaneously and intraperitoneally, then 50uL of tumor cell suspension was injected into the tail of the pancreas.

***Hemi-spleen surgery*:** For liver tumor seeding, the spleen was accessed through a Laparotomy then expressed through the skin. The spleen was then ligated into two halves inferior to the hilar vessels using medium sized ligating clips and a clip applicator. After making an incision on the

spleen, the lower half was tucked back into the peritoneum. A cell suspension with KPC FC1245 cells followed by a layer of PBS were loaded in a syringe and injected at a 30-degree angle right underneath the spleen capsule. After injecting the full volume, the needle was left inside the spleen to avoid any fluid escape. Another ligation clip was placed to ligate the superior hilar vessels and the remaining spleen was removed using scissors.

Murine Single Cell Transcriptomics: Tumors were removed and minced using a scalpel. Further dissociation was achieved with enzymatic digestion with collagenase V for pancreas tumor and collagenase IV for liver tumors (1mg/mL DMEM) for 30 mins on a MACS tissue dissociator. Tumor suspension was then filtered through 500-um, 100-um, and 40-um mesh to obtain single cells. Dead cells were subsequently removed using MACS Dead Cell Removal Kit (Miltenyi Biotec.). Single cell DNA libraries were prepared and sequenced at the UCI Genomics Research and Technology Hub. Cell Ranger version (chemistry 3' v3, pipeline version 3.1.0) was used with default settings with an initial expectation of 10,000. Cell Ranger software was used for alignment and quantification. For downstream analyses, R studio version 4.1.1 was used. Seurat version (5.2.1) was used as previously described (184). Briefly, QC was performed to exclude cells containing less than 200 or more than 2000 genes. Data were normalized using LogNormalize with a scale factor of 10,000 followed by scaling. PCA was run on the filtered data. Clusters were defined based on the gene expression using FindAllMarkers. The code is publicly available on GitHub (https://github.com/halbrook/HalbrookLab).

Human Single Cell Transcriptomics: Human single cell RNA sequencing atlas data was utilized from the following prior study(185). Briefly, this atlas included 172 primary tumors and

25 metastatic biopsies, the majority of which were from liver metastatic PDAC tissues. Tissues were a mix of treated and untreated samples. Raw data were aligned to the same human reference genome and batch correction was performed with Harmony package. Seurat v4 was used to cluster data and cell types were assigned based on major lineage markers such as *KRT18/19* for ductal identify, and *DCN, LUM, COL1A1* for CAFs. Ductal cells and CAFs were clustered separately, and DotPlot visualizations were used for specific genes of interest. Classical, basal, or hybrid identify in ductal subpopulations was determined by scoring of gene signatures.

Histology: Mice were sacrificed by CO_2 asphyxiation then tissue was quickly harvested and fixed overnight at room temperature with Z-fix solution (Anatech LTD). Tissues were processed using a Leica ASP300S Tissue Processor, paraffin embedded, and cut into 5 μm sections. Immunohistochemistry was performed by deparaffinizing and rehydrating tissues then performing antigen retrieval with a Sodium Citrate Buffer (10mM Sodium Citrate, 0.05% Tween 20, pH 6.0). Blocking was performed with serum free protein block (Dako), then PDGFRβ (Abcam, #32570, 1:300) and Cytokeratin 19 antibody (Abcam, #ab133496, 1:500) were used as primary antibodies. After washing, Rabbit-on-Rodent HRP Polymer (Biocare Medical) was used as secondary antibody, then chromogen deposited using DAB plus (Dako). Slides were then counterstained with hematoxylin. Hematoxylin and eosin staining were performed per manufacturer's instructions. Immunohistochemistry for PDGFRβ (Abcam, #32570) or MASP1 (ThermoFisher, #PA5-47992) was performed separately with standard conditions on a Discovery ULTRA stainer (Roche) and antibodies were detected with DAB, and counter stained for nuclear detection. Brightfield images were taken on a Leica THUNDER microscope.

Fluorescence ISH **:** Five-micron sections were cut from adjacent or pancreatic cancer metastatic liver biopsy tissues onto charged slides. Slides were then baked at 60°C for 30 minutes, deparaffinized with xylene for 10 minutes, dehydrated in 100% ethanol for 2 minutes, and washed with 0.1% Tween-20 RNAse-free 1x phosphate-buffered saline (PBST). RNA scope Multiplex Fluorescent Detection v2 kit assay was performed according to manufacture instructions (Advance Cell Diagnostics; ACD). Briefly, slides were incubated with hydrogen peroxide for 10 minutes at room temperature followed by target retrieval at 98°C for 15 minutes. Slides were then blocked with the Co-Detection antibody diluent for 30-60 minutes and incubated with Pan cytokeratin (PanCK) (Invitrogen, #53-9009-82, 1:400) for 16 hours at 4°C. The following day tissue sections were post-fixed with neutral buffered formalin and treated with the ProteasePlus Reagent for 13 min at 40°C in a hybridization oven. Amplification and signal enhancement (AMP) were performed for either a single probe (C1) or two different probe (C1 and C2) combinations. UPP1-C1 was a 1x probe and DCN-C2 was a 50x probes. Probes were diluted in ACD probe diluent per manufacturer's instructions and slides were incubated with them at 40°C for 2 hours. Following two washes with RNA scope washing buffer, the signal for each probe was amplified with AMP reagents, horseradish peroxidase, and tyramide signal amplification kit at 40°C. Slides were then incubated with anti-mouse or anti-rabbit secondary Alexa Fluor 488 IgG (H + L) antibody (1:400) for 1 hour at room temperature. Tissue sections were counterstained with DAPI for 15 minutes at room temperature and washed three times with PBST before being mounted with ProLong Diamond Antifade mounting medium. Images were taken on a white light laser confocal STELLARIS (Leica) microscope.

Immunofluorescence: Immunofluorescence for MASP1 (ThermoFisher, #PA5-47992, 1:100), PDGFRβ (Abcam, #32570, 1:300), or αSMA (Sigma, #A2547, 1:1000) was performed as previously described (Steele et al., Nature Cancer, 2020). Briefly, slides were deparaffinized and underwent citric acid retrieval in a microwave for 20 minutes. After cooling slides were blocked in 20% donkey serum for 30 minutes at room temperature. Following this, primary antibodies were added at 4°C for 16 hours. Tissue sections were counterstained with DAPI for 15 minutes at room temperature and washed three times with PBST before secondaries were added (Jackson Immuno donkey secondaries at 1:400 in PBS were used against goat, mouse or rabbit) for 45 minutes at room temperature and then slides were mounted with ProLong Diamond Antifade mounting medium. Images were taken at 20x or 40x on a white light laser confocal STELLARIS (Leica) microscope. Images were quantified with HALO software and at least 5 large-scale regions (N=3 Primary PDA, N=4 Liver metastasis) were analyzed for each 40X tile scanned image (average number of cells per high power field were averaged for each patient within these regions).

***CellChat Network Analysis*:** Differential cell–cell communication analysis was conducted using the CellChat framework. Specifically, intercellular communication probabilities between each cell-type pair were inferred independently for liver and pancreas tumor, utilizing the curated interaction database provided by CellChatDB. Subsequently, differential communication strength between the two conditions was computed for each cell-type pair to identify context-specific alterations in signaling networks.

Bulk RNA Sequencing: Primary fibroblasts and CAFs were brought up in culture and upon

reaching 70-80% confluency, RNA was harvested using RNeasy Plus Mini kit (Qiagen, #74126). RNA quality was verified using Nanodrop. Samples were sent for sequencing. Quality was ensured using RIN (above 8). FastQFiles were then aligned using STAR, bedgraphs were generated, and RNA counts were obtained in tpm format. Downstream analyses were performed in R studio. Briefly, differential expression of genes was performed to generate Venn diagram and z-scores were obtained to plot heatmaps.

ELISA: Serum free conditioned media was harvested from primary fibroblasts. ELISA was performed using the Human HGF Quantikine ELISA kit (R&D, #DHG00B) and following manufacturer's instructions.

Western Blotting: Cells were lysed with 1X RIPA lysis buffer (Sigma-Aldrich Cat# 20188) supplemented with protease inhibitors (cOmplete™, EDTA-free Protease Inhibitor Cocktail, Sigma-Aldrich Cat# 11873580001) as well as phosphatase inhibitors (PhosSTOP™, Roche Cat# 4906845001). Protein quantification of cleared lysates was performed using a bicinchoninic acid (BCA) assay kit (Pierce™ BCA Protein Assay Kits, ThermoFisher Cat# 23227). Lysates were subsequently electrophoresed and immunoblotted with the indicated primary antibodies: Phospho-Met (Tyr1234/1235) (1:1000, Cell Signaling Technology Cat# 3077T); Met (1:1000, Cell Signaling Technology Cat# 3127); p44/42 MAPK (Erk1/2) (1:1000, Cell Signaling Technology Cat# 4695S); Phospho-p44/42 MAPK (Erk1/2) (Thr202/Tyr204) (1:1000, Cell Signaling Technology Cat# 4370S); β-Actin (1:5000, Santa Cruz Biotechnology Cat# sc-47778); Vinculin (1:5000, Cell Signaling Technology Cat# 13901S). Nitrocellulose membranes(Bio-Rad) were then incubated with the appropriate HRP-conjugated secondary antibodies: Anti-rabbit IgG,

HRP-linked Antibody (1:10,000, Cell Signaling Technologies Cat# 7074S); Anti-mouse IgG, HRP-linked Antibody (1:10,000, Cell Signaling Technologies Cat# 7076S); or IRDye 800CW Goat anti-Mouse IgG Secondary Antibody (1:15,000, Licor, 926-32210). Imaging was performed on a Thermo iBright Imaging System using an enhanced chemiluminescence (ECL) kit (SuperSignal™ West Femto Maximum Sensitivity Substrate, Thermo Fisher Cat# 34095) or on a Li-Cor Odyssey CLx.

Cell Signaling Assays: PATC53 and PATC53 sgMet cells were grown in DMEM+10% FBS (Gibco) they reached 75% confluence. PATC53 plates were then switched to serum free DMEM for 12 hours prior to the assay. Serum free media was aspirated and plates were washed with PBS (Gibco) then subjected to treatments. Here, cells were treated with 1μm cabozantinib (ChemGood Cat# C-1333) or vehicle (0.5% DMSO) for 20 min then treated with 1ng/mL human HGF (Peprotech Cat#100-39-10UG) or vehicle (water) then incubated at 37°C for the times indicated in the figure legend for each assay.

Condition Media Assays: Liver fibroblasts, Liver CAFS, and PDAC CAFs were grown in DMEM+10% FBS (Gibco) they reached 75% confluence. Cells were washed with PBS then serum-free DMEM was added. Media was allowed to condition for 48 hours, then filtered through a 0.45μM filter. PATC53 and PATC53 sgMet cells were grown in DMEM+10% FBS (Gibco) until they reached 75% confluence. PATC53 plates were then switched to serum free DMEM for 12 hours prior to the assay. Serum free media was aspirated and plates were washed with PBS (Gibco) then incubated in serum free DMEM at 37°C. After 20 minutes, DMEM or 3:1 conditioned media – serum free DMEM was and incubated at 37°C for the time indicated in each

figure legend. The conditioned media+Vehicle condition was incubated with DMEM+0.5% DMSO for 20 minutes at 37°C. For Cabozantinib treatment experiments, 1μm drug (or 0.5%DMSO) was added for 20 minutes at 37°C prior to treatment with 3:1 conditioned media or fresh DMEM.

CRISPR/Cas9 editing of PDAC Cell lines: Genetic targeting of MET in PDAC cell lines was achieved using CRISPR/Cas9 method described previously (186). Briefly, sgRNA sequences targeting *MET* or *Met* were selected from the human and mouse GeCKOv2 CRISPR knockout pooled library, respectively. Overlapping oligonucleotides were purchased, annealed, phosphorylated, then ligated into the overhangs of PX459 V2.0 vector (Addgene plasmid #62988) that was digested with BbsI. The resulting CRISPR/Cas9 plasmid was transformed into chemically competent Stbl3 cells, miniprepped for plasmid DNA, and sequence-verified. sgRNA oligonucleotide pairs hMET-PX459F CACCgCACATGGCAGATCGATCCAT and hMET-PX459R AAACATGGATCGATCTGCCATGTGc or mMET-PX459F CACCgCACATGGCAGATCGATCCAT mMET-PX459R AAACTGAATAAGTCGACGCGCTGCc were used. PDAC cells were transiently transfected using Lipofectamine 3000 according to the manufacturer's instructions. Cells were selected with 2μg/mL puromycin for 72 hours, where a parallel non-transfected control plate was observed to be completely killed. To select clones, polyclonal pools were seeded into 96-well plates at a density of 1 cell per well. Individual clones were expanded and editing efficiency assessed via western blot.

Mouse tumor treatments: C57BL/6J mice were injected with KPC FC1245 (250k/mouse).

Tumors were established for 6 days before mice were randomized into vehicle or treatment arms. Mice (n= 5-7 per group) were treated with vehicle or cabozantinib (ChemGood #C-1333) (30mg/kg) every day for 12 days via oral gavage. After 12 days of treatment, mice were sacrificed and liver tissues were harvested upon sacrificing the mice.

***Data availability*:** scRNA sequencing data and bulk RNA sequencing data will be uploaded to GEO upon acceptance of manuscript. Human single cell RNAseq atlas is uploaded to Zenodo (https://zenodo.org/records/14199536). Other data will be provided upon reasonable request.

Statistics & Reproducibility: All experiments were run a minimum of two times with at least 3 biological replicates. Statistics were performed using Graph Pad Prism 8 (Graph Pad Software Inc). Groups of 2 were analyzed with two-tailed students t test, groups greater than 2 were compared using one-way ANOVA analysis with Tukey post hoc test. All error bars, group numbers, and explanation of significant values are presented within the figure legends. The following values are used to denote significance; * $P \leq 0.05$; ** $P \leq 0.01$; *** $P \leq 0.001$; **** $P \leq 0.0001$. Sample sizes were determined by previous experiments performed in our groups. No data were excluded from the analyses.

CHAPTER 3: COMPARATIVE ANALYSES OF PRIMARY PDAC & LIVER METASTASIS

ABSTRACT

The tumor microenvironment drives many malignant features of pancreatic ductal adenocarcinoma (PDAC). The fibroblasts within pancreatic tumors promote tissue remodeling, immune suppression, and resistance to therapy. However, the interactions between stromal populations and pancreatic cancer cells are less understood in the liver, the most frequent site of PDAC metastasis. To address this, I employed single cell transcriptomics to compare primary pancreatic vs. liver PDAC lesions. My data revealed a unique population of fibroblasts present specifically in the metastatic site that I named- Liver CAFs. Further experiments revealed liver CAFs as prominent source of HGF in the liver tumor niche. Here, I report that the expression of hepatocyte growth factor (*HGF*) in fibroblasts and its receptor *MET* in cancer cells are both markedly increased in the PDAC liver niche. Using functional assays, I validated that mitogenic MET signaling is activated in PDAC cells by liver-derived fibroblasts.

BACKGROUND

Pancreatic Ductal Adenocarcinoma (PDAC) remains one of the deadliest major cancers (187). The diversity of cell populations within pancreatic tumors have been shown to provide numerous avenues supporting cancer growth and survival (5). Cancer associated fibroblasts (CAFs) often constitute the majority of overall cellularity within the dense stroma, driving an intense fibroinflammatory reaction (188). This characteristic tissue remodeling by CAFs impairs drug

and nutrient diffusion within primary PDAC tumors (45,98), but also acts to restrain metastasis (99,100,102). Accordingly, there have been extensive efforts to understand the varied, occasionally paradoxical, roles of CAFs in the pancreatic tumor microenvironment.

Early efforts to understand the stroma during pancreatic tumorigenesis predominantly identified CAFs as an expansion of a pancreatic stellate cell population based on features reminiscent of liver stellate cells, such as vitamin A droplet accumulation. However, a compendium of work has uncovered a remarkable heterogeneity among CAFs within pancreatic tumors. Recent lineage tracing of *Fabp4*$^{+}$ cells suggests that only a small, but functionally important, subset of pancreatic CAFs are derived from a stellate cell origin (79). In contrast, up to half of the PDAC CAF population can arise from *Gli1*$^{+}$ pancreas resident fibroblasts (80). Regardless of origin, pancreatic CAFs have been shown to have functional phenotypes that include myofibroblast CAFs (myCAFs) responsible for stromal remodeling, inflammatory CAFs (iCAFs) that modulate immune suppression, antigen-presenting CAFs (apCAFs) characterized by high MHC II expression, and senescent CAFs that have been shown to have pro-tumorigenic role. Pancreatic CAFs can also be separated into functionally distinct roles by CD105 expression. Moreover, CAF heterogeneity fuels spatially distinct immune hot “reactive” and matrix rich “deserted” sub-tumor microenvironments that often co-exist within individual pancreatic tumors (124).

Importantly, the volume and diversity of CAFs allow for a multitude of avenues to dynamically interact with PDAC cells in a way that actively supports tumor growth. For example; IGF1, GAS6, and LIF released from CAFs provide paracrine signals to PDAC cells that support numerous pro-tumor pathways (189). Further, CAFs can directly supply metabolites including

lipoproteins, amino acids, nucleotides, and glycosylation intermediates to support PDAC metabolism which is notoriously dysregulated by poor nutrient availability within the pancreatic tumor microenvironment. Similarly, Netrin $G1^{+}$ CAFs support PDAC progression through the modulation of glutamine metabolism while suppressing an anti-tumor immune response (190).

Many of these crosstalk pathways between pancreatic CAFs and cancer cells have been investigated as therapeutic targets to improve the poor prognosis of PDAC patients. However, only 20% of patients diagnosed with this deadly malignancy present with early stage disease where surgical resection, combined with (neo)adjuvant chemotherapy, is the preferred treatment approach (34). In contrast, 80% of PDAC patients present with metastatic disease, with the liver being the most frequently colonized secondary organ (33). In addition, the liver also represents the most frequent site of distant recurrence in patients who have undergone primary tumor resection. The liver harbors its own diverse resident fibroblast populations (191). While some of these liver-resident fibroblasts exhibit similarity to some that are found in the pancreas, such as hepatic stellate cells, CAFs that arise in the PDAC liver niche interact with different cell populations encountered in their microenvironment as compared to CAFs found in primary pancreatic tumors (192,193). Consequently, approaches developed to target stromal-cancer crosstalk that have been derived from studying pancreatic CAFs may or may not retain therapeutic benefit in metastatic disease.

To address this, we set out to contrast the phenotype of CAFs in liver tumors vs. pancreatic tumors derived from PDAC. Leveraging single cell RNA sequencing of murine tumors derived from the same cancer cells, we identify that the majority of the CAFs isolated from liver PDAC

do not correspond to transcriptomic profiles that describe CAFs present in primary PDAC. Using the receptor-ligand pairing tool CellChat, we identify a putative *HGF-MET* crosstalk axis that is exclusive to liver CAFs and PDAC cells. Isolating primary human fibroblasts, we functionally demonstrate that liver-derived fibroblasts release HGF that can activate mitogenic signaling pathways in PDAC cells. Finally, we demonstrate that both pharmacological and genetic MET targeting markedly impair the growth of liver PDAC in immune competent mice. Collectively, these data demonstrate that programming of cancer-associated fibroblasts is influenced heavily by the tissue from which they arise. This leads to potential opportunities to develop new approaches tailored to target stromal-cancer crosstalk in an organ-specific fashion.

MAIN RESULTS

Fibroblast populations in the liver are expanded in the PDAC metastatic tumor niche:

To compare the changes in the stromal compartment between the pancreas and liver in response to the presence of PDAC, I performed histology on matched tissues from the autochthonous $Kras^{+/LSL\text{-}G12D}$;$Trp53^{+/LSL\text{-}R172H}$;Pdx1-Cre (KPC) murine PDAC model vs. wildtype mice. In both the liver and the pancreas, PDAC lesions are accompanied by an expansion of the stroma within tumor region (**Fig. 3.1a**) as shown by hematoxylin and eosin staining where hematoxylin stains the nucleus (purple) and eosin stains the cytoplasm and surrounding structures such as collagen (pink). To further confirm the desmoplasia, I performed immunostaining for the pan-fibroblast marker Platelet-derived Growth Factor Receptor (PDGFR). Here, I observed that fibroblasts are readily present across the normal liver and that their numbers are markedly expanded in PDAC metastatic lesions, similar to the stromal expansion seen in primary pancreatic tumors vs. normal pancreas (**Fig. 3.1b,c**). I, next, wanted to verify is this phenotype is conserved in patient samples.

To do that, I did in situ hybridization for the human fibroblast marker Decorin (*DCN)* in human PDAC liver biopsy samples, which revealed an abundance of fibroblasts across nearby normal liver tissues that remain closely associated with the epithelial cells (**Fig. 3.1d**). Collectively, these data suggest that the abundant fibroblast populations in the liver have potential to serve many of the pro-tumorigenic roles that have been previously ascribed to pancreatic CAF populations.

Single-cell transcriptomics show liver CAFs are distinct from pancreatic CAF populations.

Previous studies have consistently found that single cell sequencing of pancreatic biopsies underrepresent fibroblast populations in samples obtained from tumor resections (194). As liver PDAC metastasis specimens are nearly always obtained via biopsy, even large collections of data such as our Human Pancreatic Cancer Single-Cell Atlas have complicated studying liver PDAC CAFs in detail. Finally, the genetic diversity across patients with very few paired primary and liver metastatic lesions limits the ability to compare stromal cells between tumor sites.

I leveraged comparative murine allograft models by either injecting syngeneic KPC FC1245 PDAC cells into the liver of C57BL/6J mice via a hemi-splenic injection method or injected the same PDAC cells orthotopically into the pancreas and harvested the tumors on day 18 and day 15, respectively (**Fig. 3.1e**). These tumors, then, underwent physical and enzymatic digestion followed by three rounds of filtration to obtain a single cell suspension. To gain insight into global programming of the pancreas vs. liver PDAC lesions we performed 10X chromium single cell RNA sequencing on the total cell population dissociated from microdissected tumors. After

aligning the data, using the Louvain algorithm, I clustered the cells from both tumor sites together in an unbiased manner which yielded 38 different clusters (**Supplemental Fig. 1a**). The major cell types were annotated using canonical markers (**Supp. Fig. 1b,c**) allowing me to identify eleven different populations of epithelial, immune, and stromal cells in these tumors. These populations were largely represented across both tumor sites (**Supplemental Fig. 1d**), however the fractional distribution of the populations captured varied (**Supplemental Fig. 1e**). However, there was sufficient transcriptional overlap that I was able to directly compare the two sites. Thus, while single cell transcriptomics are not necessarily a quantitative measure of absolute cell numbers, these trends can nonetheless inform some of the potential differences in the immune infiltration in the pancreatic vs. liver PDAC tumor microenvironment.

Importantly, we captured a sufficient population of fibroblasts between the pancreatic and liver PDAC lesions to enable further sub-clustering. Within the total fibroblast population, I identified 11 sub-populations (**Supplemental Fig. 2a**) that largely mapped to the previously described myCAF, iCAF, and apCAF transcriptional subtypes that have previously been described. However, beyond a cluster of clearly proliferating fibroblasts which was identified by the expression of proliferation and cell cycle genes, one population was clearly distinct and did not share transcriptional overlap with other reported pancreatic CAF subtypes such as senCAFs. Splitting the object by tumor site we find that this population is exclusively present in PDAC liver tumors (**Fig. 3.1f**) and hence, we named it liver CAFs. Comparing the ratio of different CAFs between the two sites, I found that these liver CAFs account for approximately half of the non-proliferating stromal object (**Fig. 3.1g**). Using transcriptional characterization of CAF sub-populations by top gene expression, we found previously established markers of CAF

populations such as *Il6* in iCAFs, *Acta2* in myCAFs, and *Msln* in apCAFs, and additionally, I was able to define putative marker genes for liver CAFs that include *Masp1, Frzb, Epha4, and Ptch1* (**Fig. 3.1h**). Of these, we observed that the specificity of *Masp1* expression in murine liver CAFs vs. pancreatic CAFs is mirrored in the CAFs found in human liver metastasis vs. primary CAF populations in the compendium of human single cell data (**Fig. 3.1i**). Lastly, I validated MASP1 using staining and saw that the expression is indeed specific to liver vs. pancreatic CAFs in murine and human PDAC (**Supplemental Fig. 2b-d**).

Collectively, these data establish that the stromal populations associated with liver PDAC lesions are distinct from those that have been extensively characterized in primary pancreatic tumors. Accordingly, I inferred that liver CAFs will also employ mechanisms to shape the microenvironment of the metastatic niche unique from those that have been identified by studying pancreatic CAFs.

PDAC cells display preferential metabolic programming in liver vs pancreas tumors

To determine how liver CAFs communicate with cancer cells, I proceeded to define the PDAC cell populations present between our syngeneic murine liver and pancreas tumors. Out of initial 20 clusters, (**Supplemental Fig. 3a**) I was able to consolidate these 20 clusters into 6 clusters on the basis of the gene overlap. I next wanted to perform pathway analyses using different pathway databases. I found 4 main populations that displayed clear themes by pathway analysis of upregulated genes in each cluster (**Fig. 3.2a**) and two minor populations with unclear functions. Further investigating top genes associated with these pathways, I found that the two largest populations separated based on different metabolic preferences: glycolysis, or redox metabolism

centered around protection from oxidative stress that I termed “Redox” (**Fig. 3.2b-d, Supplemental Fig. 3b**). The other two main populations were either centered on proliferation, or an enrichment of genes associated with extracellular interaction that I termed “ECM-related”. Given their unclear function, I termed the remaining minor populations “Epithelial 5”, and “Epithelial 6”.

Interestingly, I observed that with the exception of Epithelial 5, all the other PDAC cell populations can be observed in both pancreatic and liver allografts (**Fig. 3.2d**). However, the distribution of the PDAC subclusters between tumor sites varied dramatically (**Fig. 3.2e**). Here, I observed that the pancreatic tumors demonstrated fairly even heterogeneity, with glycolytic, redox, and ECM-related populations in approximately equal proportion among the non-proliferating cells. In contrast, the vast majority of PDAC cells in liver tumors show a gene expression program centered on redox metabolism, potentially due to higher availability of oxygen and nutrient availability in the liver vs. the hypoxic and nutrient-challenged environment of the primary pancreatic tumors (**Fig. 3.2f**).

To validate the metabolic preferences of PDAC cells residing in the liver vs. the pancreas, I compared the expression of the master redox protein NRF2 (*NFE2l2*) and canonical downstream NRF2 targets in our murine and published human datasets. Here, I observed a clear upregulation of *NFE2L2, GCLC, GCLM, and NQO1* in the liver PDAC populations compared to those isolated from pancreatic tumors (Fig. 2f). Interestingly, the preference of redox metabolism in liver resident PDAC cells is conserved regardless of basal, classical, or hybrid transcriptional subtype (**Supplemental Fig. 3c**) which was verified using the human single cell atlas publicly

available. Knocking down *Nfe2l2* using small interfering RNA (siRNA) in KPC cells and then injecting in mice significantly increased survival when compared with mice receiving the wildtype KPC cells. This data taken together with increased expression in redox genes specifically in the liver suggest that pancreatic cancer cells either reprogram their metabolism in response to the nutrient availability and organotrophic factors, or the initial establishment of tumors in these different environments selects for specific metabolic populations that that we have previously shown co-exist within PDAC.

The HGF-MET signaling axis is specifically upregulated in the liver metastatic tumors

With defined stromal and cancer epithelial clusters, I next proceeded to probe the potential interactions between these populations within the liver PDAC lesions. To accomplish this, I leveraged the ligand-receptor interaction tool CellChat (195) to build a liver PDAC signaling network (**Fig. 3.3a**) and a pancreatic PDAC signaling network (**Supplemental Fig. 4a**). My data showed key differences in the number of interactions and interaction strengths between different populations in liver vs. pancreatic tumors. I also noticed that stromal populations appear to be the dominate source of signal (**Fig. 3.3a**). Interestingly, in liver PDAC lesions, liver CAFs are the most active source of signaling to other populations (**Fig. 3.3b**). I then looked at the most significantly upregulated signaling pathways between stromal and cancer cells. Comparing these different pathways and focusing our analysis on unique signaling pathways showing significant communications and identified to be outputs from liver CAFs and input by PDAC populations, I identified that the Hepatocyte Growth Factor (HGF) pathway fits these criteria (**Fig. 3.3c**). In contrast, several other pathways that derive signals from stromal populations are conserved

between liver and pancreatic PDAC tumor networks including PTN and IL6 (**Supplemental Fig. 4b**).

HGF, as discussed in previous chapter, is produced by mesenchymal cells, including both pancreatic and liver CAF populations. HGF is the only known ligand to the tyrosine kinase receptor c-MET. Using the Seurat wrapper function plotGeneExpression, I validated that liver CAFs are by far the most abundant source of *Hgf* expression among all the populations, and the expression of the *Met* receptor is exclusive to the PDAC populations (**Fig. 3.3d**). Further visualizing the distribution of the HGF pathway across these cell populations by chord diagram, the data showed that liver CAFs are indeed the primary sender of the HGF signal to multiple epithelial clusters as depicted in the chord diagram (**Fig. 3.3e**) whereas myCAFs and iCAFs only make minor contributions. Finally, we validated that the *HGF* ligand expression is upregulated in liver PDAC CAFs vs. primary pancreatic CAFs (**Fig. 3.3f**), and the expression of the *MET* receptor is upregulated in liver PDAC cells vs. pancreatic PDAC cells in murine datasets. This trend is conserved in humans as I validated HGF and MET expression in fibroblasts and cancer cells, respectively in our human single cell atlas.

Human liver fibroblasts produce HGF to activate MET-ERK signaling in PDAC cells

To functionally examine the signaling promoted by liver vs. pancreatic fibroblast populations in human models, I established several primary fibroblast cultures from surgical resections that included a primary PDAC specimen (PDAC CAF), a liver-metastatic colorectal tumor (Liver CAF), and nearby normal liver tissue (Liver Fibroblast). I first collected RNA and performed bulk RNA-sequencing to compare these populations (**Fig. 3.4a**). Principal Component Analysis (PCA) showed distinct clustering of all three fibroblast populations (**Supplemental Fig. 5a**). The liver CAFs and liver fibroblasts cluster closer together as compared to the PDAC CAFs. Differential gene expression and analyzing the overlap of gene signatures among the three groups showed more similarity between the two liver-derived fibroblasts than PDAC CAFs (**Supplemental Fig. 5b**). Unbiased clustering based on the z-scores of the top 50 differentially expressed genes which also included MASP1, further corroborated that fibroblasts tend to cluster on the organ of origin (**Supplemental Fig. 5c**).

Using the bulk RNA sequencing data, I compared specific gene expression between these fibroblast groups. First, I looked at the expression of pan-fibroblast markers. Here, I found the expression of the fibroblast marker gene *PDGFRA* to be largely similar across both CAFs and the liver fibroblast cultures (**Fig. 3.4b**). In comparison, I observed that both the liver CAF marker *MASP1* and expression of *HGF* are markedly upregulated in both liver-derived fibroblasts and CAFs vs. PDAC CAFs (**Fig. 3.4c**). I next validated that the differences in *HGF* gene expression translated to a difference in protein production and release using an enzyme linked immunosorbent assay (ELISA) on conditioned media harvested from the fibroblast cultures. As expected, I observe dramatically higher production of HGF by both liver-derived fibroblast and

CAF populations vs. primary PDAC CAFs (**Fig. 3.4d**).

HGF is known to be the only ligand for its receptor c-MET. This binding results in autophosphorylation of this tyrosine kinase and activating multiple downstream pathways including ERK (MAPK), AKT, and STAT3. The increased production of HGF by CAFs and fibroblasts in the liver, can dramatically alter these downstream signaling networks.

To determine if the HGF released by liver-derived fibroblasts has a functional impact on human pancreatic cancer cells, I treated the human PDAC cell line- PATC53 with fibroblast conditioned media and examined MET activation (**Fig. 3.4e**). Indeed, I observed that the conditioned media from both human Liver-CAF and human adjacent normal liver fibroblasts resulted in increased MET phosphorylation vs. PDAC CAF conditioned media. Investigating potential downstream implications of MET activation in PDAC cells, I next treated PATC53 cells with human recombinant HGF and observed an increase in ERK and AKT1 activation (**Fig. 3.4f**). This activation of MET, ERK, and AKT1 by HGF can be disrupted by treatment with the pharmacological MET inhibitor cabozantinib (XL-184). Importantly, I observe MET, ERK, AKT1 and STAT3 activation in PATC53 cells when treated with liver fibroblast conditioned media. Here I also show that this activation can be reduced by treatment with cabozantinib (**Fig. 3.4g**). Interestingly, the ERK and STAT3 activation by fibroblast conditioned media is only partially disrupted by MET inhibition, suggesting that other upstream pathways are likely being stimulated in parallel.

Since cabozantinib is known to target other receptors such as VEGFR and RON due to shared homology, I wanted to eliminate the possibility of other receptors getting activated in the phenotype I observed. To further investigate the role of MET in activating mitogenic pathways

and use a different approach to target c-MET, I genetically targeted MET using CRISPR editing. Here, I observe that partial loss of MET is sufficient to promote dramatic compensatory rewiring of mitogenic pathways downstream of MET in PATC53 cells (**Fig. 3.4h**). This includes a marked upregulation of the total protein levels of ERK, AKT, and to a lesser extent, STAT3 in sg*MET* PATC53 cells. Importantly, despite the increased overall protein levels, the activation of these pathways in response to treatment with liver fibroblast conditioned media is greatly diminished in sg*MET* vs. parental control. Again, I observe some ERK activation in sg*MET* relative to AKT, further suggesting the presence of other factors such as potential fibroblast-produced EGFR ligands may also be present.

Collectively, these data show that human liver-derived fibroblast populations are uniquely equipped to activate MET signaling in PDAC cells. MET activation drives multiple mitogenic signaling pathways that play centrally important roles in PDAC. Importantly, MET activation by stromal HGF can be targeted by clinically available pharmacological inhibitors such as cabozantinib.

Figure 3.1: PDAC stromal expansion in liver shows distinct fibroblasts from primary tumors

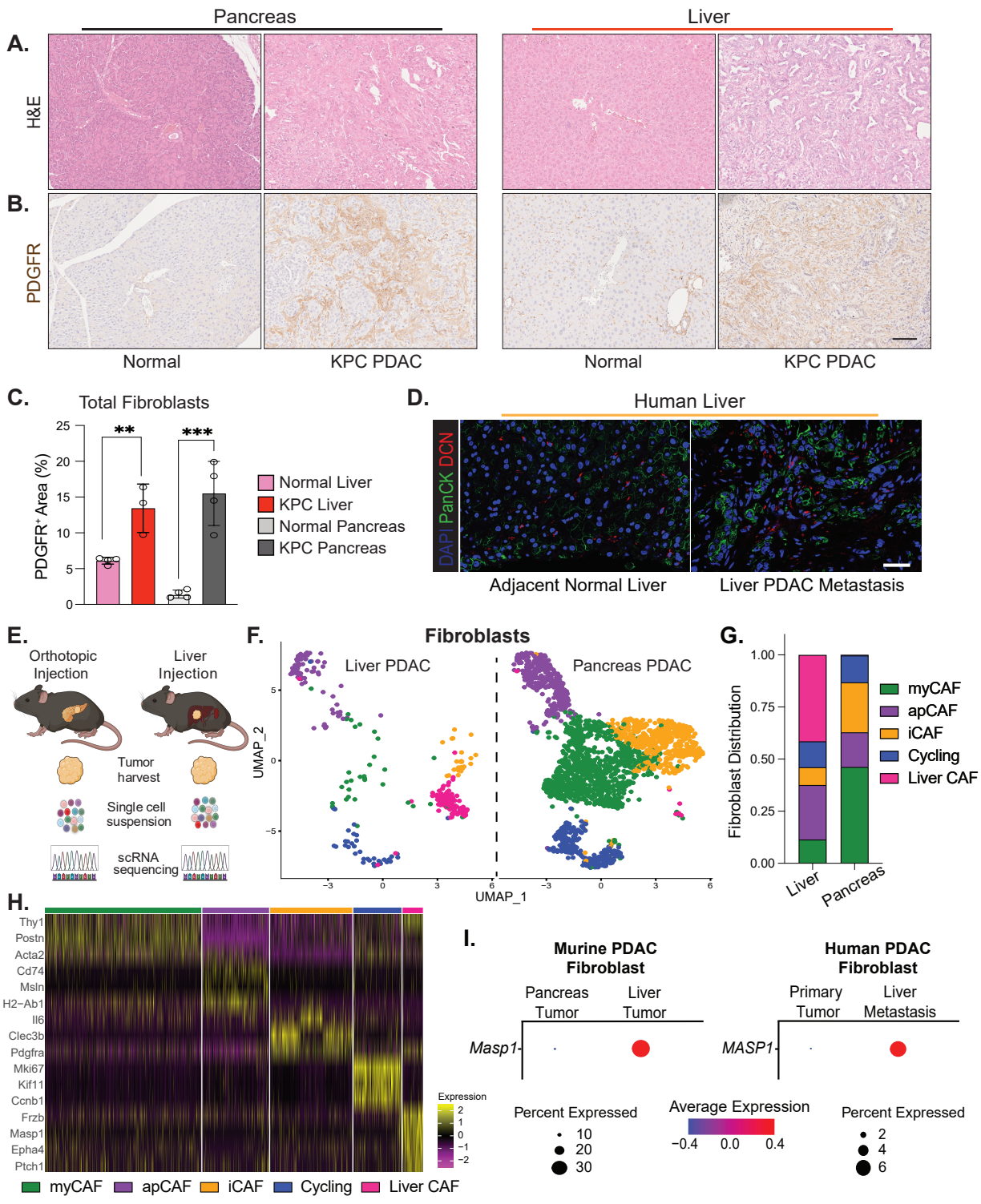

Figure 3.1:

Stromal expansion occurs in PDAC liver lesions with distinct fibroblasts from pancreatic tumors. **A.** Hematoxylin and Eosin (H&E) staining of normal tissue pancreas or liver tissues from wildtype mice compared with PDAC primary and liver metastatic tumors from KPC mice. **B.** Representative immunohistochemistry of the pan-fibroblast marker PDGFRb in tumor tissue vs. normal liver and pancreas. **C.** Quantification of $PDGFRb^{+}$ area in (**B**) (n=3 liver samples, n=4 pancreas). **D.** Fluorescent ISH staining for the fibroblast marker Decorin (DCN, red) coupled with IF for the epithelial marker Pan-Cytokeratin (PanCK, green) in primary human PDAC and liver metastasis. **E.** Schematic illustration of experimental design for single cell RNA sequencing comparing pancreas vs. liver PDAC tumors. Here, syngeneic KPC cells are injected in mice orthotopically to form tumors in the pancreas or via hemi-spleen injection to seed tumors in the liver and processed for sequencing. **F.** Uniform manifold approximation and projection (UMAP) plot showing the fibroblasts populations present in either pancreas or liver PDAC lesions. **G.** Ratio of the distribution of cells between myCAF, apCAF, iCAF, cycling, or Liver CAF sub-populations in either pancreas or liver PDAC tumors. **H.** Top 5 heatmap of genes that separate fibroblast sub-populations. **I**. Dot plot representation of the gene expression of the Liver CAF marker *MASP1* between fibroblast populations present in pancreas or liver lesions in murine or human PDAC. Scale bar = 100μM. Error bars are mean ±SD, ** $P \leq 0.01$; *** $P \leq 0.001$ by two-tail student's t test.

Figure 3.2: PDAC cells display preferential metabolic programming between tumor sites

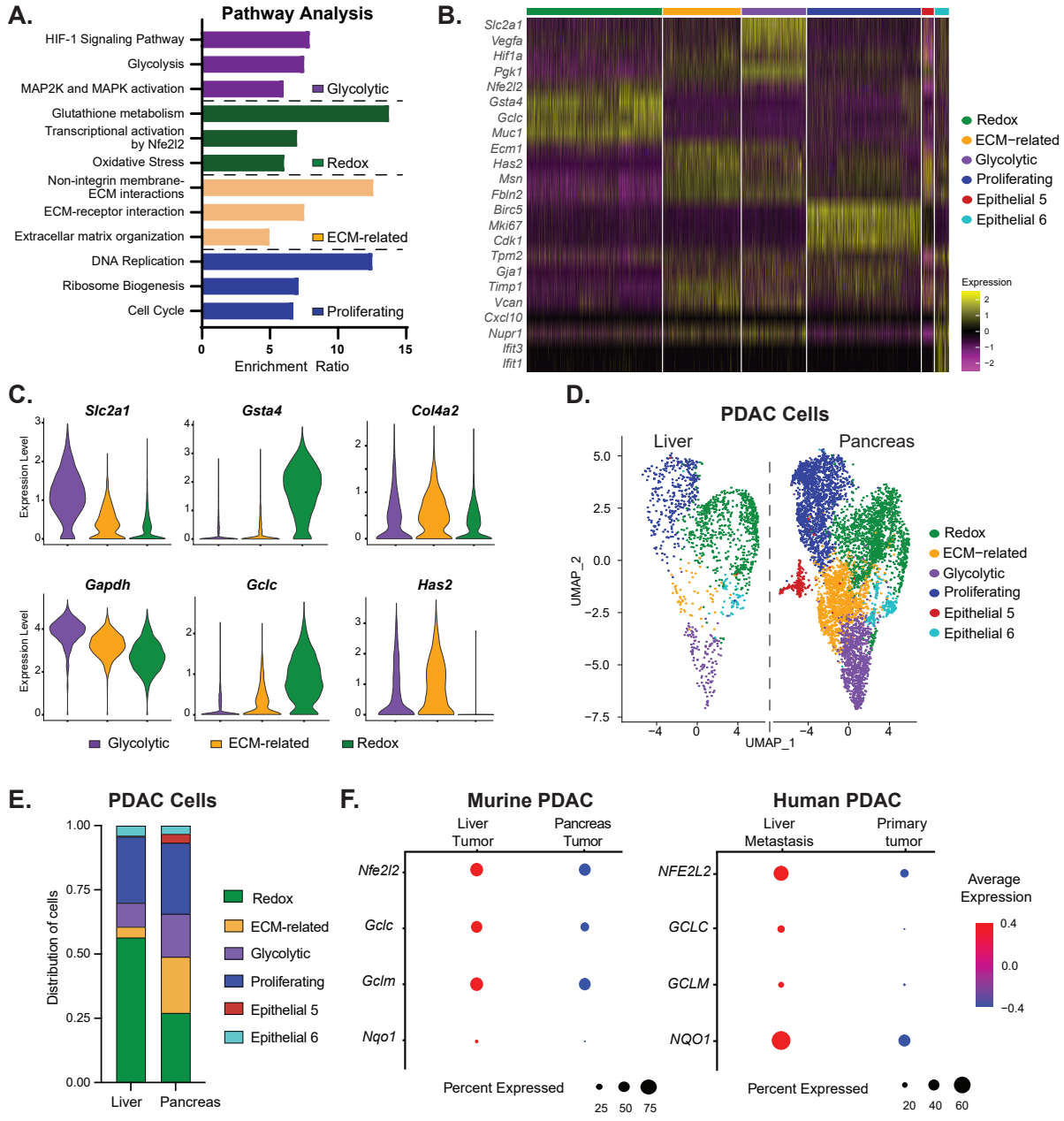

Figure 3.2:

PDAC cells display metabolic heterogeneity and differential preferences between pancreas and liver tumors. **A.** Analysis of overrepresented genes in the main PDAC clusters grouped in distinct biological pathways centered on glycolysis, redox metabolism, extracellular matrix-related genes, or proliferation. **B.** Heatmap of highly expressed genes within each PDAC subpopulation. **C.** Violin plots showing expression of representative genes that distinguish the main PDAC clusters including *Slc2a1* and *Gapdh* (Glycolysis), *Gsta4 and Gclc* (Redox), or *Col4a2* and *Has2* (ECM-related). **D.** UMAP and bar graph (**E**) representation of PDAC population distribution between pancreas and liver lesions. **F.** Dot plot representation of redox metabolism genes *NFE2L2, GCLC, GCLM*, and *NQO1* between liver and pancreas PDAC cells from human or mouse tumors.

Figure 3.3: A paracrine HGF-MET signaling axis is upregulated in liver PDAC lesions

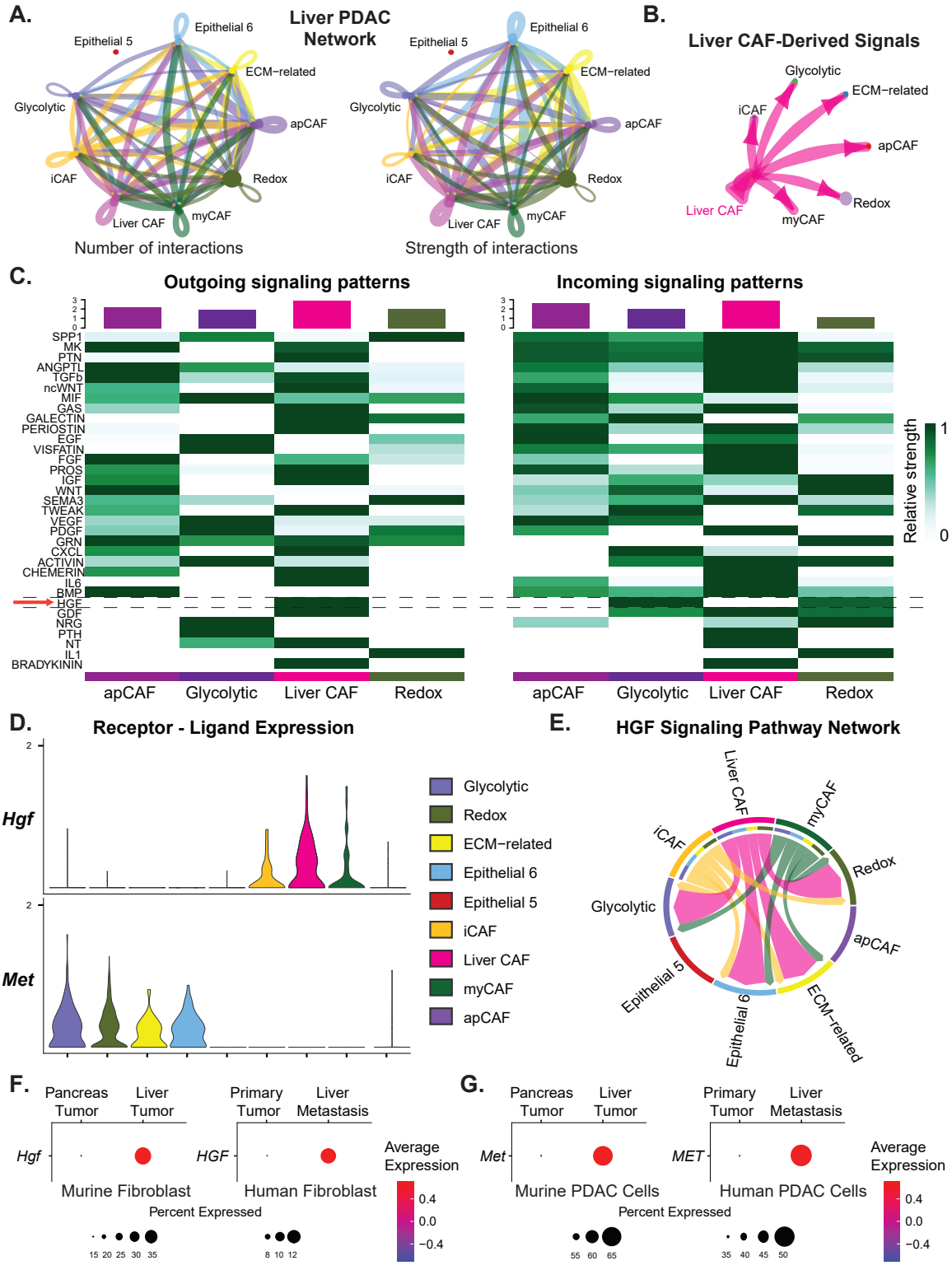

Figure 3.3:

A paracrine HGF-MET signaling axis is upregulated in liver PDAC lesions. **A.** Circle plot depiction of the CellChat aggregated cell-cell communication network showing number of ligand-receptor interactions (left) and strength these interactions (right) between each indicated two populations in murine PDAC liver lesions. **B.** Isolated signaling from Liver CAFs to stromal and cancer populations in the liver niche. **C.** Top signaling pathways with the most outgoing or incoming signaling in PDAC liver, with HGF highlighted (red arrow). Violin plots showing gene expression of the ligand HGF (**D**) and the HGF receptor MET by stromal and PDAC sub-populations. **E.** The HGF signaling pathway visualized by chord diagram showing different CAF sub-populations signaling to the cancer cells, line width is proportional to interaction strength. **F.** Dot plot representation of the *HGF* gene expression between fibroblasts isolated from pancreas or liver PDAC lesions in mouse and human tissues. **G.** Dot plot representation of the *MET* gene expression between cancer cells isolated from pancreas or liver PDAC lesions in mouse and human tissues.

Figure 3.4: Human liver fibroblasts release HGF to activate mitogenic MET signaling in PDAC

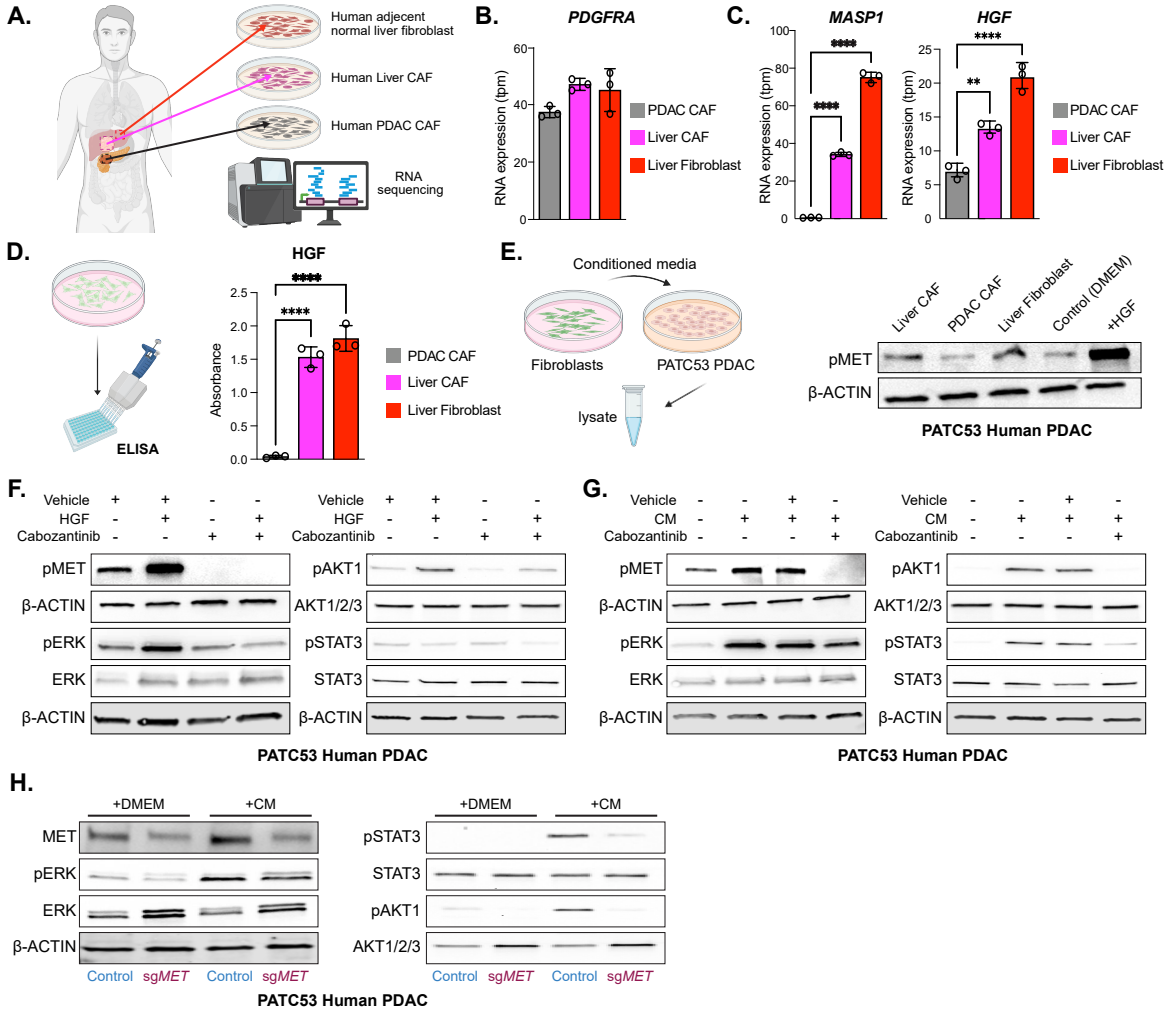

Figure 3.4:

Human liver fibroblasts release HGF to activate mitogenic MET signaling in PDAC cells. **A.** RNA was isolated and sequenced from primary fibroblast cultures that were established from a resected liver colorectal metastasis (Liver CAF), the paired nearby normal liver tissue (Liver Fibroblast), or a primary PDAC tumor specimen (PDA CAF). **B.** Quantification of the fibroblast marker gene *PDGFRA* across fibroblast populations. **C.** Quantification of Liver CAF marker *MASP1* and *HGF* gene expression across fibroblast populations. **D.** Quantification of HGF released by fibroblasts into conditioned media by ELISA. **E.** Western blot analysis of MET activation in human PDAC cell line PATC53 by a 3:1 ratio of conditioned media - fresh complete media from different fibroblast cultures as compared to HGF (1ng/mL) after 30 seconds. **F.** Western blot analysis of MET (30 seconds), STAT3, AKT, and ERK (15 minutes) in PATC53 PDAC cells treated with either HGF (1 ng/mL), the MET inhibitor cabozantinib (1μM) or combination. **G.** Western blot analysis of MET (30 seconds), STAT3, AKT and ERK (15 minutes) in PATC53 PDAC cells treated with either 3:1 liver fibroblast conditioned media:fresh media or fresh media alone or in combination with the MET inhibitor cabozantinib (1μM) or vehicle. **H.** Western blot analysis of MET, ERK, AKT, and STAT3 in sg*MET* vs. parental control PATC53 PDAC cells treated with a 3:1 ratio of liver fibroblast conditioned media:fresh media or fresh media. β-ACTIN was used as a loading control in all conditions. Error bars are mean ±SD; ** $P \leq 0.01$; *** $P \leq 0.001$; **** $P \leq 0.0001$, by one-way Anova with Tukey post hoc.

Supplementary Fig. 1: Characterization of cell populations in PDAC lesions

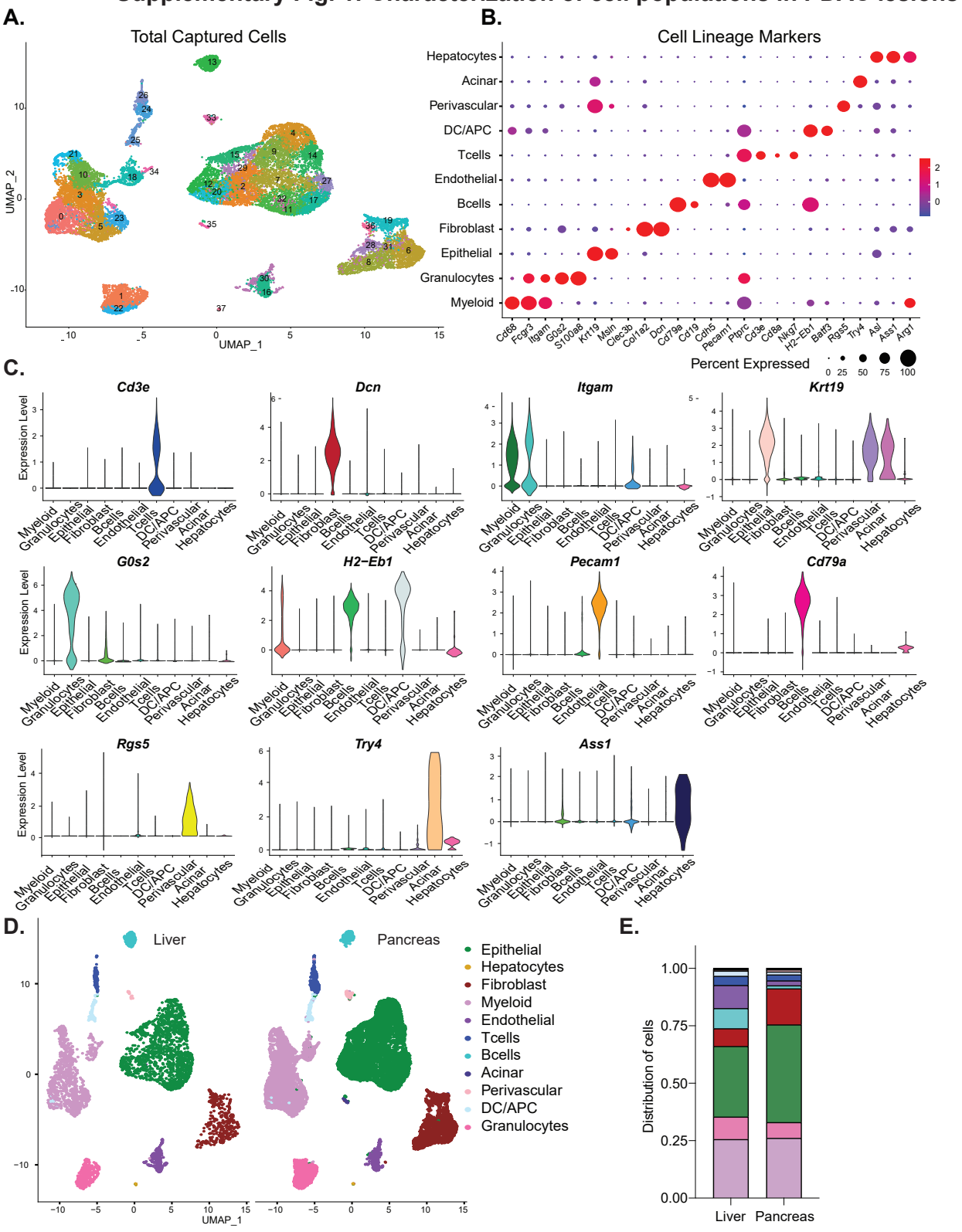

Supplemental Figure 1:

Characterization of cell populations in PDAC lesions. **A.** UMAP plot of 38 different clusters calculated by Seurat representing all cells captured from single cell RNA sequencing of murine pancreas and liver PDAC tumors. **B.** Dot plot representation of marker genes used to define clusters in (**A**). **C.** Violin plots validating key defining genes- *Cd3e, Dcn, Itgam, Krt19, G0s2*, *H2-Eb1, Pecam1, Cd79a, Rgs5, Try4,* and *Ass1* used to identify each population. **D.** UMAP split by tumor site of identified cell lineages. **E.** Fractional distribution of cell populations between liver and pancreas tumors.

Supplemental Fig. 2: MASP1 is expressed in liver, not pancreatic, fibroblasts

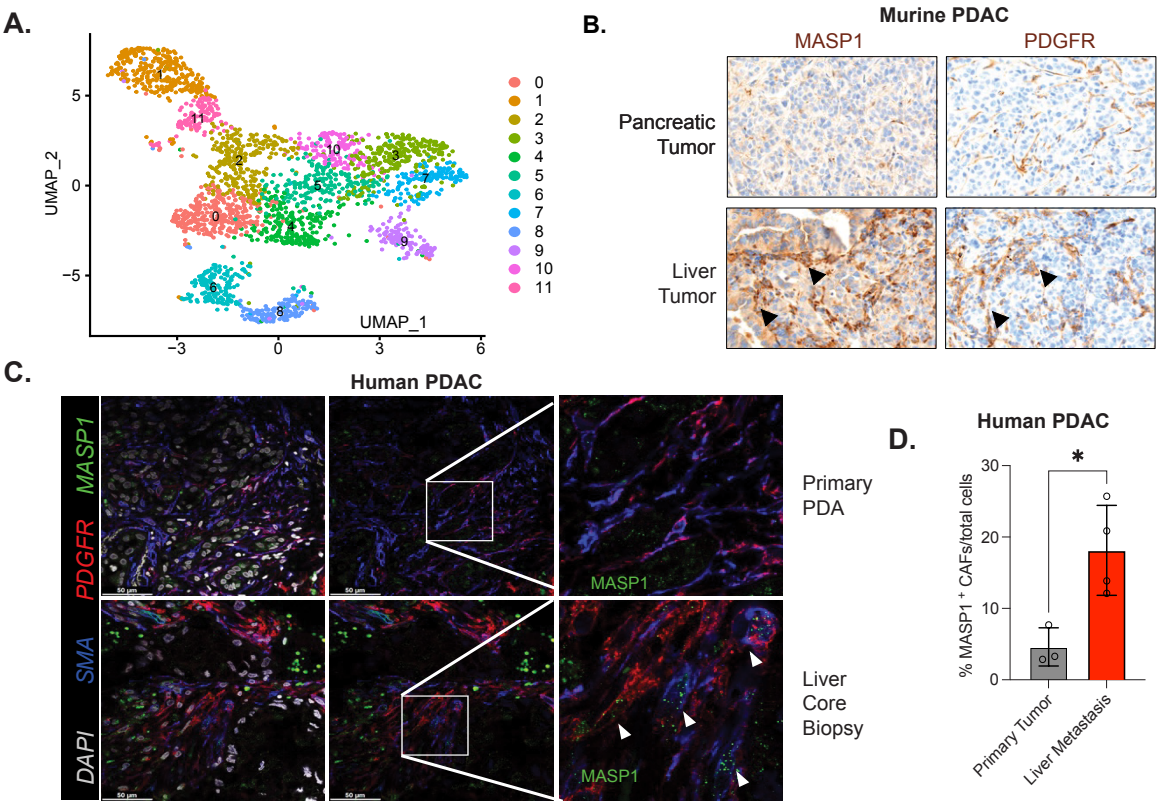

Supplemental Figure 2:

MASP1 is expressed in liver, not pancreatic, fibroblasts. **A.** UMAP plot of 12 different clusters of PDAC fibroblasts. **B.** IHC staining on serial murine PDAC liver and pancreas tumors for the pan-fibroblast marker PDGFR and liver CAF marker MASP1. **C.** Representative co-immunofluorescence staining for MASP1 (green), PDGFR (red), fibroblast marker SMA (blue), and DAPI (white) in primary human PDAC tumor and metastatic liver core biopsies. **D.** Quantification of $MASP1^{+}$ fibroblasts in primary human PDAC vs. liver metastasis, n= 4 per group, ** $P \leq 0.05$ by two-tailed student's t test.

Supplemental Fig. 3: Murine PDAC cell clustering and human correlation

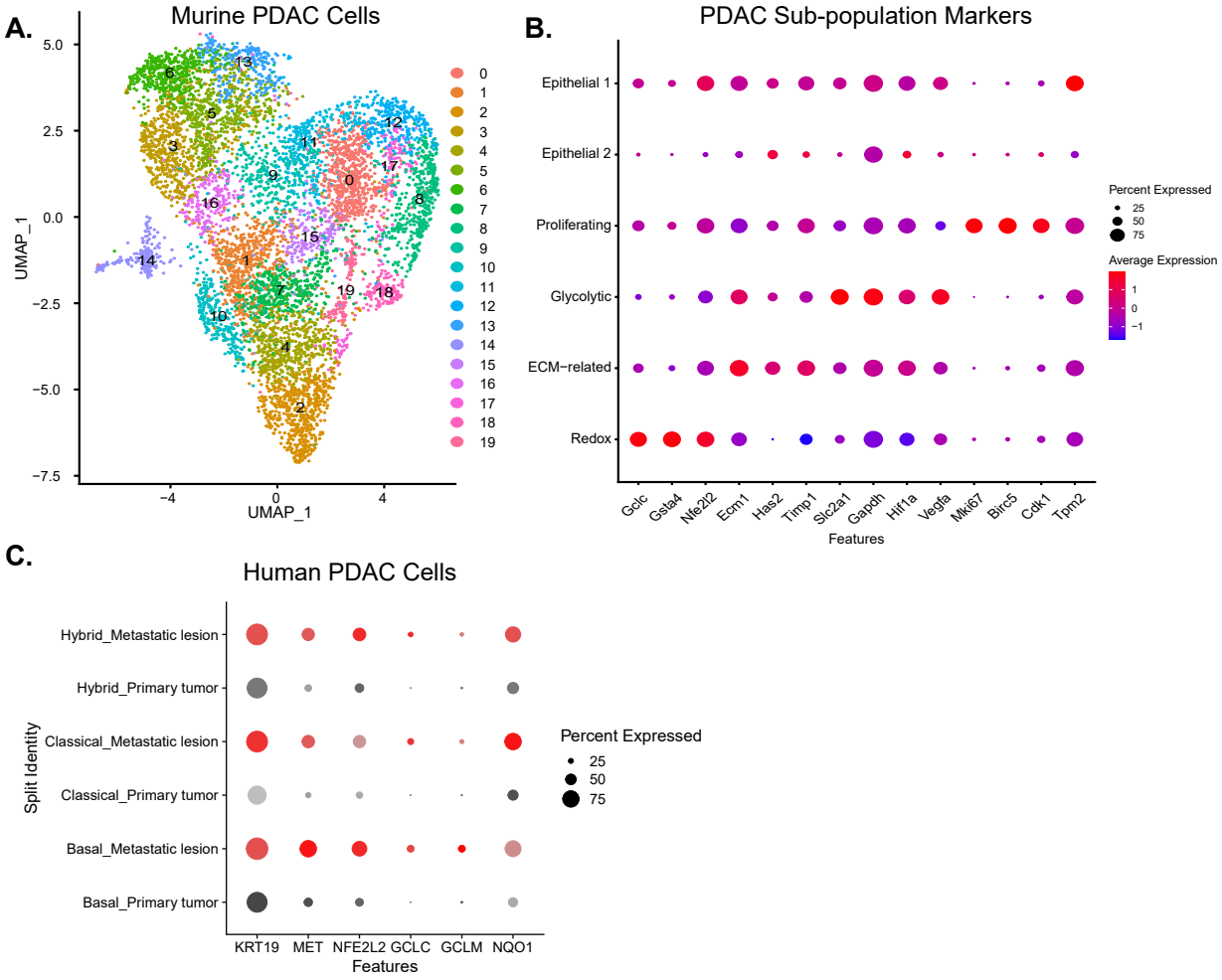

Supplemental Figure 3:

Murine PDAC cell clustering and human correlation. **A.** UMAP of the 20 clusters of the PDAC cell object. **B.** Dot plot representation of key genes that were used to collapse clusters and denote sub-populations. **C.** Dot plot representation of redox metabolism genes *NFE2L2, GCLC, GCLM*, and *NQO1* in *KRT19* expressing human PDAC cells separated into Basal, Classical, or Hybrid transcriptional subtypes.

Supplemental Fig. 4: HGF is not a feature of the pancreatic tumor signaling network

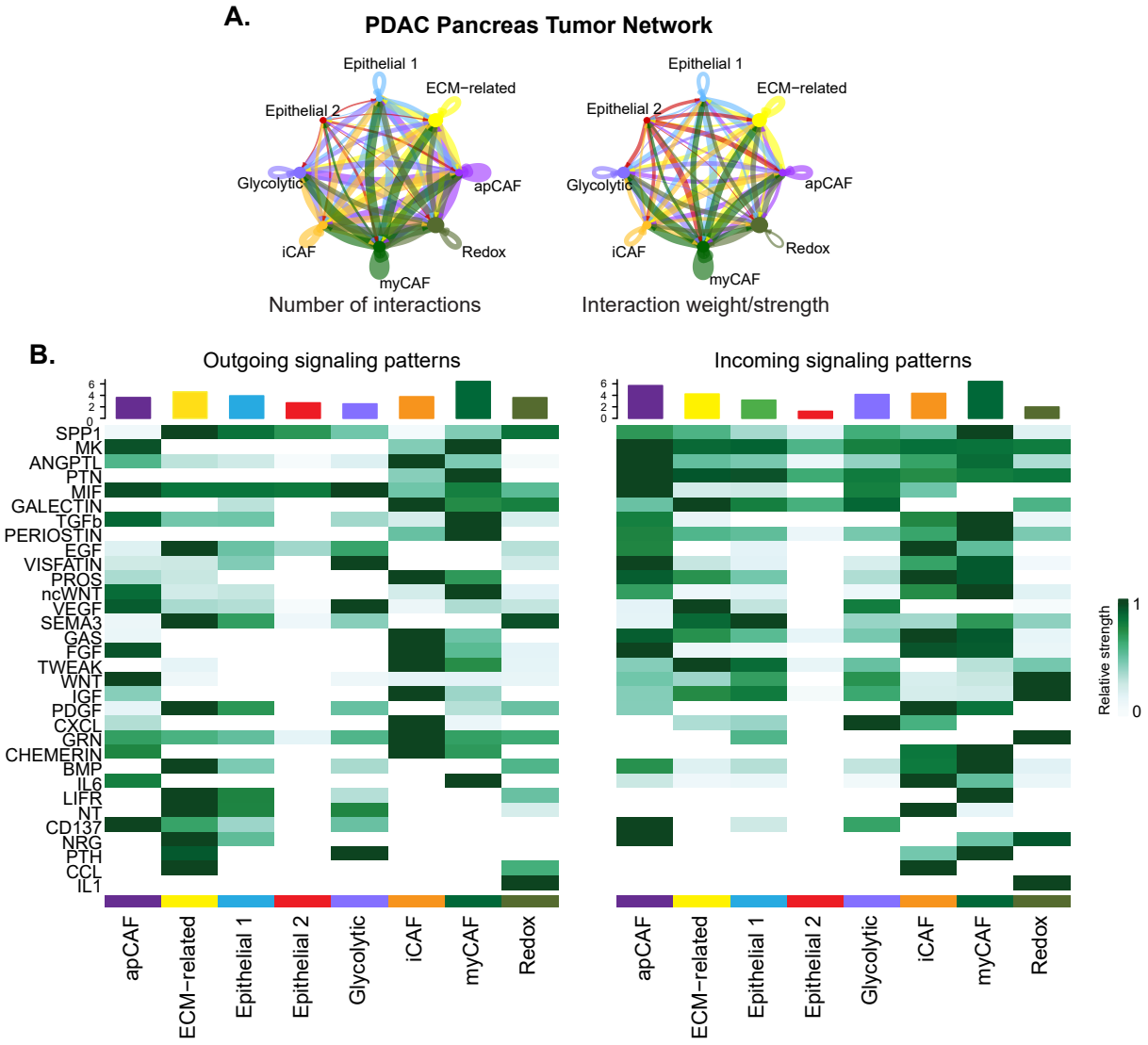

Supplemental Figure 4:

HGF is not a feature of the pancreatic tumor signaling network. **A.** Circle plot depiction of the CellChat aggregated cell-cell communication network showing number of ligand-receptor interactions (left) and strength of these interactions (right) between each indicated two populations in murine PDAC pancreatic tumors. **B.** Top signaling pathways with the most outgoing or incoming signaling in PDAC pancreatic tumors.

Supplemental Fig. 5: Fibroblast Transcriptomics and sg*MET* PDAC signaling

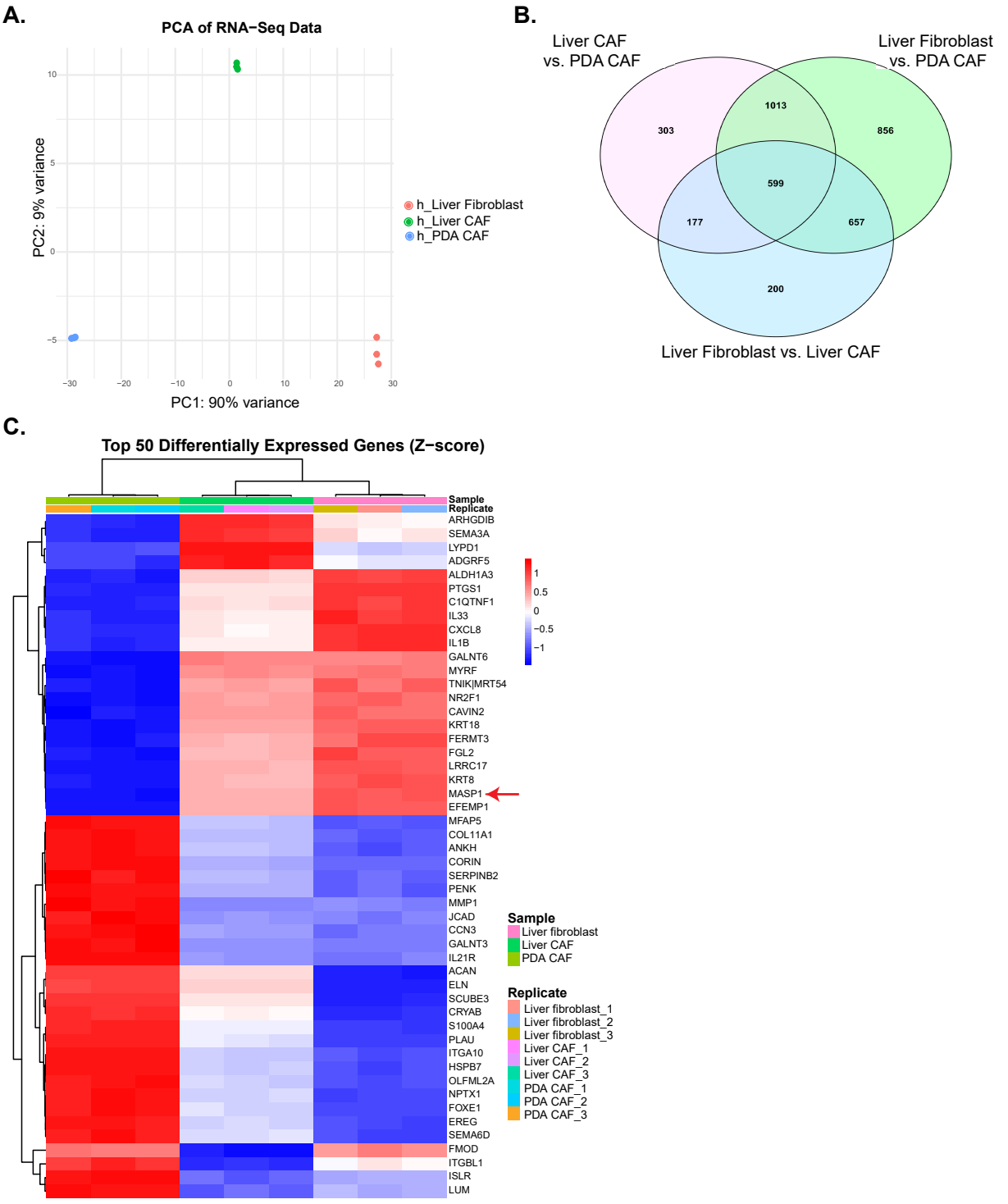

Supplemental Figure 5:

Fibroblast Transcriptomics. **A.** Principal Component Analysis (PCA) performed on RNA sequencing data of human PDAC CAFs, Liver CAFs, and Liver Fibroblasts. **B.** Venn diagram depiction of the upregulated genes identified by differential expression gene analyses between the three fibroblasts lineages. **C.** Heat-map showing top 50 differentially expressed genes across all samples and groups, highlighting *MASP1* in RED.

CHAPTER 4: TARGETING MET IN PRECLINICAL AND CLINICAL SETTING

BACKGROUND

The HGF-MET signaling axis represents a critical pathway in both development and disease. c-MET, a receptor tyrosine kinase, is activated exclusively by its cognate ligand HGF. Upon ligand binding, c-MET undergoes dimerization and autophosphorylation of its intracellular tyrosine residues, which serves as a docking platform for adaptor proteins and downstream effectors (176). These initiates multiple intracellular signaling cascades, including the RAS–MAPK, PI3K–AKT, and STAT3 pathways, collectively regulating cell proliferation, motility, invasion, and survival (179).

Physiologically, HGF/c-MET signaling is indispensable during embryogenesis, where it governs processes such as gastrulation, myoblast migration, angiogenesis, and organogenesis. In adults, this pathway remains quiescent under homeostatic conditions but becomes reactivated in response to tissue injury, playing a pivotal role in wound healing and liver regeneration. Dysregulation of this pathway, through overexpression, amplification, or aberrant activation of c-MET, has been implicated in oncogenesis across multiple malignancies, including renal cell carcinoma, thyroid cancer, hepatocellular carcinoma, and PDAC (152). Elevated c-MET expression is frequently correlated with tumor aggressiveness, therapy resistance, and poor clinical prognosis**.**

Given its central role in tumor progression, the HGF/c-MET axis has emerged as an attractive therapeutic target. Several approaches, including small-molecule tyrosine kinase inhibitors, monoclonal antibodies, and ligand antagonists**,** are under clinical investigation to attenuate aberrant c-MET signaling and improve patient outcomes.

C-MET is a proto-oncogene located on the chromosome 7q21-31 and encodes for the protein C-MET (167). HGF secreted by mesenchymal cells, mostly fibroblasts, binds to c-MET causing its intracellular domains to auto-phosphorylate. This binding leads to the recruitment of other proteins such as GRB2 and GAB1 further activating multiple crucial pathways such as ERK, STAT3, and AKT. These downstream proteins can translocate into the nucleus and initiate transcription of genes involved in cell cycle, cell progression, and cell survival.

Two approaches have been explored in targeting c-MET for therapeutic benefits- 1) small molecule inhibitors and 2) monoclonal antibody. Crizotinib and cabozantinib were the first two small molecule inhibitors that have also received FDA approval (181). Since then several other drugs have received FDA approval and are currently being used in clinic to treat various cancers such as RCC, thyroid cancer, NSCLC, and some types of gliomas.

In this project, I used the c-MET inhibitor cabozantinib (also known as XL-184 and cabometyx) to study its efficacy in liver metastatic PDAC. Cabozantinib targets 3 receptors including- MET, AXL, and VEGFR. Currently, cabozantinib is FDA approved to treat the following types of cancers: 1) metastatic pancreatic neuroendocrine tumor, 2) advanced RCC (in combination with

nivolumab), 3) HCC (if the patient has previously been treated with sorafenib), and 4) locally advanced or metastatic thyroid cancer (resistant to VEGFR targeted therapy).

There have been toxicity issues related to cabozantinib due to its higher half-life (~4.5 days in humans) and multiple receptor targeting (196). The receptor VEGFR is known to be involved in formation, proliferation, and motility of endothelial cells, and subsequently angiogenesis- the process of formation of vascular networks (197). Therefore, off-targeting of this receptor leads to leaky vasculature and fatal hemorrhages have been reported in patients under cabozantinib. Hepatic toxicity has also been reported in many cases with elevation in enzymes such as ALT and AST. Other cabozantinib related side effects include adrenal insufficiency, osteonecrosis of the jaw, dysregulated or inefficient wound healing, thyroid dysfunction, diarrhea, disruption of gut lining, hypocalcemia, loss of appetite followed by weight loss etc (198). Despite the drug toxicity, cabozantinib has shown promising results in various clinical trials and therefore, has been FDA and EMA (European Medicine Agency) approved.

My data showed increased *c-Met* expression in tumors harvested from liver PDAC vs primary tumors. This trend was conserved in human patient samples as well. To investigate the effects of c-Met inhibition in mice, I used the pharmacological inhibitor cabozantinib to inhibit Met. Mice were injected with KPC tumors in the liver and after letting the cells establish a tumor niche, I randomized the mice into two groups: 1) Vehicle and 2) Treatment with cabozantinib. Mice started receiving their designated treatments orally on day 06. This was done to allow the cancer cells to seed and establish a tumor niche. After 12 days of treatments, mice were sacrificed, and liver tissues were harvested to measure tumor size. Our data show significant reduction in tumor

weight in mice that received cabozantinib as compared to the control group. These data suggest a newer approach in treating liver metastatic PDAC.

RESULTS

MET inhibition impair growth of liver PDAC tumors in mice

My data demonstrated that HGF production by liver stromal cells has functional consequences on pancreatic cancer cells in culture; this has the potential to be even more impactful in liver PDAC tumors given their increased MET expression we have observed on PDAC cells in the liver niche. Accordingly, I examined the impact of the MET inhibitor cabozantinib on liver PDAC tumors. To accomplish this, I established syngeneic KPC-FC1245 tumors in the livers of mice C57BL/6J through hemispleen injections. After letting tumors establish for 6 days, I randomized mice onto treatment arms with either cabozantinib or vehicle (30mg/kg) via daily oral gavage (**Fig. 4.1a**). This dosage was decided based off previous published pre-clinical studies (199). I monitored the mice every day and found no significant weight loss in the animals in this 16-day study (**Fig. 4.2a**). On day 16, mice were sacrificed, and liver tissues were harvested. All liver harvested from control mice presented with clear macroscopic tumor lesions, whereas the majority of cabozantinib treated mice showed no obvious tumors (**Fig. 4.1b,c, Figure 4.2b,c**). These observations were mirrored by a markedly lower liver mass in the cabozantinib treatment group vs. vehicle control (**Fig. 4.1d**). To quantify microscopic malignant lesions, I further validated this finding by immunostaining for cytokeratin-19 (CK-19) as a marker for PDAC cells. Here, I observed that cabozantinib treated liver tissues showed either no tumors or a few small tumor masses within the liver tissue (**Fig. 4.1e,f**). In contrast, as expected the livers of vehicle treated mice were largely comprised of $CK19^{+}$ tumor cells. I, next,

performed a similar 16 day experiment to study the effects of cabozantinib on primary PDAC. To do so, I established orthotopic tumors using syngeneic KPC cells in mice and randomized the mice into 2 groups- vehicle and treatment with cabozantinib. My data showed reduced primary tumors in mice that received cabozantinib as compared to the vehicle treated mice. Interestingly, cabozantinib did not lead to complete clearance of tumors in any of the mice as we observed in our hemi-spleen tumors. Nevertheless, I report reduced tumors in the primary and metastatic site upon treatment with cabozantinib.

Reduction in tumor weight is specific to MET inhibition

As previously pointed out, most pharmacological MET inhibitors, including cabozantinib also inhibit other MET family receptor tyrosine kinases including VEGFR and RET. To demonstrate the specific impact of targeting MET on PDAC liver tumor growth, I targeted MET expression in KPC FC1245 cells with CRISPR editing. Here, I was able to obtain a robust loss of MET expression in sg*Met* clonal cell lines (**Fig. 4.2d**). I selected 4 sg*Met* clonal lines that individually grew slightly slower than the parental FC1245 control (**Fig. 4.2e**), again demonstrating an important role for MET on PDAC biology. However, this defect was less obvious in a cocktail of the 4 sg*Met* clonal lines that I combined to use for in vivo studies.

I then established syngeneic liver tumors in mice C57BL/6J mice through hemispleen injections of sg*Met* KPC-FC1245 or parental controls (**Fig. 4.1g**). These mice were sacrificed and liver tissue were harvested at Day 16. Here, we observed that the majority of sg*Met* tumors lacked gross macroscopic lesions that were observed in all the parental KPC-FC1245 tumors (**Fig. 4.1h,i, Fig. 4.2f,g**). This was further reflected in a significantly lower liver mass in the sg*Met*

compared to the control tumors (**Fig. 4.1j**). Assessing CK19 immunostaining, we observed that parental controls showed the liver tissue is largely replaced by PDAC cells, whereas the $CK19^{+}$ sg*Met* tumors were either small or not seen (**Fig. 4.1k,l**).

Collectively, these data confirm that MET signaling is a key pathway promoting the growth of liver PDAC tumors. Importantly, this pathway can be leveraged to impair tumor growth using clinically available pharmacological inhibitors such as cabozantinib.

Figure 4.1 MET inhibition impairs the growth of liver PDAC tumors

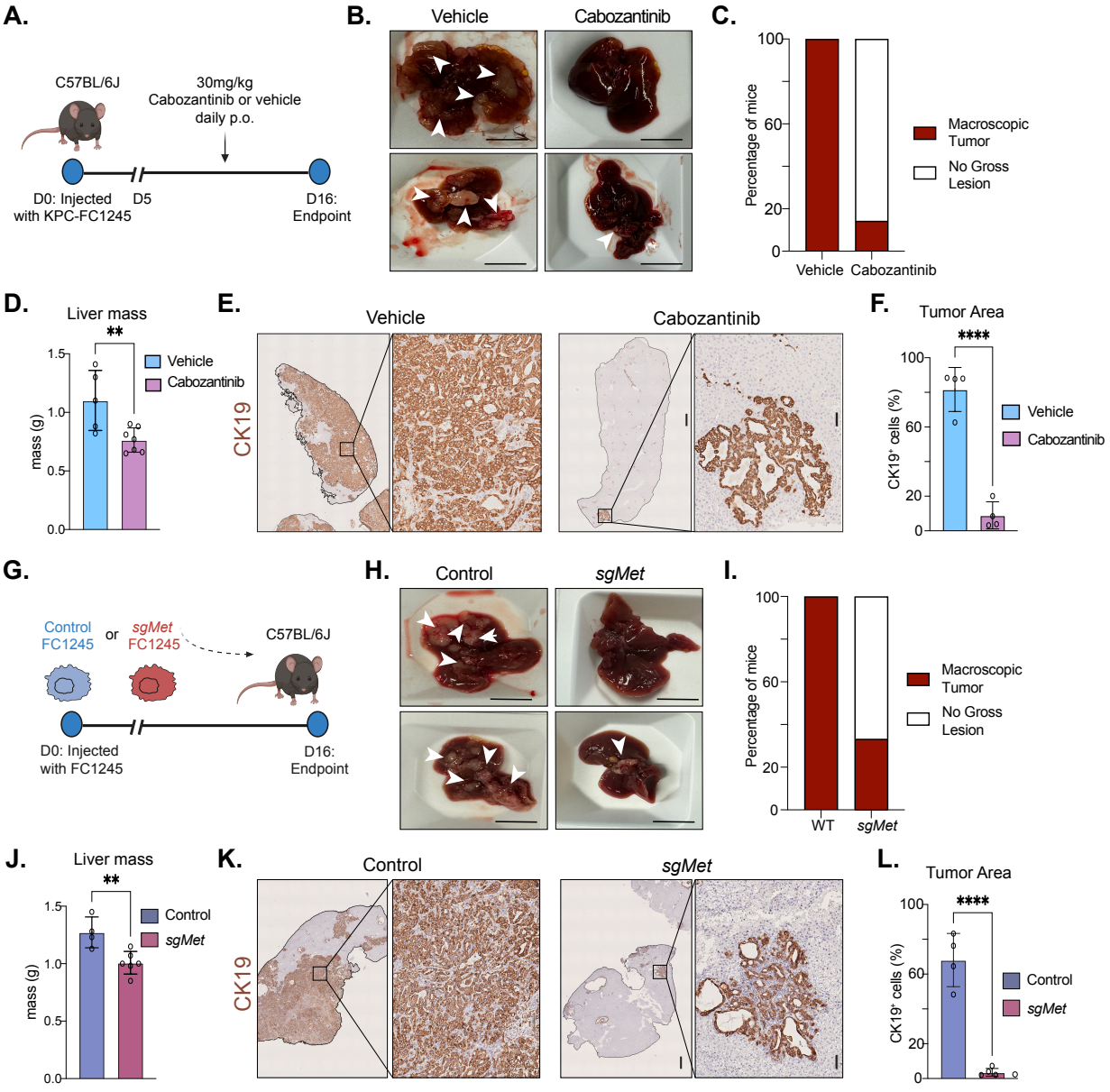

Figure 4.1:

MET inhibition impairs the growth of PDAC in the liver. **A.** Schematic of experimental design for pharmacological MET inhibition. Here, KPC-FC1245 PDAC cells were implanted into the liver via hemi-spleen injections. 6 days later mice were randomly divided onto vehicle or 30mg/kg cabozantinib treatment arms p.o. daily for 12 days. **B.** Representative images of liver at endpoint from vehicle or cabozantinib treated mice. **C.** Quantification of the number of liver tissues that in **(B)** contained observable macroscopic tumors at harvest or appeared grossly normal. **D.** Liver mass of vehicle or treated group at endpoint (n=5 vehicle, n=7 cabozantinib). **E.** Representative IHC for Cytokeratin-19 (CK19) from liver tissue sections treated with vehicle or cabozantinib. **F.** Quantification of percent $CK19^+$ cells per section, n= 4 per group. **G.** Schematic of experimental design for genetic *Met* targeting. Here, control or sg*Met* KPC-FC1245 PDAC cells were implanted into the liver via hemi-spleen injections and mice were sacrificed 16 days later. **H.** Representative images at endpoint of livers implanted with control or sg*Met* KPC cells. **I.** Quantification of the number of liver tissues that contained observable macroscopic tumors at harvest or appeared grossly normal. **J.** Mass of control or sg*MET* implanted livers at harvest (n=4 control, n=6 sg*Met*). **K.** Representative CK-19 IHC staining of control or sg*Met* FC1245 implanted liver tissues. **L.** Quantification percent $CK19^+$ cells per section (n=4 control, n=5 sg*Met*). Scale bars are 1cM for gross tissues, 500μM for low magnification IHC, 50μM for high IHC magnification. Error bars are mean ±SD; ** $P \leq 0.01$; *** $P \leq 0.001$; **** $P \leq 0.0001$ by two-tail student's t test.

Fig. 4.2: In vivo data supplements and sgMet validation

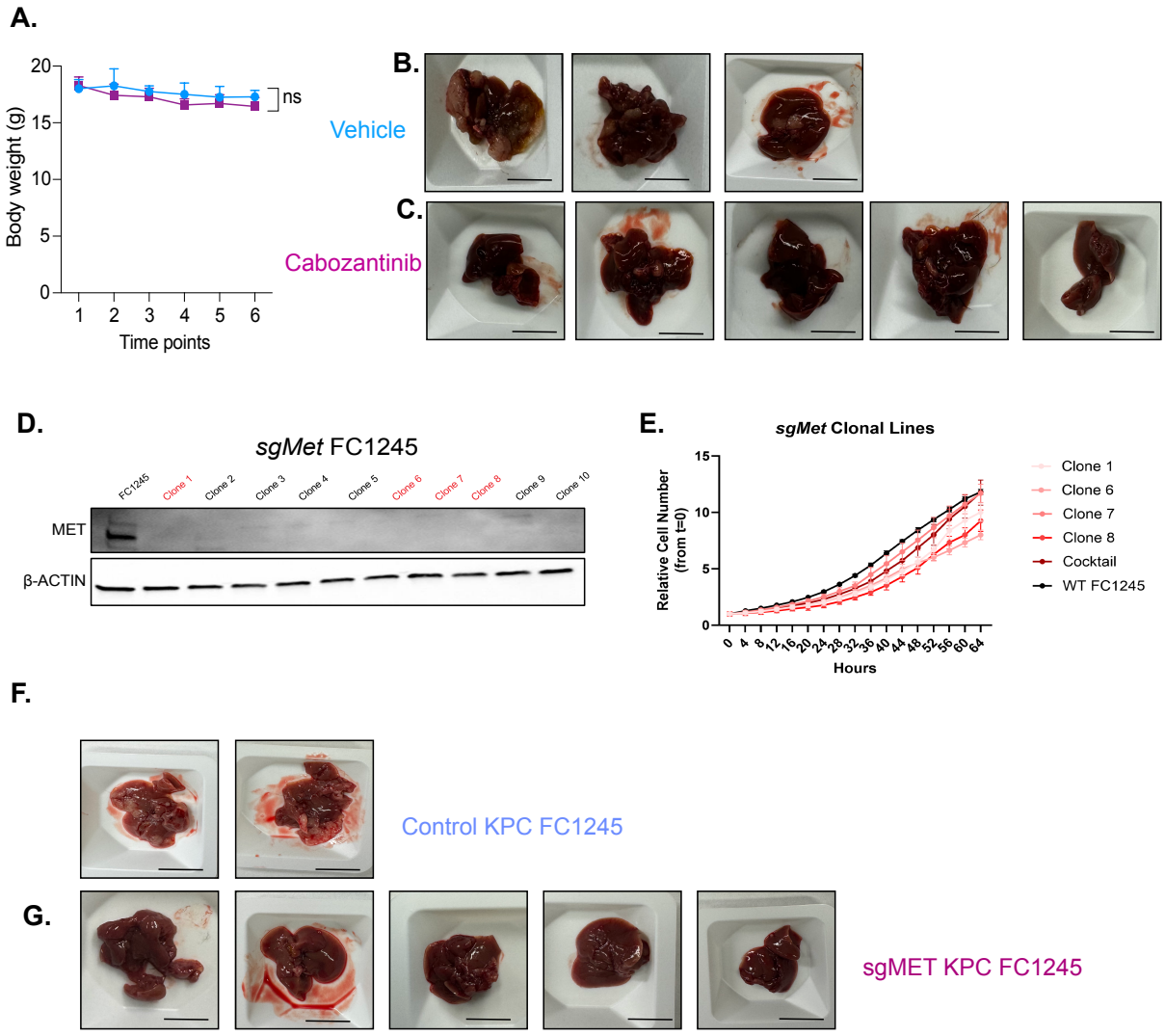

Figure 4.2: ***In vivo data supplements and murine*** **sg*Met validation*. A.** Body weight of vehicle and cabozantinib treated mice throughout the experiment outline in **Figure 4.1a**. **B.** Gross liver images of remaining vehicle and **(C)** cabozantinib treated mice harvested at the endpoint of the experiment. **D** Western blot showing extent of MET loss sg*Met* KPC FC1245 cells in 10 different clonal populations vs. parental control, later pooled clones highlighted in red. β-ACTIN was used as the loading control. **E.** Growth curves of 4 selected sg*Met* FC1245 clones, the 4 clones pooled together (cocktail), and parental FC1245 cell line as relative cell number (from t=o) over 64 hours analyzed by Cytation5 imaging. **F.** Gross liver images of mice injected with control FC1245 or **(I)** sg*MET* FC1245 taken at the endpoint.

Cabozantinib related drug toxicity

My 16-day study showed reduced tumors with no overall impact on mice after treatment with cabozantinib. I then performed a survival study after injected mice with KPC cells via hemi-spleen injections. The mice maintained their weight until D18-D20. However, the mice in the treatment group started dropping weight rapidly. Upon performing necropsy on these mice, the livers in these mice were free of tumors but had compromised tissue structure. This is in alignment with hepatic impairment and hepatic toxicity that is often reported in patients treated with cabozantinib. My data show a significant increase in survival in mice treated with cabozantinib vs vehicle. However, drug efficacy and toxicity when used for longer duration remain questionable.

Current undergoing clinical trials on cabozantinib

The sensitivity of PDAC cells to MET inhibition has been reported in the context of primary pancreatic tumors. I used clinically available MET inhibitor cabozantinib to demonstrate the therapeutic potential in liver metastatic pancreatic cancer. This drug is currently approved to treat patients with renal cell carcinoma, thyroid cancer, and hepatocellular carcinoma where it has demonstrated clinical efficacy. Cabozantinib was also recently approved for the treatment of pancreatic neuroendocrine tumors after phase 3 trial showed 13.8 month of progression free survival compared to 4.4 months in the placebo group (200). Cabozantinib was explored in combination with gemcitabine in a small cohort of PDAC patients and showed some response that would warrant further investigation. However, dose limiting toxicities were an issue in this phase 1 trial and a maximum tolerated dose could not be obtained (201). A similar observation

was made on this project where survival study needed to be halted due to tolerability issues in mice. To overcome this, alternative approaches need to be tested in PDAC. For example, combining cabozantinib with immunotherapy or other targeted agents may offer a less toxic therapeutic strategy. This approach is currently under evaluation in clinical trials in PDAC, including cabozantinib + atezolizumab (NCT04820179), cabozantinib + pembrolizumab (NCT05052723), and cabozantinib + erlotinib (NCT03213626). Accordingly, while there is potential for MET inhibitors to be used in PDAC, the right contexts will need to be found and tested in further trials.

KRAS inhibitors have been an active area of investigation in multiple cancer types including NSCLC and PDAC (202). Multiple KRAS inhibitors targeting common mutations such as G12C and G12D are currently in clinical trials. MRTX1133 which targets the PDAC specific G12D mutation in the gene KRAS showed promising results in pre-clinical setting and is currently in the first phase of clinical trial (203). Other KRAS inhibitors such as sotorasib and adagrasib are currently FDA approved for solid tumors with mutation in G12C (usually found in KRAS mutated NSCLC) (204). Preclinical results suggest that resistance to KRAS inhibitors in NSCLC is driven by amplification or overexpression in c-MET (205). Therefore, this opens an opportunity to study the effects of combinatorial treatment to overcome KRAS inhibition resistance. It is believed that KRAS inhibitors will be the future of PDAC treatments. The emerging role of c-MET in KRAS mutated cancer has sparked an interest among clinicians in combining RAS inhibitors with MET inhibitors.

Given my observations, we expect that cabozantinib could be an ideal application as a first line

single agent or in combination regimens with other targeted agents as chemotherapy is unlikely to have a durable response in PDAC liver metastasis. Further, given the frequency of recurrence in the liver, after curative intended tumor resection, a sequential treatment strategy such as adjuvant treatment cabozantinib following standard of care chemotherapy may be effective to eliminate disseminated cells before they can establish a liver tumor niche.

CHAPTER 5: ADDITIONAL FINDINGS AND FUTURE DIRECTIONS

BACKGROUND

The TME of PDAC is highly complex and composed of dynamic interactions among malignant epithelial cells, stromal populations, and infiltrating immune cells. Although CAFs and ECM components constitute the majority of the PDAC stroma, immune cells form a crucial and functionally diverse compartment that profoundly shapes tumor biology (105).

Oncogenic KRAS, a hallmark driver mutation in PDAC, orchestrates immune evasion by inducing secretion of cytokines and growth factors such as GM-CSF, which in turn recruits MDSCs and TAMs to the TME (107,108). Similarly, subsets of CAFs, including apCAFs, have been shown to modulate adaptive immunity by promoting the conversion of naïve $CD4^+$ T cells into Tregs, thereby contributing to a profoundly immunosuppressive niche (81).

Myeloid cells, particularly macrophages, represent the most abundant immune population within PDAC tumors. Tumor-secreted cytokines and chemokines polarize macrophages toward an M2-like phenotype, characterized by pro-tumorigenic functions such as immune suppression, angiogenesis, and metabolic support for cancer cells. Both tissue-resident macrophages and monocyte-derived macrophages have been identified as sources of TAMs in PDAC. Importantly, macrophages not only suppress cytotoxic T cell activity but also provide essential nutrients that sustain tumor cell metabolism, further reinforcing malignant progression.

Therapeutic strategies targeting the myeloid compartment have shown promise in preclinical models. For instance, blockade of CD11b, a key integrin expressed on myeloid cells, has been demonstrated to deplete immunosuppressive myeloid populations and sensitize tumors to immune checkpoint blockade (116,117). Based on these encouraging findings, CD11b inhibition is currently being evaluated in clinical trials. Another immunomodulatory approach involves CD40 agonists, which activate dendritic cells (DCs) and enhance priming of $CD8^+$ T cells, thereby promoting antitumor immunity (206,207). While early-phase trials with CD40 agonists have yielded only modest clinical responses and were limited by toxicity, they nonetheless highlight the potential of targeting dendritic cell biology in PDAC.

Collectively, these findings underscore the pivotal role of immune cell programming in PDAC progression. The interplay between malignant, stromal, and immune populations establishes a highly immunosuppressive TME that remains a significant barrier to effective therapy. A deeper mechanistic understanding of immune regulation in PDAC is essential to guide the development of combinatorial therapeutic strategies aimed at overcoming immunosuppression and improving patient outcomes.

There has been extensive research on the TME of primary PDAC. It is known that myeloid cells are the primary source of immune suppression and chemotherapy resistance. Accordingly, efforts have been made to target myeloid cells to sensitize PDAC cells to chemotherapy and immunotherapy. However, it is not known if a similar myeloid cell dependent immune suppression mechanism take place in a metastatic organ such as the liver. To determine the mechanism of immune suppression in metastatic PDAC, I further analyzed the single cell

sequencing data between primary PDAC and liver PDAC. I re-scaled and re-clustered the myeloid and T cell clusters. After carefully filtration of CD45+ cells, I further classified and defined different sub-types of T cells and myeloid cells. My data show that, similar to the CAFs, there are key differences in the immune populations that get established in the primary vs metastatic niche in PDAC. This further stresses the importance of designing and having treatments specific to the organ of metastases rather than the niche found in primary tumor.

MAIN RESULTS

Distinct myeloid cell populations in the liver vs primary PDAC

Myeloid cells were the most abundant immune cell type present in our single cell sequencing data. This is an accurate reflection of human PDAC tumor microenvironment. To further classify and characterize these myeloid cells, I re-normalized and re-scaled the myeloid cluster. Using differential expression gene signature, I labeled the distinct myeloid clusters (**Fig. 5.1**). The data showed various sub-clusters of macrophages including MHCII high and Arg high macrophages **(Fig. 5.1a)**. I was able to identify a cluster of dendritic cells in my dataset. I also found a population of undifferentiated monocytes in the liver which usually represent as MDSCs in the primary PDAC. In addition, I was able to cluster of Kupffer cells in the liver. Kupffer cells are resident macrophage population in the liver and are also known to be the largest tissue resident population in human body. This population of innate immune cells is usually the host's first line of defense against pathogens entering the liver either through portal vein or arterial circulation (208). In addition, Kupffer cells can also provide protection to the hepatic tissue in times of drug induced liver toxicity or fibrosis. However, it has been shown that Kupffer cells can contribute to chronic inflammation as a stress response in conditions such as alcoholic or non-alcoholic fatty

disease (NAFD) and non-alcoholic steatohepatitis (NASH) (209). It has also been shown that these Kupffer cells, along with circulating monocytes, can give rise to TAMs in episodes of malignancy such as hepatocellular carcinoma (HCC) (210). My data show reduction in MHCII high macrophages in the liver as compared to the pancreas. However, this is compensated by the abundance of Kupffer cells in the liver **(Fig. 5.1b)**. I also noted higher proportion of undifferentiated monocytes in the liver as compared to primary PDAC. This suggests enrichment of alternative subsets of myeloid cells in the metastatic site vs primary PDAC and therefore, possibly alternative cell crosstalk between these populations. The functional role of these myeloid cells in the liver and their relationship with PDAC cells remain an active area of investigation.

Increased number of T cells in the liver as compared to primary PDAC

After classifying myeloid cells, I performed a similar analysis on T cells. Using commonly used gene signatures, I was able to cluster and label naïve, CD8, NK, Tregs, and double negative T cells. Similar to other cancer cells and fibroblasts, there was a cluster with active cell cycle genes that I labeled cycling T cells. My data also suggest higher expression of certain genes defining cytotoxicity such as *Cd8*, *Ifng* (Interferon gamma), and *Gzmb* (Granzyme B) upon comparing the gene expression. Conversely, I also noted higher expression of stem-like progenitor exhausted (Tpex) genes such as *Slamf6* and *Tcf7* in the liver T cells vs primary pancreas. Tpex are known to be a memory like T cells with self-renewal ability and long life. Tpex are usually the result of chronic stimulation of the T cell receptor (TCR) and therefore, can give rise to terminally exhausted T cells (211). It has also been shown that presence of Tpex cells can be indicative to a positive response to check point blockade therapy in certain tumors (212,213). Some of these

results were verified at protein level by performing cytometry by time of flight (CyTOF). CyTOF is a mass cytometry technique which stains antigen on cells using metal conjugation instead of fluorophores as done in the traditional flow cytometry. This technology allows panels with multiple markers without having to worry about spectral overlap and compensation issues. I used a 29-marker panel to compare immune differences between primary PDAC and liver PDAC tumors. Preliminary results from this experiment confirm some of the phenotype observed in our single cell dataset. For example, I see a higher number of B cells and CD8 T cells in liver tumors vs primary pancreas tumor. Additionally, there is also an increased percentage of activated CD8 T cells as noted by the expression of CD44 in liver tumors vs pancreas. However, this experiment requires heavy optimization in panel designing and sample preparation. Nevertheless, this is exciting data and opens additional avenues for further research and experimentation.

Figure 5.1 Myeloid populations in primary vs metastatic PDAC

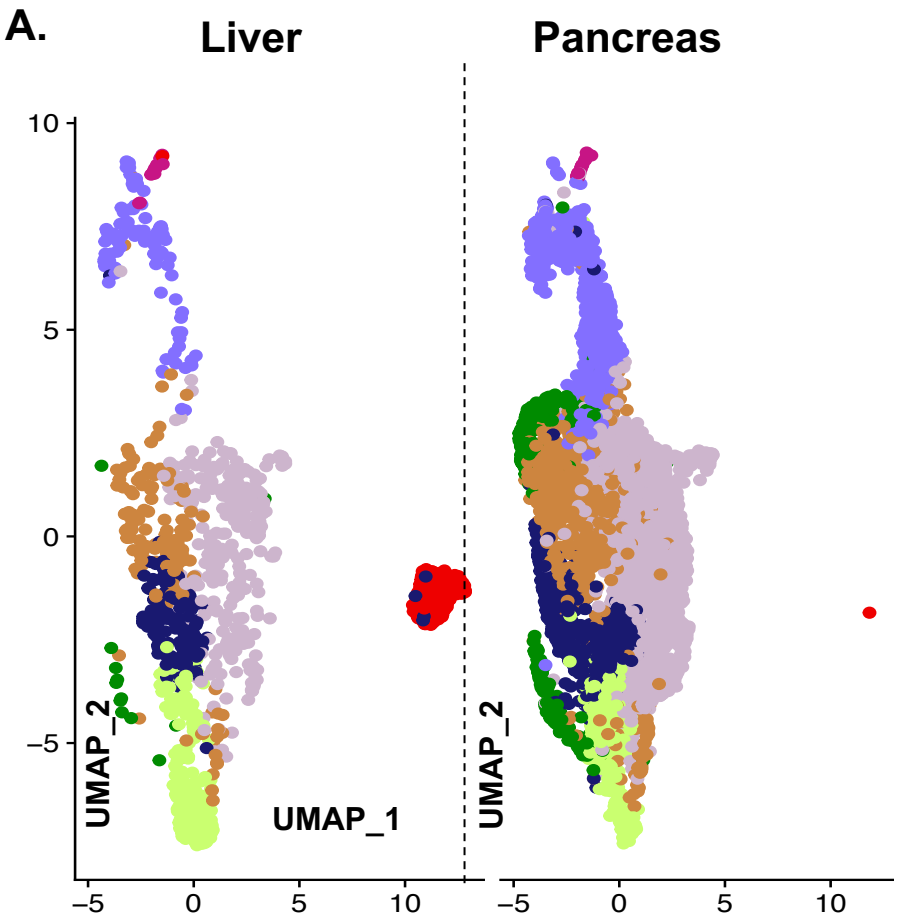

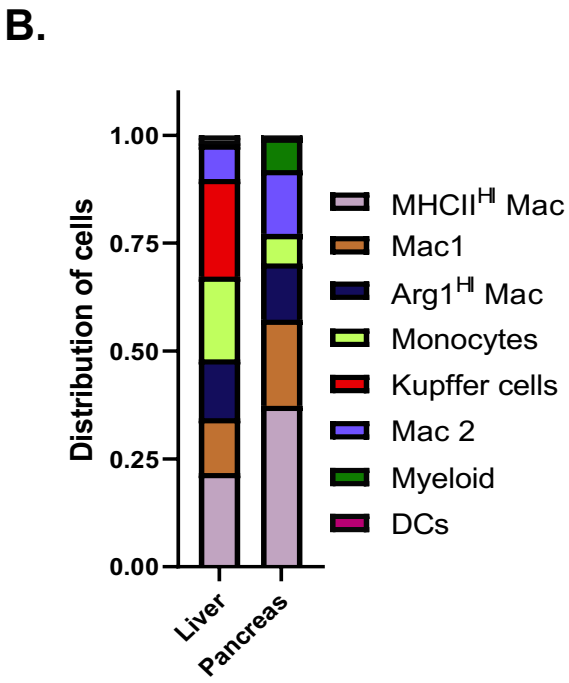

Figure 5.1 Myeloid clusters in primary vs metastatic tumors. **A.** UMAP displaying distinct myeloid clusters including monocytes, macrophages, dendritic cells, and Kupffer cells**. B.** Fractional distribution of the different myeloid sub-populations between primary PDAC and liver PDAC.

A.

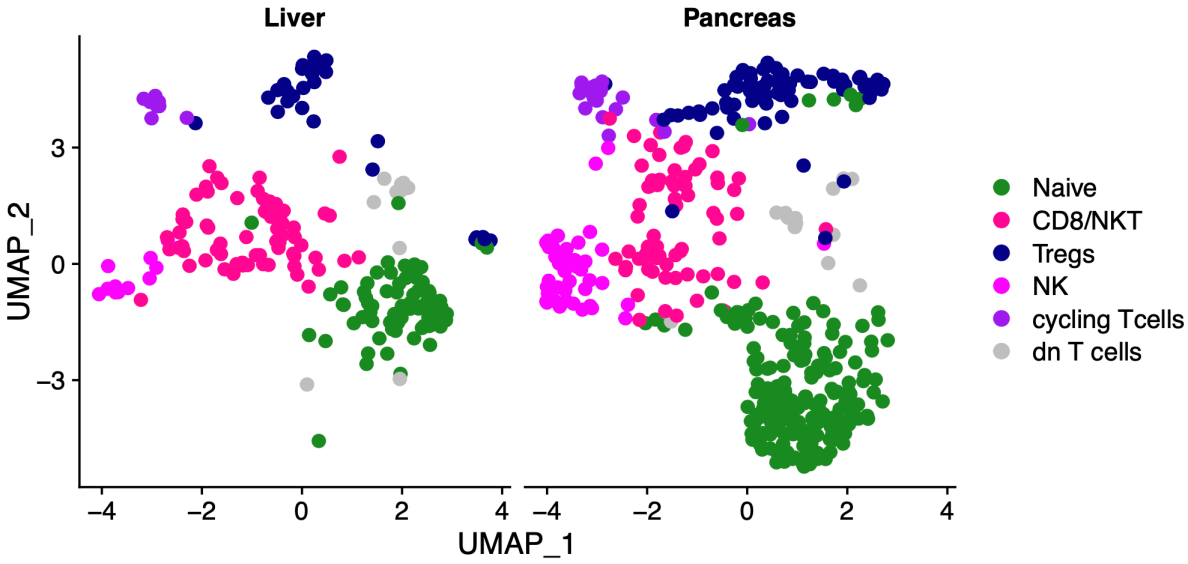
Liver
Pancreas
UMAP_2
UMAP_1
Naive
CD8/NKT
Tregs
NK
cycling Tcells
dn T cells

B.

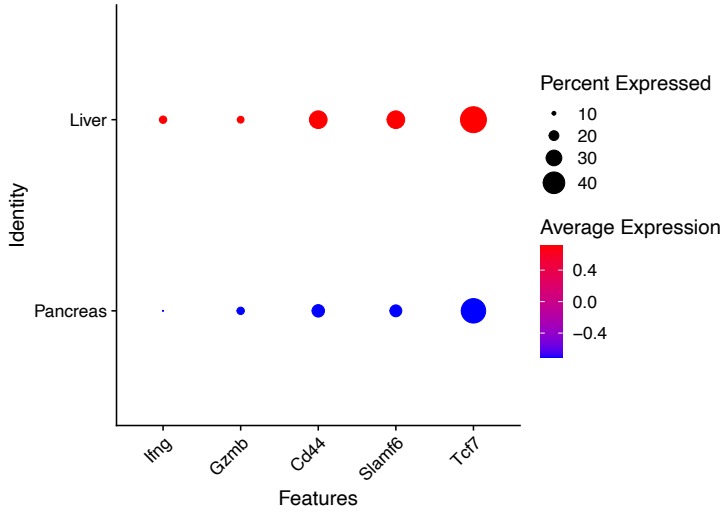
Liver
Pancreas
Identity
Ifng
Gzmb
Cd44
Slamf6
Tcf7
Features
Percent Expressed
10
20
30
40
Average Expression
0.4
0.0
−0.4

C.

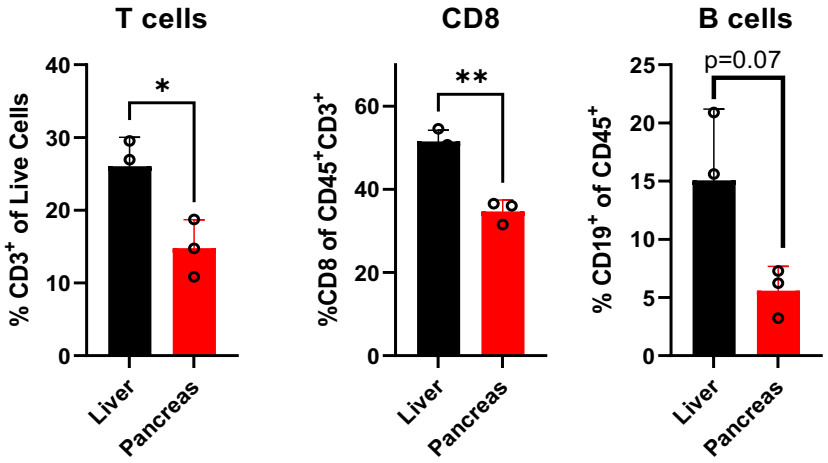
T cells
CD8
B cells
% CD3+ of Live Cells
%CD8 of CD45+CD3+
% CD19+ of CD45+
p=0.07
Liver
Pancreas

***Figure 5.2 T cell variability in primary vs metastatic PDAC*. A.** UMAP displaying different sub-clusters of T cells including CD8, Tregs, cycling T cells, NK, naïve, and double negative T cells. **B.** Increased expression of activation (*Ifng, Gzmb,* and *Cd44*) and exhaustion (*Slamf6* and *Tcf7*) in liver vs pancreas. **C.** CyTOF quantification and comparison of CD3+ T cells, CD8+T cells, and B cells between primary PDAC and liver lesions.

DISCUSSION AND FUTURE DIRECTIONS

Desmoplasia has long been recognized as a characteristic feature of PDAC (214). Accordingly, pancreatic fibroblasts have been extensively studied to understand how they remodel the pancreas to support carcinogenesis and PDAC progression. These insights have led to better understanding of how CAFs coordinate with malignant epithelial and immune cells to create an environment permissive to PDAC growth. Among the first characterized stromal-PDAC crosstalk pathways was the activation of hedgehog signaling in CAFs by ligands released from malignant epithelial cells that promote stromal expansion and fibrosis (97). While disruption of this signaling axis has thus far proven disappointing in the clinical setting potentially either due to loss of a tumor restraining populations, or enrichment of more immune suppressive fibroblasts, this illustrates the central impact that CAFs mediate in PDAC biology.

The stromal populations in PDAC liver tumors have also been suggested to have tumor-promoting and restraining functions (79). In this study, I sought to directly compare how different immune and stromal populations that arise in response to the same PDAC cells program liver lesions vs. pancreatic tumors. Here, I verified that the expansion of stroma associated with tumorigenesis in the pancreas is also observed in regions of the tumor-bearing liver. Using single cell RNA sequencing we observed that the vast majority of liver CAFs show transcriptional profiles distinct from those that map onto fibroblasts that occur in primary pancreatic tumors. Thus, although pancreatic fibroblasts have often been compared to liver fibroblasts, as stellate populations have been isolated from both organs, liver fibroblasts are clearly different from those found in the pancreas even when exposed to signals from the same cancer cells.

Importantly, this also indicates that stromal-cancer support networks between PDAC cells and CAFs are highly variable between tumor sites. Here, I observe that HGF expression is a feature of normal and cancer-associated fibroblast populations in the liver. Accordingly, the mitogenic signaling provided by MET activation in PDAC cells likely plays important roles in both the establishment and maintenance of the liver metastatic tumor niche. The role of HGF-MET signaling axis has emerged as a potential target in PDAC under the context of pancreatic stellate cells in primary tumors (171,172,215). Here, targeting HGF or MET was shown to potentiate response to several treatment approaches and inhibit metastasis of primary tumors. However, the focus on isolated pancreatic stellate cells in this study might overstate the impact of this axis in primary tumors as stellate-derived CAFs are a minority population in PDAC. HGF-MET signaling has also been identified as a signaling axis in liver iCAF populations, although the therapeutic potential remained unknown (193). Here, I confirm that the *HGF* expression in fibroblast populations from both human and mouse PDAC liver tumors and fibroblasts isolated from nearby normal human liver tissue is markedly higher than that found in primary pancreatic tumors. Accordingly, this HGF-MET crosstalk likely plays an important role in both establishment and maintenance of the liver metastatic niche.

As I sought to compare the interactions across many different populations of cells in pancreatic and liver PDAC lesions, the number of fibroblasts captured from liver tumors occluded any confident in-depth characterization of potential subpopulations that likely co-exist within the CAFs present in the metastatic niche. However, recent studies probing the programming of CAFs in liver metastasis have suggested that *Hgf* is expressed by iCAFs or vascular-associated metastasis-associated fibroblasts (vMAFs) (192). This data also supports the extensive literature

of normal liver fibroblast HGF production in the context of wound-healing and tissue repair (179). My data show liver-derived fibroblasts are able to activate canonical mitogenic signaling pathways downstream of MET including ERK, AKT, and STAT3 phosphorylation in PDAC cells in a MET-dependent fashion. Interestingly, I find that STAT3 is not activated in PATC53 PDAC cells by HGF alone and pharmacological inhibition of MET *in vitro* does not completely reduce ERK or STAT3 activity suggesting a potentiation of these pathway with other signaling molecules or metabolites released from liver fibroblasts. Despite this complexity, MET inhibition is clearly sufficient to potently impair the ability of PDAC cells to grow within the liver.

Single cell transcriptomics studies have nearly universally observed that PDAC sub-population heterogeneity within tumors does not correspond to the transcriptional subtypes defined from bulk RNA sequences approaches (216). In our datasets, I was able to define four main PDAC cell sub-populations with functionally relevant gene signatures that are present in both tumor sites. Interestingly, despite establishing tumors with the same initial population of PDAC cells, we observed a profound preference for programming centered on redox metabolism in the cells residing in the liver. This could be influenced by the stark differences in the metabolic state encountered between the hypoxic nutrient poor pancreatic tumor microenvironment (217) as compared to the liver, which serves as a primary anabolic hub and the center of gluconeogenesis. Indeed, metastatic PDAC cells have been shown to exhibit preferential metabolic pathway utilization (218), and this can serve to allow preferential seeding in one organ over another (219). Further, our lab has already identified that differential metabolic programming can co-exist in both human and murine PDAC, and recent work has shown clonal metabolic states are key to

metabolic adaptation (220). In addition, I cannot conclude if there is plasticity between these populations or this over representation of redox metabolism preference in liver tumors is selected during seeding, although the dominance of specific clonal populations in PDAC metastasis has been reported using elegant genetic barcoding (221).

While this project uncovered some key differences between primary and metastatic PDAC, some key questions remain unanswered. Here, I identified and characterized HGF expressing liver CAFs in liver which are clearly distinct from primary PDAC CAFs. Knowing that liver is home to multiple fibroblast populations, the progenitor of liver CAFs remain an unsolved mystery. Resident liver fibroblasts such as hepatic stellate cells and portal fibroblasts are known to expand and get activated during times of tissue injury or even malignancies. Circulating mesenchymal cells can also enter the hepatic tissue and give rise to fibroblasts. More investigation is required to identify the progenitor of liver CAFs.

This project also focuses on the metabolic preferences of PDAC cells that seem to alter with the organ of seeding. Here, I report PDAC cells relying on glycolysis, oxidative phosphorylation, and ECM proteins for nutrient recycling which is in alignment with previous findings. This is also mirrored by the hypoxic and nutrient deprived nature of the pancreas. However, PDAC cells showed preference for redox metabolism while expanding a niche in the liver. This could be due to well-oxygenated and nutrient rich conditions encountered in the liver. Both the murine and human single cell data showed increased expression of the redox master regulator *NFE2L2* along with other downstream genes in the liver. Knocking down *Nfe2l2* in PDAC cells increased survival in mice. It is known that KRAS can regulate Nfe2l2 and metabolic homeostasis which is

often times dysregulated in malignancies. Here, I also show that disruption of MET axis can affect downstream mitogenic signaling including RAS proteins such as MAPK. If this disruption can also affect NRF2 and other downstream proteins remain unknown.

Lastly, this project also highlights key differences in other populations and sub-populations such as the myeloid cells and T cells. How these immune cells rewire their crosstalk with each other and with cancer cells in the liver require more investigation. Tools like CellChat can unveil the distinct signaling pathways between the primary and metastatic site. Depleting immune populations such as myeloid cells or B cells can provide important information about mechanisms of immune surveillance and suppression in the liver vs pancreas. Additionally, the presence of higher number of CD8 T cells in the liver raise an important question of whether PDAC metastasis in the liver can be sensitized to immunotherapy which has failed to yield promising results in treating primary tumor.

Overall, this project looks at changes in tumor microenvironments of primary vs metastatic organ in PDAC. My data show a novel stromal population in the liver that upregulates HGF-MET signaling axis to promote tumorigenesis. Inhibiting this axis resulted in smaller tumors and increased survival in mice. In addition, I also see key differences in other compartments such as myeloid and T cells. This is exciting data that suggest taking in consideration, along with primary tumor, the organ of metastasis and its environment when treating this deadly disease.

REFERENCES

1. Singh R, Yousefian N, Allen W, Anaraki C, Beutel A, Calderon S, et al. Comparative Analysis of Primary and Liver Fibroblasts Reveals MET as a Potent Target in Pancreatic Cancer Metastasis. bioRxiv. Cold Spring Harbor Laboratory; 2025;2025.09.06.674373.

2. Rahib L, Smith BD, Aizenberg R, Rosenzweig AB, Fleshman JM, Matrisian LM. Projecting Cancer Incidence and Deaths to 2030: The Unexpected Burden of Thyroid, Liver, and Pancreas Cancers in the United States. Cancer Res. 2014;74:2913–21.

3. Rahib L, Wehner MR, Matrisian LM, Nead KT. Estimated Projection of US Cancer Incidence and Death to 2040. JAMA Netw Open. 2021;4:e214708.

4. Cronin KA, Scott S, Firth AU, Sung H, Henley SJ, Sherman RL, et al. Annual report to the nation on the status of cancer, part 1: National cancer statistics. Cancer. 2022;128:4251–84.

5. Halbrook CJ, Lyssiotis CA, Pasca Di Magliano M, Maitra A. Pancreatic cancer: Advances and challenges. Cell. 2023;186:1729–54.

6. Petersen GM. Familial pancreatic cancer. Semin Oncol. 2016;43:548–53.

7. Singhi AD, Koay EJ, Chari ST, Maitra A. Early Detection of Pancreatic Cancer: Opportunities and Challenges. Gastroenterology. 2019;156:2024–40.

8. Velez-Delgado A, Donahue KL, Brown KL, Du W, Irizarry-Negron V, Menjivar RE, et al. Extrinsic KRAS Signaling Shapes the Pancreatic Microenvironment Through Fibroblast Reprogramming. Cell Mol Gastroenterol Hepatol. 2022;13:1673–99.

9. Maitra A, Adsay NV, Argani P, Iacobuzio-Donahue C, De Marzo A, Cameron JL, et al. Multicomponent Analysis of the Pancreatic Adenocarcinoma Progression Model Using a Pancreatic Intraepithelial Neoplasia Tissue Microarray. Mod Pathol. 2003;16:902–12.

10. Valente R, Coppola A, Scandavini CM, Halimi A, Magnusson A, Lauro A, et al. Interactions between the Exocrine and the Endocrine Pancreas. J Clin Med. 2024;13:1179.

11. Miyamoto Y, Maitra A, Ghosh B, Zechner U, Argani P, Sriuranpong V, et al. Notch mediates TGF -induced changes in epithelial differentiation during pancreatic tumorigenesis.

12. Means AL, Meszoely IM, Suzuki K, Miyamoto Y, Rustgi AK, Coffey RJ, et al. Pancreatic epithelial plasticity mediated by acinar cell transdifferentiation and generation of nestin-positive intermediates. Development. 2005;132:3767–76.

13. Guerra C, Schuhmacher AJ, Cañamero M, Grippo PJ, Verdaguer L, Pérez-Gallego L, et al. Chronic Pancreatitis Is Essential for Induction of Pancreatic Ductal Adenocarcinoma by K-Ras Oncogenes in Adult Mice. Cancer Cell. 2007;11:291–302.

14. Raphael BJ, Hruban RH, Aguirre AJ, Moffitt RA, Yeh JJ, Stewart C, et al. Integrated Genomic Characterization of Pancreatic Ductal Adenocarcinoma. Cancer Cell. 2017;32:185-203.e13.

15. Overbeek KA, Cahen DL, Canto MI, Bruno MJ. Surveillance for neoplasia in the pancreas. Best Pract Res Clin Gastroenterol. 2016;30:971–86.

16. Cystic precursors to invasive pancreatic cancer | Nature Reviews Gastroenterology & Hepatology [Internet]. [cited 2025 Aug 25]. Available from: https://www.nature.com/articles/nrgastro.2011.2

17. Zhen DB, Rabe KG, Gallinger S, Syngal S, Schwartz AG, Goggins MG, et al. BRCA1, BRCA2, PALB2, and CDKN2A mutations in familial pancreatic cancer: a PACGENE study. Genet Med. 2015;17:569–77.

18. Kanda M, Matthaei H, Wu J, Hong S, Yu J, Borges M, et al. Presence of Somatic Mutations in Most Early-Stage Pancreatic Intraepithelial Neoplasia. Gastroenterology. 2012;142:730-733.e9.

19. Fujikura K, Hosoda W, Felsenstein M, Song Q, Reiter JG, Zheng L, et al. Multiregion whole-exome sequencing of intraductal papillary mucinous neoplasms reveals frequent somatic *KLF4* mutations predominantly in low-grade regions. Gut. 2021;70:928–39.

20. Peters MLB, Eckel A, Mueller PP, Tramontano AC, Weaver DT, Lietz A, et al. Progression to pancreatic ductal adenocarcinoma from pancreatic intraepithelial neoplasia: Results of a simulation model. Pancreatology. 2018;18:928–34.

21. Carpenter ES, Elhossiny AM, Kadiyala P, Li J, McGue J, Griffith BD, et al. Analysis of Donor Pancreata Defines the Transcriptomic Signature and Microenvironment of Early Neoplastic Lesions. Cancer Discov. 2023;13:1324.

22. Ideno N, Yamaguchi H, Ghosh B, Gupta S, Okumura T, Steffen DJ, et al. GNASR201C Induces Pancreatic Cystic Neoplasms in Mice That Express Activated KRAS by Inhibiting YAP1 Signaling. Gastroenterology. 2018;155:1593-1607.e12.

23. Patra KC, Kato Y, Mizukami Y, Widholz S, Boukhali M, Revenco I, et al. Mutant GNAS drives pancreatic tumourigenesis by inducing PKA-mediated SIK suppression and reprogramming lipid metabolism. Nat Cell Biol. Nature Publishing Group; 2018;20:811–22.

24. Hosein AN, Dangol G, Okumura T, Roszik J, Rajapakshe K, Siemann M, et al. Loss of Rnf43 Accelerates Kras-Mediated Neoplasia and Remodels the Tumor Immune Microenvironment in Pancreatic Adenocarcinoma. Gastroenterology. 2022;162:1303-1318.e18.

25. Bardeesy N, Cheng K, Berger JH, Chu GC, Pahler J, Olson P, et al. Smad4 is dispensable for normal pancreas development yet critical in progression and tumor biology of pancreas cancer. Genes Dev. 2006;20:3130–46.

26. Hingorani SR, Wang L, Multani AS, Combs C, Deramaudt TB, Hruban RH, et al. Trp53R172H and KrasG12D cooperate to promote chromosomal instability and widely metastatic pancreatic ductal adenocarcinoma in mice. Cancer Cell. 2005;7:469–83.

27. Aguirre AJ, Bardeesy N, Sinha M, Lopez L, Tuveson DA, Horner J, et al. Activated Kras and Ink4a/Arf deficiency cooperate to produce metastatic pancreatic ductal adenocarcinoma. Genes Dev. 2003;17:3112–26.

28. Qiu W, Sahin F, Iacobuzio-Donahue C, Garcia-Carracedo D, Wang W, Kuo C-Y, et al. Disruption of p16 and Activation of Kras in Pancreas Increase Ductal Adenocarcinoma Formation and Metastasis in vivo. Oncotarget. Impact Journals; 2011;2:862–73.

29. Jones S, Zhang X, Parsons DW, Lin JC-H, Leary RJ, Angenendt P, et al. Core Signaling Pathways in Human Pancreatic Cancers Revealed by Global Genomic Analyses. Science [Internet]. American Association for the Advancement of Science; 2008 [cited 2025 Aug 25]; Available from: https://www.science.org/doi/10.1126/science.1164368

30. Waddell N, Pajic M, Patch A-M, Chang DK, Kassahn KS, Bailey P, et al. Whole genomes redefine the mutational landscape of pancreatic cancer. Nature. Nature Publishing Group; 2015;518:495–501.

31. Bailey P, Chang DK, Nones K, Johns AL, Patch A-M, Gingras M-C, et al. Genomic analyses identify molecular subtypes of pancreatic cancer. Nature. Nature Publishing Group; 2016;531:47–52.

32. Intraductal Papillary Mucinous Neoplasms of the Pancreas:... : Annals of Surgery [Internet]. LWW. [cited 2025 Aug 25]. Available from: https://journals.lww.com/annalsofsurgery/fulltext/2001/09000/intraductal_papillary_mucinous_neoplasms_of_the.5.aspx

33. Kleeff J, Korc M, Apte M, La Vecchia C, Johnson CD, Biankin AV, et al. Pancreatic cancer. Nat Rev Dis Primer. 2016;2:16022.

34. Beutel AK, Halbrook CJ. Barriers and opportunities for gemcitabine in pancreatic cancer therapy. Am J Physiol-Cell Physiol. 2023;324:C540–52.

35. Burris3rd HA, Moore MJ, Andersen J, Green MR, Rothenberg ML, Modiano MR, et al. Improvements in survival and clinical benefit with gemcitabine as first-line therapy for patients with advanced pancreas cancer: a randomized trial. J Clin Oncol [Internet]. 1997 [cited 2025 Aug 25]; Available from: https://ascopubs.org/doi/10.1200/JCO.1997.15.6.2403

36. Evans DB, George B, Tsai S. Non-metastatic Pancreatic Cancer: Resectable, Borderline Resectable, and Locally Advanced-Definitions of Increasing Importance for the Optimal Delivery of Multimodality Therapy. Ann Surg Oncol. 2015;22:3409–13.

37. Evans DB. What Makes a Pancreatic Cancer Resectable? Am Soc Clin Oncol Educ Book [Internet]. American Society of Clinical OncologyAlexandria, VA; 2018 [cited 2025 Aug 25]; Available from: https://ascopubs.org/doi/10.1200/EDBK_200861

38. Conroy T, Desseigne F, Ychou M, Bouché O, Guimbaud R, Bécouarn Y, et al. FOLFIRINOX versus Gemcitabine for Metastatic Pancreatic Cancer [Internet]. N. Engl. J. Med. Massachusetts Medical Society; 2011 [cited 2025 Aug 25]. Available from: https://www.nejm.org/doi/full/10.1056/NEJMoa1011923

39. Moore MJ, Goldstein D, Hamm J, Figer A, Hecht JR, Gallinger S, et al. Erlotinib Plus Gemcitabine Compared With Gemcitabine Alone in Patients With Advanced Pancreatic Cancer: A Phase III Trial of the National Cancer Institute of Canada Clinical Trials Group. J Clin Oncol [Internet]. American Society of Clinical Oncology; 2007 [cited 2025 Aug 25]; Available from: https://ascopubs.org/doi/10.1200/JCO.2006.07.9525

40. Von Hoff DD, Ervin T, Arena FP, Chiorean EG, Infante J, Moore M, et al. Increased Survival in Pancreatic Cancer with nab-Paclitaxel plus Gemcitabine [Internet]. N. Engl. J. Med. Massachusetts Medical Society; 2013 [cited 2025 Aug 25]. Available from: https://www.nejm.org/doi/full/10.1056/NEJMoa1304369

41. Sohal DPS, Kennedy EB, Cinar P, Conroy T, Copur MS, Crane CH, et al. Metastatic Pancreatic Cancer: ASCO Guideline Update. J Clin Oncol [Internet]. American Society of Clinical Oncology; 2020 [cited 2025 Aug 25]; Available from: https://ascopubs.org/doi/10.1200/JCO.20.01364

42. Golan T, Hammel P, Reni M, Cutsem EV, Macarulla T, Hall MJ, et al. Maintenance Olaparib for Germline BRCA-Mutated Metastatic Pancreatic Cancer. N Engl J Med [Internet]. Massachusetts Medical Society; 2019 [cited 2025 Aug 25]; Available from: https://www.nejm.org/doi/full/10.1056/NEJMoa1903387

43. Le DT, Uram JN, Wang H, Bartlett BR, Kemberling H, Eyring AD, et al. PD-1 Blockade in Tumors with Mismatch-Repair Deficiency [Internet]. N. Engl. J. Med. Massachusetts Medical Society; 2015 [cited 2025 Aug 25]. Available from: https://www.nejm.org/doi/full/10.1056/NEJMoa1500596

44. Lee DU, Han BS, Jung KH, Hong S-S. Tumor Stroma as a Therapeutic Target for Pancreatic Ductal Adenocarcinoma. Biomol Ther. The Korean Society of Applied Pharmacology; 2024;32:281–90.

45. Provenzano PP, Cuevas C, Chang AE, Goel VK, Von Hoff DD, Hingorani SR. Enzymatic Targeting of the Stroma Ablates Physical Barriers to Treatment of Pancreatic Ductal Adenocarcinoma. Cancer Cell. 2012;21:418–29.

46. Väyrynen SA, Zhang J, Yuan C, Väyrynen JP, Costa AD, Williams H, et al. Composition, spatial characteristics, and prognostic significance of myeloid cell infiltration in pancreatic cancer. Clin Cancer Res Off J Am Assoc Cancer Res. 2020;27:1069.

47. DuFort CC, DelGiorno KE, Carlson MA, Osgood RJ, Zhao C, Huang Z, et al. Interstitial Pressure in Pancreatic Ductal Adenocarcinoma Is Dominated by a Gel-Fluid Phase. Biophys J. 2016;110:2106.

48. Collisson EA, Sadanandam A, Olson P, Gibb WJ, Truitt M, Gu S, et al. Subtypes of pancreatic ductal adenocarcinoma and their differing responses to therapy. Nat Med. Nature Publishing Group; 2011;17:500–3.

49. Moffitt RA, Marayati R, Flate EL, Volmar KE, Loeza SGH, Hoadley KA, et al. Virtual microdissection identifies distinct tumor- and stroma-specific subtypes of pancreatic ductal adenocarcinoma. Nat Genet. Nature Publishing Group; 2015;47:1168–78.

50. Puleo F, Nicolle R, Blum Y, Cros J, Marisa L, Demetter P, et al. Stratification of Pancreatic Ductal Adenocarcinomas Based on Tumor and Microenvironment Features. Gastroenterology. 2018;155:1999-2013.e3.

51. Maurer C, Holmstrom SR, He J, Laise P, Su T, Ahmed A, et al. Experimental microdissection enables functional harmonisation of pancreatic cancer subtypes. Gut. BMJ Publishing Group; 2019;68:1034–43.

52. Chan-Seng-Yue M, Kim JC, Wilson GW, Ng K, Figueroa EF, O'Kane GM, et al. Transcription phenotypes of pancreatic cancer are driven by genomic events during tumor evolution. Nat Genet. Nature Publishing Group; 2020;52:231–40.

53. Bailey P, Chang DK, Nones K, Johns AL, Patch A-M, Gingras M-C, et al. Genomic analyses identify molecular subtypes of pancreatic cancer. Nature. Nature Publishing Group; 2016;531:47–52.

54. Wu J, Liang C, Chen M, Su W. Association between tumor-stroma ratio and prognosis in solid tumor patients: a systematic review and meta-analysis. Oncotarget. Impact Journals; 2016;7:68954–65.

55. R K. The biology and function of fibroblasts in cancer. Nat Rev Cancer [Internet]. Nat Rev Cancer; 2016 [cited 2025 Aug 25];16. Available from: https://pubmed.ncbi.nlm.nih.gov/27550820/

56. E H, Mk O, Mh S. Fibroblast Heterogeneity in the Pancreatic Tumor Microenvironment. Cancer Discov [Internet]. Cancer Discov; 2020 [cited 2025 Aug 25];10. Available from: https://pubmed.ncbi.nlm.nih.gov/32014869/

57. Sahai E, Astsaturov I, Cukierman E, DeNardo DG, Egeblad M, Evans RM, et al. A framework for advancing our understanding of cancer-associated fibroblasts. Nat Rev Cancer. 2020;20:174–86.

58. Sherman MH, Magliano MP di. Cancer-Associated Fibroblasts: Lessons from Pancreatic Cancer. Annu Rev Cancer Biol. Annual Reviews; 2023;7:43–55.

59. LeBleu VS, Kalluri R. A peek into cancer-associated fibroblasts: origins, functions and translational impact. Dis Model Mech [Internet]. The Company of Biologists; 2018 [cited 2025 Aug 26];11. Available from: https://dx.doi.org/10.1242/dmm.029447

60. Von Ahrens D, Bhagat TD, Nagrath D, Maitra A, Verma A. The role of stromal cancer-associated fibroblasts in pancreatic cancer. J Hematol OncolJ Hematol Oncol. 2017;10:76.

61. Zhang Y, Crawford HC, Magliano MP di. Epithelial-Stromal Interactions in Pancreatic Cancer. Annu Rev Physiol. Annual Reviews; 2019;81:211–33.

62. Auciello FR, Bulusu V, Oon C, Tait-Mulder J, Berry M, Bhattacharyya S. A Stromal Lysolipid–Autotaxin Signaling Axis Promotes Pancreatic Tumor Progression. Cancer Discov. 2019;9:199–209.

63. Kim PK, Halbrook CJ, Kerk SA, Radyk M, Wisner S, Kremer DM, et al. Hyaluronic acid fuels pancreatic cancer cell growth. Finley LW, White RM, editors. eLife. eLife Sciences Publications, Ltd; 2021;10:e62645.

64. Sousa CM, Biancur DE, Wang X, Halbrook CJ, Sherman MH, Zhang L, et al. Pancreatic stellate cells support tumour metabolism through autophagic alanine secretion. Nature. Nature Publishing Group; 2016;536:479–83.

65. Djurec M, Graña O, Lee A, Troulé K, Espinet E, Cabras L, et al. Saa3 is a key mediator of the protumorigenic properties of cancer-associated fibroblasts in pancreatic tumors. Proc Natl Acad Sci. 2018;115:E1147–56.

66. Feig C, Jones JO, Kraman M, Wells RJB, Deonarine A, Chan DS, et al. Targeting CXCL12 from FAP-expressing carcinoma-associated fibroblasts synergizes with anti–PD-L1 immunotherapy in pancreatic cancer. Proc Natl Acad Sci. 2013;110:20212–7.

67. Lo A, Wang L-CS, Scholler J, Monslow J, Avery D, Newick K, et al. Tumor-Promoting Desmoplasia Is Disrupted by Depleting FAP-Expressing Stromal Cells. Cancer Res. American Association for Cancer Research; 2015;75:2800–10.

68. Randomized Phase Ib/II Study of Gemcitabine Plus Placebo or Vismodegib, a Hedgehog Pathway Inhibitor, in Patients With Metastatic Pancreatic Cancer | Journal of Clinical Oncology [Internet]. [cited 2025 Aug 25]. Available from: https://ascopubs.org/doi/full/10.1200/JCO.2015.62.8719

69. De Jesus-Acosta A, Sugar EA, O'Dwyer PJ, Ramanathan RK, Von Hoff DD, Rasheed Z, et al. Phase 2 study of vismodegib, a hedgehog inhibitor, combined with gemcitabine and nab-paclitaxel in patients with untreated metastatic pancreatic adenocarcinoma. Br J Cancer. Nature Publishing Group; 2020;122:498–505.

70. Kim EJ, Sahai V, Abel EV, Griffith KA, Greenson JK, Takebe N, et al. Pilot Clinical Trial of Hedgehog Pathway Inhibitor GDC-0449 (Vismodegib) in Combination with Gemcitabine in Patients with Metastatic Pancreatic Adenocarcinoma. Clin Cancer Res. American Association for Cancer Research; 2014;20:5937–45.

71. A Phase I Study of FOLFIRINOX Plus IPI-926, a Hedgehog... : Pancreas [Internet]. LWW. [cited 2025 Aug 25]. Available from:

https://journals.lww.com/pancreasjournal/fulltext/2016/03000/a_phase_i_study_of_folfirinox_plus_ipi_926,_a.9.aspx

72. Cutsem EV, Tempero MA, Sigal D, Oh D-Y, Fazio N, Macarulla T, et al. Randomized Phase III Trial of Pegvorhyaluronidase Alfa With Nab-Paclitaxel Plus Gemcitabine for Patients With Hyaluronan-High Metastatic Pancreatic Adenocarcinoma. J Clin Oncol [Internet]. American Society of Clinical Oncology; 2020 [cited 2025 Aug 25]; Available from: https://ascopubs.org/doi/10.1200/JCO.20.00590

73. Erkan M, Weis N, Pan Z, Schwager C, Samkharadze T, Jiang X, et al. Organ-, inflammation- and cancer specific transcriptional fingerprints of pancreatic and hepatic stellate cells. Mol Cancer. 2010;9:88.

74. Wang Z, Dong S, Zhou W. Pancreatic stellate cells: Key players in pancreatic health and diseases (Review). Mol Med Rep. Spandidos Publications; 2024;30:1–18.

75. Phillips P. Pancreatic stellate cells and fibrosis. In: Grippo PJ, Munshi HG, editors. Pancreat Cancer Tumor Microenviron [Internet]. Trivandrum (India): Transworld Research Network; 2012 [cited 2025 Aug 26]. Available from: http://www.ncbi.nlm.nih.gov/books/NBK98937/

76. Allam A, Thomsen AR, Gothwal M, Saha D, Maurer J, Brunner TB. Pancreatic stellate cells in pancreatic cancer: In focus. Pancreatology. 2017;17:514–22.

77. Apte MV, Park S, Phillips PA, Santucci N, Goldstein D, Kumar RK, et al. Desmoplastic reaction in pancreatic cancer: Role of pancreatic stellate cells. Pancreas. 2004;29:179–87.

78. Sherman MH. Stellate Cells in Tissue Repair, Inflammation, and Cancer. Annu Rev Cell Dev Biol. Annual Reviews; 2018;34:333–55.

79. Helms EJ, Berry MW, Chaw RC, DuFort CC, Sun D, Onate MK, et al. Mesenchymal Lineage Heterogeneity Underlies Nonredundant Functions of Pancreatic Cancer–Associated Fibroblasts. Cancer Discov. American Association for Cancer Research; 2022;12:484–501.

80. Garcia PE, Adoumie M, Kim EC, Zhang Y, Scales MK, El-Tawil YS, et al. Differential Contribution of Pancreatic Fibroblast Subsets to the Pancreatic Cancer Stroma. Cell Mol Gastroenterol Hepatol. 2020;10:581–99.

81. Huang H, Wang Z, Zhang Y, Pradhan RN, Ganguly D, Chandra R, et al. Mesothelial cell-derived antigen-presenting cancer-associated fibroblasts induce expansion of regulatory T cells in pancreatic cancer. Cancer Cell. 2022;40:656-673.e7.

82. Han L, Wu Y, Fang K, Sweeney S, Roesner UK, Parrish M, et al. The splanchnic mesenchyme is the tissue of origin for pancreatic fibroblasts during homeostasis and tumorigenesis. Nat Commun. Nature Publishing Group; 2023;14:1.

83. Öhlund D, Handly-Santana A, Biffi G, Elyada E, Almeida AS, Ponz-Sarvise M, et al. Distinct populations of inflammatory fibroblasts and myofibroblasts in pancreatic cancer. J Exp Med. 2017;214:579–96.

84. Velez-Delgado A, Donahue KL, Brown KL, Du W, Irizarry-Negron V, Menjivar RE, et al. Extrinsic KRAS Signaling Shapes the Pancreatic Microenvironment Through Fibroblast Reprogramming. Cell Mol Gastroenterol Hepatol. 2022;13:1673–99.

85. Zhang Y, Yan W, Collins MA, Bednar F, Rakshit S, Zetter BR, et al. Interleukin-6 Is Required for Pancreatic Cancer Progression by Promoting MAPK Signaling Activation and Oxidative Stress Resistance. Cancer Res. American Association for Cancer Research; 2013;73:6359–74.

86. Hosein AN, Huang H, Wang Z, Parmar K, Du W, Huang J, et al. Cellular heterogeneity during mouse pancreatic ductal adenocarcinoma progression at single-cell resolution. JCI Insight. 4:e129212.

87. Biffi G, Oni TE, Spielman B, Hao Y, Elyada E, Park Y, et al. IL1-Induced JAK/STAT Signaling Is Antagonized by TGFβ to Shape CAF Heterogeneity in Pancreatic Ductal Adenocarcinoma. Cancer Discov. American Association for Cancer Research; 2019;9:282–301.

88. Dominguez CX, Müller S, Keerthivasan S, Koeppen H, Hung J, Gierke S, et al. Single-Cell RNA Sequencing Reveals Stromal Evolution into LRRC15+ Myofibroblasts as a Determinant of Patient Response to Cancer Immunotherapy. Cancer Discov. American Association for Cancer Research; 2020;10:232–53.

89. Perez VM, Kearney JF, Yeh JJ. The PDAC Extracellular Matrix: A Review of the ECM Protein Composition, Tumor Cell Interaction, and Therapeutic Strategies. Front Oncol [Internet]. Frontiers; 2021 [cited 2025 Aug 26];11. Available from: https://www.frontiersin.org/journals/oncology/articles/10.3389/fonc.2021.751311/full

90. Quantitative Analysis of Collagen and Collagen Subtypes I,... : Pancreas [Internet]. LWW. [cited 2025 Aug 26]. Available from: https://journals.lww.com/pancreasjournal/fulltext/1995/11000/quantitative_analysis_of_collagen_and_collagen.7.aspx

91. Hosein AN, Brekken RA, Maitra A. Pancreatic cancer stroma: an update on therapeutic targeting strategies. Nat Rev Gastroenterol Hepatol. Nature Publishing Group; 2020;17:487–505.

92. Iaconisi GN, Lunetti P, Gallo N, Cappello AR, Fiermonte G, Dolce V, et al. Hyaluronic Acid: A Powerful Biomolecule with Wide-Ranging Applications—A Comprehensive Review. Int J Mol Sci. 2023;24:10296.

93. Berman DM, Karhadkar SS, Maitra A, Montes De Oca R, Gerstenblith MR, Briggs K, et al. Widespread requirement for Hedgehog ligand stimulation in growth of digestive tract tumours. Nature. 2003;425:846–51.

94. Bailey JM, Mohr AM, Hollingsworth MA. Sonic hedgehog paracrine signaling regulates metastasis and lymphangiogenesis in pancreatic cancer. Oncogene. 2009;28:3513–25.

95. Fendrich V, Oh E, Bang S, Karikari C, Ottenhof N, Bisht S, et al. Ectopic overexpression of Sonic Hedgehog (Shh) induces stromal expansion and metaplasia in the adult murine pancreas. Neoplasia N Y N. 2011;13:923–30.

96. Mao J, Ligon KL, Rakhlin EY, Thayer SP, Bronson RT, Rowitch D, et al. A novel somatic mouse model to survey tumorigenic potential applied to the Hedgehog pathway. Cancer Res. 2006;66:10171–8.

97. Thayer SP, di Magliano MP, Heiser PW, Nielsen CM, Roberts DJ, Lauwers GY, et al. Hedgehog is an early and late mediator of pancreatic cancer tumorigenesis. Nature. 2003;425:851–6.

98. Inhibition of Hedgehog Signaling Enhances Delivery of Chemotherapy in a Mouse Model of Pancreatic Cancer | Science [Internet]. [cited 2025 Aug 26]. Available from: https://www.science.org/doi/10.1126/science.1171362

99. Rhim AD, Oberstein PE, Thomas DH, Mirek ET, Palermo CF, Sastra SA, et al. Stromal Elements Act to Restrain, Rather Than Support, Pancreatic Ductal Adenocarcinoma. Cancer Cell. 2014;25:735–47.

100. Lee JJ, Perera RM, Wang H, Wu D-C, Liu XS, Han S, et al. Stromal response to Hedgehog signaling restrains pancreatic cancer progression. Proc Natl Acad Sci [Internet]. 2014 [cited 2025 Aug 26];111. Available from: https://pnas.org/doi/full/10.1073/pnas.1411679111

101. Jiang H, Torphy RJ, Steiger K, Hongo H, Ritchie AJ, Kriegsmann M, et al. Pancreatic ductal adenocarcinoma progression is restrained by stromal matrix. J Clin Invest. American Society for Clinical Investigation; 2020;130:4704–9.

102. Özdemir BC, Pentcheva-Hoang T, Carstens JL, Zheng X, Wu C-C, Simpson TR, et al. Depletion of Carcinoma-Associated Fibroblasts and Fibrosis Induces Immunosuppression and Accelerates Pancreas Cancer with Reduced Survival. Cancer Cell. 2014;25:719–34.

103. Dominguez CX, Müller S, Keerthivasan S, Koeppen H, Hung J, Gierke S, et al. Single-Cell RNA Sequencing Reveals Stromal Evolution into LRRC15+ Myofibroblasts as a Determinant of Patient Response to Cancer Immunotherapy. Cancer Discov. American Association for Cancer Research; 2020;10:232–53.

104. Elyada E, Bolisetty M, Laise P, Flynn WF, Courtois ET, Burkhart RA, et al. Cross-Species Single-Cell Analysis of Pancreatic Ductal Adenocarcinoma Reveals Antigen-Presenting Cancer-Associated Fibroblasts. Cancer Discov. 2019;9:1102–23.

105. Muller M, Haghnejad V, Schaefer M, Gauchotte G, Caron B, Peyrin-Biroulet L, et al. The Immune Landscape of Human Pancreatic Ductal Carcinoma: Key Players, Clinical Implications, and Challenges. Cancers. 2022;14:995.

106. Krishnamoorthy M, Lenehan JG, Burton JP, Maleki Vareki S. Immunomodulation in Pancreatic Cancer. Cancers. Multidisciplinary Digital Publishing Institute; 2020;12:3340.

107. Bayne LJ, Beatty GL, Jhala N, Clark CE, Rhim AD, Stanger BZ, et al. Tumor-Derived Granulocyte-Macrophage Colony-Stimulating Factor Regulates Myeloid Inflammation and T Cell Immunity in Pancreatic Cancer. Cancer Cell. 2012;21:822–35.

108. Pylayeva-Gupta Y, Lee KE, Hajdu CH, Miller G, Bar-Sagi D. Oncogenic Kras-Induced GM-CSF Production Promotes the Development of Pancreatic Neoplasia. Cancer Cell. 2012;21:836–47.

109. Xiong C, Zhu Y, Xue M, Jiang Y, Zhong Y, Jiang L, et al. Tumor-associated macrophages promote pancreatic ductal adenocarcinoma progression by inducing epithelial-to-mesenchymal transition. Aging. 2021;13:3386–404.

110. Singh A, Talekar M, Raikar A, Amiji M. Macrophage-targeted delivery systems for nucleic acid therapy of inflammatory diseases. J Control Release Off J Control Release Soc. 2014;190:515–30.

111. Boyer S, Lee H-J, Steele N, Zhang L, Sajjakulnukit P, Andren A, et al. Multiomic characterization of pancreatic cancer-associated macrophage polarization reveals deregulated metabolic programs driven by the GM-CSF–PI3K pathway. Fertig EJ, Zaidi M, DeNardo D, editors. eLife. eLife Sciences Publications, Ltd; 2022;11:e73796.

112. Lorestani P, Dashti M, Nejati N, Habibi MA, Askari M, Robat-Jazi B, et al. The complex role of macrophages in pancreatic cancer tumor microenvironment: a review on cancer progression and potential therapeutic targets. Discov Oncol. 2024;15:369.

113. Mitchem JB, Brennan DJ, Knolhoff BL, Belt BA, Zhu Y, Sanford DE, et al. Targeting Tumor-Infiltrating Macrophages Decreases Tumor-Initiating Cells, Relieves Immunosuppression, and Improves Chemotherapeutic Responses. Cancer Res. American Association for Cancer Research; 2013;73:1128–41.

114. Zhu Y, Knolhoff BL, Meyer MA, Nywening TM, West BL, Luo J, et al. CSF1/CSF1R Blockade Reprograms Tumor-Infiltrating Macrophages and Improves Response to T-cell Checkpoint Immunotherapy in Pancreatic Cancer Models. Cancer Res. American Association for Cancer Research; 2014;74:5057–69.

115. Candido JB, Morton JP, Bailey P, Campbell AD, Karim SA, Jamieson T, et al. CSF1R+ Macrophages Sustain Pancreatic Tumor Growth through T Cell Suppression and Maintenance of Key Gene Programs that Define the Squamous Subtype. Cell Rep. 2018;23:1448–60.

116. DeNardo DG, Galkin A, Dupont J, Zhou L, Bendell J. GB1275, a first-in-class CD11b modulator: rationale for immunotherapeutic combinations in solid tumors. J Immunother Cancer [Internet]. BMJ Publishing Group Ltd; 2021 [cited 2025 Aug 26];9. Available from: https://jitc.bmj.com/content/9/8/e003005

117. Panni RZ, Herndon JM, Zuo C, Hegde S, Hogg GD, Knolhoff BL, et al. Agonism of CD11b reprograms innate immunity to sensitize pancreatic cancer to immunotherapies. Sci

Transl Med [Internet]. American Association for the Advancement of Science; 2019 [cited 2025 Aug 26]; Available from: https://www.science.org/doi/10.1126/scitranslmed.aau9240

118. Halbrook CJ, Pontious C, Kovalenko I, Lapienyte L, Dreyer S, Lee H-J, et al. Macrophage-Released Pyrimidines Inhibit Gemcitabine Therapy in Pancreatic Cancer. Cell Metab. 2019;29:1390-1399.e6.

119. Daley D, Zambirinis CP, Seifert L, Akkad N, Mohan N, Werba G, et al. γδ T Cells Support Pancreatic Oncogenesis by Restraining αβ T Cell Activation. Cell. 2016;166:1485-1499.e15.

120. McAllister F, Bailey JM, Alsina J, Nirschl CJ, Sharma R, Fan H, et al. Oncogenic Kras Activates a Hematopoietic-to-Epithelial IL-17 Signaling Axis in Preinvasive Pancreatic Neoplasia. Cancer Cell. 2014;25:621–37.

121. Perusina Lanfranca M, Zhang Y, Girgis A, Kasselman S, Lazarus J, Kryczek I, et al. Interleukin 22 Signaling Regulates Acinar Cell Plasticity to Promote Pancreatic Tumor Development in Mice. Gastroenterology. 2020;158:1417-1432.e11.

122. Zhang Y, Yan W, Mathew E, Bednar F, Wan S, Collins MA, et al. CD4+ T Lymphocyte Ablation Prevents Pancreatic Carcinogenesis in Mice. Cancer Immunol Res. American Association for Cancer Research; 2014;2:423–35.

123. Zhang Y, Lazarus J, Steele NG, Yan W, Lee H-J, Nwosu ZC, et al. Regulatory T-cell Depletion Alters the Tumor Microenvironment and Accelerates Pancreatic Carcinogenesis. Cancer Discov. American Association for Cancer Research; 2020;10:422–39.

124. Li J, Byrne KT, Yan F, Yamazoe T, Chen Z, Baslan T, et al. Tumor cell-intrinsic factors underlie heterogeneity of immune cell infiltration and response to immunotherapy. Immunity. 2018;49:178.

125. Dp H, N X, A T, C G, S G-R, Kr M, et al. B Cells and T Follicular Helper Cells Mediate Response to Checkpoint Inhibitors in High Mutation Burden Mouse Models of Breast Cancer. Cell [Internet]. Cell; 2019 [cited 2025 Aug 26];179. Available from: https://pubmed.ncbi.nlm.nih.gov/31730857/

126. Ba H, Sm R, J G, S Z, R B, R T, et al. B cells and tertiary lymphoid structures promote immunotherapy response. Nature [Internet]. Nature; 2020 [cited 2025 Aug 26];577. Available from: https://pubmed.ncbi.nlm.nih.gov/31942075/

127. R C, M L, A S, M D, M SL, S M, et al. Tertiary lymphoid structures improve immunotherapy and survival in melanoma. Nature [Internet]. Nature; 2020 [cited 2025 Aug 26];577. Available from: https://pubmed.ncbi.nlm.nih.gov/31942071/

128. Petitprez F, de Reyniès A, Keung EZ, Chen TW-W, Sun C-M, Calderaro J, et al. B cells are associated with survival and immunotherapy response in sarcoma. Nature. 2020;577:556–60.

129. Largeot A, Pagano G, Gonder S, Moussay E, Paggetti J. The B-Side of Cancer Immunity: The Underrated Tune. Cells. 2019;8:449.

130. He Y, Qian H, Liu Y, Duan L, Li Y, Shi G. The Roles of Regulatory B Cells in Cancer. J Immunol Res. 2014;2014:215471.

131. Mirlekar B, Wang Y, Li S, Zhou M, Entwistle S, Buysscher TD, et al. Balance between immunoregulatory B cells and plasma cells drives pancreatic tumor immunity. Cell Rep Med. 2022;3:100744.

132. Jacobetz MA, Chan DS, Neesse A, Bapiro TE, Cook N, Frese KK, et al. Hyaluronan impairs vascular function and drug delivery in a mouse model of pancreatic cancer. Gut. BMJ Publishing Group; 2013;62:112–20.

133. P O, Gc C, Sr P, O N-S, D H. Imaging guided trials of the angiogenesis inhibitor sunitinib in mouse models predict efficacy in pancreatic neuroendocrine but not ductal carcinoma. Proc Natl Acad Sci U S A [Internet]. Proc Natl Acad Sci U S A; 2011 [cited 2025 Aug 26];108. Available from: https://pubmed.ncbi.nlm.nih.gov/22084065/

134. Js Y, Ce L, Al S. The significance of the tissue pressure of normal testicular and of neoplastic (Brown-Pearce carcinoma) tissue in the rabbit. J Pathol Bacteriol [Internet]. J Pathol Bacteriol; 1950 [cited 2025 Aug 26];62. Available from: https://pubmed.ncbi.nlm.nih.gov/14784896/

135. M S, Y B, M S, Rk J. Oncotic pressure in solid tumors is elevated. Cancer Res [Internet]. Cancer Res; 2000 [cited 2025 Aug 26];60. Available from: https://pubmed.ncbi.nlm.nih.gov/10945638/

136. Sussman JH, Kim N, Kemp SB, Traum D, Katsuda T, Kahn BM, et al. Multiplexed Imaging Mass Cytometry Analysis Characterizes the Vascular Niche in Pancreatic Cancer. Cancer Res. American Association for Cancer Research; 2024;84:2364–76.

137. Y U, O M, C M, K S, J K, T N, et al. Placental defect and embryonic lethality in mice lacking hepatocyte growth factor/scatter factor. Nature [Internet]. Nature; 1995 [cited 2025 Aug 27];373. Available from: https://pubmed.ncbi.nlm.nih.gov/7854453/

138. Schmidt C, Bladt F, Goedecke S, Brinkmann V, Zschiesche W, Sharpe M, et al. Scatter factor/hepatocyte growth factor is essential for liver development. Nature. Nature Publishing Group; 1995;373:699–702.

139. Bachleitner-Hofmann T, Sun MY, Chen C-T, Tang L, Song L, Zeng Z, et al. HER kinase activation confers resistance to MET tyrosine kinase inhibition in MET oncogene-addicted gastric cancer cells. Mol Cancer Ther. 2008;7:3499–508.

140. Khoury H, Naujokas MA, Zuo D, Sangwan V, Frigault MM, Petkiewicz S, et al. HGF converts ErbB2/Neu epithelial morphogenesis to cell invasion. Mol Biol Cell. 2005;16:550–61.

141. Yeh C-Y, Shin S-M, Yeh H-H, Wu T-J, Shin J-W, Chang T-Y, et al. Transcriptional activation of the Axl and PDGFR-α by c-Met through a ras- and Src-independent mechanism in human bladder cancer. BMC Cancer. 2011;11:139.

142. Danilkovitch-Miagkova A, Zbar B. Dysregulation of Met receptor tyrosine kinase activity in invasive tumors. J Clin Invest. American Society for Clinical Investigation; 2002;109:863–7.

143. Miller CT, Lin L, Casper AM, Lim J, Thomas DG, Orringer MB, et al. Genomic amplification of MET with boundaries within fragile site FRA7G and upregulation of MET pathways in esophageal adenocarcinoma. Oncogene. 2006;25:409–18.

144. Hara T, Ooi A, Kobayashi M, Mai M, Yanagihara K, Nakanishi I. Amplification of c-myc, K-sam, and c-met in gastric cancers: detection by fluorescence in situ hybridization. Lab Investig J Tech Methods Pathol. 1998;78:1143–53.

145. Kuniyasu H, Yasui W, Kitadai Y, Yokozaki H, Ito H, Tahara E. Frequent amplification of the c-met gene in scirrhous type stomach cancer. Biochem Biophys Res Commun. 1992;189:227–32.

146. Houldsworth J, Cordon-Cardo C, Ladanyi M, Kelsen DP, Chaganti RS. Gene amplification in gastric and esophageal adenocarcinomas. Cancer Res. 1990;50:6417–22.

147. Tong CYK, Hui ABY, Yin X-L, Pang JCS, Zhu X-L, Poon W-S, et al. Detection of oncogene amplifications in medulloblastomas by comparative genomic hybridization and array-based comparative genomic hybridization. J Neurosurg. 2004;100:187–93.

148. Di Renzo MF, Poulsom R, Olivero M, Comoglio PM, Lemoine NR. Expression of the Met/hepatocyte growth factor receptor in human pancreatic cancer. Cancer Res. 1995;55:1129–38.

149. Bean J, Brennan C, Shih J-Y, Riely G, Viale A, Wang L, et al. MET amplification occurs with or without T790M mutations in EGFR mutant lung tumors with acquired resistance to gefitinib or erlotinib. Proc Natl Acad Sci U S A. 2007;104:20932–7.

150. Engelman JA, Zejnullahu K, Mitsudomi T, Song Y, Hyland C, Park JO, et al. MET amplification leads to gefitinib resistance in lung cancer by activating ERBB3 signaling. Science. 2007;316:1039–43.

151. Organ SL, Tsao M-S. An overview of the c-MET signaling pathway. Ther Adv Med Oncol. 2011;3:S7–19.

152. Huang X, Li E, Shen H, Wang X, Tang T, Zhang X, et al. Targeting the HGF/MET Axis in Cancer Therapy: Challenges in Resistance and Opportunities for Improvement. Front Cell Dev Biol. 2020;8:152.

153. Molnarfi N, Benkhoucha M, Funakoshi H, Nakamura T, Lalive PH. Hepatocyte growth factor: A regulator of inflammation and autoimmunity. Autoimmun Rev. 2015;14:293–303.

154. Nakamura T. Structure and function of hepatocyte growth factor. Prog Growth Factor Res. 1991;3:67–85.

155. Shima N, Itagaki Y, Nagao M, Yasuda H, Morinaga T, Higashio K. A fibroblast-derived tumor cytotoxic factor/F-TCF(hepatocyte growth factor/HGF) has multiple functions in vitro. Cell Biol Int Rep. 1991;15:397–408.

156. Montesano R, Matsumoto K, Nakamura T, Orci L. Identification of a fibroblast-derived epithelial morphogen as hepatocyte growth factor. Cell. 1991;67:901–8.

157. Rubin JS, Osada H, Finch PW, Taylor WG, Rudikoff S, Aaronson SA. Purification and characterization of a newly identified growth factor specific for epithelial cells. Proc Natl Acad Sci. Proceedings of the National Academy of Sciences; 1989;86:802–6.

158. Direct Evidence That Hepatocyte Growth Factor Is A... : Hepatology [Internet]. LWW. [cited 2025 Aug 27]. Available from: https://journals.lww.com/hep/fulltext/1992/11000/direct_evidence_that_hepatocyte_growth_factor_is_a.19.aspx

159. YAEKASHIWA M, NAKAYAMA S, OHNUMA K, SAKAI T, ABE T, SATOH K, et al. Simultaneous or Delayed Administration of Hepatocyte Growth Factor Equally Represses the Fibrotic Changes in Murine Lung Injury Induced by Bleomycin. Am J Respir Crit Care Med [Internet]. American Thoracic SocietyNew York, NY; 2012 [cited 2025 Aug 27]; Available from: https://www.atsjournals.org/doi/10.1164/ajrccm.156.6.9611057

160. Hepatocyte Growth Factor Modulates Matrix... : Journal of the American Society of Nephrology [Internet]. LWW. [cited 2025 Aug 27]. Available from: https://journals.lww.com/jasn/fulltext/2003/12000/hepatocyte_growth_factor_modulates_matrix.6.aspx

161. Hepatocyte growth factor counteracts transforming growth factor-β1, through attenuation of connective tissue growth factor induction, and prevents renal fibrogenesis in 5/6 nephrectomized mice [Internet]. [cited 2025 Aug 27]. Available from: https://faseb.onlinelibrary.wiley.com/doi/epdf/10.1096/fj.02-0442fje?getft_integrator=scopus&src=getftr&utm_source=scopus

162. Dworkin LD, Gong R, Tolbert E, Centracchio J, Yano N, Zanabli AR, et al. Hepatocyte growth factor ameliorates progression of interstitial fibrosis in rats with established renal injury. Kidney Int. 2004;65:409–19.

163. Xiao G-H, Jeffers M, Bellacosa A, Mitsuuchi Y, Vande Woude GF, Testa JR. Anti-apoptotic signaling by hepatocyte growth factor/Met via the phosphatidylinositol 3-kinase/Akt and mitogen-activated protein kinase pathways. Proc Natl Acad Sci U S A. 2001;98:247–52.

164. Zhang Y, Du Z, Zhang M. Biomarker development in MET-targeted therapy. Oncotarget. 2016;7:37370.

165. Liu W-T, Jing Y-Y, Yu G, Chen H, Han Z, Yu D-D, et al. Hepatic stellate cell promoted hepatoma cell invasion via the HGF/c-Met signaling pathway regulated by p53. Cell Cycle Georget Tex. 2016;15:886–94.

166. Hass R, Jennek S, Yang Y, Friedrich K. c-Met expression and activity in urogenital cancers – novel aspects of signal transduction and medical implications. Cell Commun Signal. 2017;15:10.

167. A mini-review of c-Met as a potential therapeutic target in melanoma. Biomed Pharmacother. Elsevier Masson; 2017;88:194–202.

168. Gandino L, Di Renzo MF, Giordano S, Bussolino F, Comoglio PM. Protein kinase-c activation inhibits tyrosine phosphorylation of the c-met protein. Oncogene. 1990;5:721–5.

169. Phosphorylation of serine 985 negatively regulates the hepatocyte growth factor receptor kinase. J Biol Chem. Elsevier; 1994;269:1815–20.

170. Pothula SP, Xu Z, Goldstein D, Merrett N, Pirola RC, Wilson JS, et al. Targeting the HGF/c-MET pathway: stromal remodelling in pancreatic cancer. Oncotarget. 2017;8:76722–39.

171. Pang TCY, Xu Z, Mekapogu AR, Pothula S, Becker T, Corley S, et al. HGF/c-Met Inhibition as Adjuvant Therapy Improves Outcomes in an Orthotopic Mouse Model of Pancreatic Cancer. Cancers. 2021;13:2763.

172. Mekapogu AR, Xu Z, Pothula S, Perera C, Pang T, Hosen SMZ, et al. HGF/c-Met pathway inhibition combined with chemotherapy increases cytotoxic T-cell infiltration and inhibits pancreatic tumour growth and metastasis. Cancer Lett. 2023;568:216286.

173. Orian-Rousseau V, Morrison H, Matzke A, Kastilan T, Pace G, Herrlich P, et al. Hepatocyte Growth Factor-induced Ras Activation Requires ERM Proteins Linked to Both CD44v6 and F-Actin. Mol Biol Cell. 2007;18:76–83.

174. Role of the hepatocyte growth factor receptor, c-Met, in oncogenesis and potential for therapeutic inhibition. Cytokine Growth Factor Rev. Pergamon; 2002;13:41–59.

175. Maulik G, Madhiwala P, Brooks S, Ma PC, Kijima T, Tibaldi EV, et al. Activated c-Met signals through PI3K with dramatic effects on cytoskeletal functions in small cell lung cancer. J Cell Mol Med. 2002;6:539–53.

176. Organ SL, Tsao M-S. An overview of the c-MET signaling pathway. Ther Adv Med Oncol. 2011;3:S7–19.

177. Syed ZA, Yin W, Hughes K, Gill JN, Shi R, Clifford JL. HGF/c-met/Stat3 signaling during skin tumor cell invasion: indications for a positive feedback loop. BMC Cancer. 2011;11:180.

178. Boccaccio C, Andò M, Tamagnone L, Bardelli A, Michieli P, Battistini C, et al. Induction of epithelial tubules by growth factor HGF depends on the STAT pathway. Nature. 1998;391:285–8.

179. Ilangumaran S, Villalobos-Hernandez A, Bobbala D, Ramanathan S. The hepatocyte growth factor (HGF)–MET receptor tyrosine kinase signaling pathway: Diverse roles in modulating immune cell functions. Cytokine. 2016;82:125–39.

180. Fogli S, Tabbò F, Capuano A, Del Re M, Passiglia F, Cucchiara F, et al. The expanding family of c-Met inhibitors in solid tumors: a comparative analysis of their pharmacologic and clinical differences. Crit Rev Oncol Hematol. 2022;172:103602.

181. Puccini A, Marín-Ramos NI, Bergamo F, Schirripa M, Lonardi S, Lenz H-J, et al. Safety and Tolerability of c-MET Inhibitors in Cancer. Drug Saf. 2019;42:211–33.

182. Maroto P, Porta C, Capdevila J, Apolo AB, Viteri S, Rodriguez-Antona C, et al. Cabozantinib for the treatment of solid tumors: a systematic review. Ther Adv Med Oncol. 2022;14:17588359221107112.

183. Grünwald BT, Devisme A, Andrieux G, Vyas F, Aliar K, McCloskey CW, et al. Spatially confined sub-tumor microenvironments in pancreatic cancer. Cell. Elsevier; 2021;184:5577-5592.e18.

184. Steele NG, Carpenter ES, Kemp SB, Sirihorachai V, The S, Delrosario L, et al. Multimodal Mapping of the Tumor and Peripheral Blood Immune Landscape in Human Pancreatic Cancer. Nat Cancer. 2020;1:1097.

185. Loveless IM, Kemp SB, Hartway KM, Mitchell JT, Wu Y, Zwernik SD, et al. Human Pancreatic Cancer Single-Cell Atlas Reveals Association of CXCL10+ Fibroblasts and Basal Subtype Tumor Cells. Clin Cancer Res. American Association for Cancer Research; 2025;31:756–72.

186. Kim PK, Halbrook CJ, Kerk SA, Radyk M, Wisner S, Kremer DM, et al. Hyaluronic acid fuels pancreatic cancer cell growth. eLife. 2021;10:e62645.

187. Siegel RL, Miller KD, Fuchs HE, Jemal A. Cancer statistics, 2022. CA Cancer J Clin. 2022;72:7–33.

188. Apte MV, Park S, Phillips PA, Santucci N, Goldstein D, Kumar RK, et al. Desmoplastic Reaction in Pancreatic Cancer: Role of Pancreatic Stellate Cells. Pancreas. 2004;29:179–87.

189. Shi Y, Gao W, Lytle NK, Huang P, Yuan X, Dann AM, et al. Targeting LIF-mediated paracrine interaction for pancreatic cancer therapy and monitoring. Nature. Nature Publishing Group; 2019;569:131–5.

190. Francescone R, Barbosa Vendramini-Costa D, Franco-Barraza J, Wagner J, Muir A, Lau AN, et al. Netrin G1 Promotes Pancreatic Tumorigenesis through Cancer-Associated

Fibroblast–Driven Nutritional Support and Immunosuppression. Cancer Discov. 2021;11:446–79.

191. Affo S, Yu L-X, Schwabe RF. The Role of Cancer-Associated Fibroblasts and Fibrosis in Liver Cancer. Annu Rev Pathol. 2016;12:153.

192. Raymant M, Astuti Y, Alvaro-Espinosa L, Green D, Quaranta V, Bellomo G, et al. Macrophage-fibroblast JAK/STAT dependent crosstalk promotes liver metastatic outgrowth in pancreatic cancer. Nat Commun. Nature Publishing Group; 2024;15:3593.

193. Bhattacharjee S, Hamberger F, Ravichandra A, Miller M, Nair A, Affo S, et al. Tumor restriction by type I collagen opposes tumor-promoting effects of cancer-associated fibroblasts. J Clin Invest. 2021;131:e146987.

194. Werba G, Weissinger D, Kawaler EA, Zhao E, Kalfakakou D, Dhara S, et al. Single-cell RNA sequencing reveals the effects of chemotherapy on human pancreatic adenocarcinoma and its tumor microenvironment. Nat Commun. Nature Publishing Group; 2023;14:797.

195. Jin S, Guerrero-Juarez CF, Zhang L, Chang I, Ramos R, Kuan C-H, et al. Inference and analysis of cell-cell communication using CellChat. Nat Commun. Nature Publishing Group; 2021;12:1088.

196. Sa L, Dr M, Lt N. Clinical Pharmacokinetics and Pharmacodynamics of Cabozantinib. Clin Pharmacokinet [Internet]. Clin Pharmacokinet; 2017 [cited 2025 Aug 30];56. Available from: https://pubmed.ncbi.nlm.nih.gov/27734291/

197. Shibuya M. VEGF-VEGFR Signals in Health and Disease. Biomol Ther. 2014;22:1.

198. CABOMETYX® (cabozantinib) Mechanism of Action [Internet]. [cited 2025 Aug 30]. Available from: https://www.cabometyxhcp.com/mechanism-of-action

199. Wu Y, Chen S, Yang X, Sato K, Lal P, Wang Y, et al. Combining the Tyrosine Kinase Inhibitor Cabozantinib and the mTORC1/2 Inhibitor Sapanisertib Blocks ERK Pathway Activity and Suppresses Tumor Growth in Renal Cell Carcinoma. Cancer Res. 2023;83:4161–78.

200. Chan JA, Geyer S, Zemla T, Knopp MV, Behr S, Pulsipher S, et al. Phase 3 Trial of Cabozantinib to Treat Advanced Neuroendocrine Tumors. N Engl J Med [Internet]. Massachusetts Medical Society; 2025 [cited 2025 Aug 30]; Available from: https://www.nejm.org/doi/abs/10.1056/NEJMoa2403991

201. Zhen DB, Griffith KA, Ruch JM, Camphausen K, Savage JE, Kim EJ, et al. A Phase I Trial of Cabozantinib and Gemcitabine in Advanced Pancreatic Cancer. Invest New Drugs. 2016;34:733.

202. KRAS inhibitors: resistance drivers and combinatorial strategies. Trends Cancer. Cell Press; 2025;11:91–116.

203. The KRASG12D inhibitor MRTX1133 elucidates KRAS-mediated oncogenesis. Nat Med. Nature Publishing Group; 2022;28:2017–8.

204. The next-generation KRAS inhibitors…What comes after sotorasib and adagrasib? Lung Cancer. Elsevier; 2024;194:107886.

205. Suzuki S, Yonesaka K, Teramura T, Takehara T, Kato R, Sakai H, et al. KRAS Inhibitor Resistance in MET-Amplified KRASG12C Non–Small Cell Lung Cancer Induced By RAS- and Non–RAS-Mediated Cell Signaling Mechanisms. Clin Cancer Res. American Association for Cancer Research; 2021;27:5697–707.

206. Byrne KT, Betts CB, Mick R, Sivagnanam S, Bajor DL, Laheru DA, et al. Neoadjuvant Selicrelumab, an Agonist CD40 Antibody, Induces Changes in the Tumor Microenvironment in Patients with Resectable Pancreatic Cancer. Clin Cancer Res. American Association for Cancer Research; 2021;27:4574–86.

207. Hogg GD, Weinstein AG, Kingston NL, Liu X, Dres OM, Kang L-I, et al. Combined Flt3L and CD40 agonism restores dendritic cell–driven T cell immunity in pancreatic cancer. Sci Immunol [Internet]. American Association for the Advancement of Science; 2025 [cited 2025 Aug 30]; Available from: https://www.science.org/doi/10.1126/sciimmunol.adp3978

208. Nguyen-Lefebvre AT, Horuzsko A. Kupffer Cell Metabolism and Function. J Enzymol Metab. 2015;1:101.

209. Dixon LJ, Barnes M, Tang H, Pritchard MT, Nagy LE. Kupffer Cells in the Liver. Compr Physiol. 2013;3:785–97.

210. Zheng H, Peng X, Yang S, Li X, Huang M, Wei S, et al. Targeting tumor-associated macrophages in hepatocellular carcinoma: biology, strategy, and immunotherapy. Cell Death Discov. Nature Publishing Group; 2023;9:1–15.

211. Targeting the PSGL-1 Immune Checkpoint Promotes Immunity to PD-1–Resistant Melanoma | Cancer Immunology Research | American Association for Cancer Research [Internet]. [cited 2025 Aug 30]. Available from: https://aacrjournals.org/cancerimmunolres/article-abstract/10/5/612/694719/Targeting-the-PSGL-1-Immune-Checkpoint-Promotes?redirectedFrom=fulltext

212. He R, Hou S, Liu C, Zhang A, Bai Q, Han M, et al. Follicular CXCR5-expressing CD8+ T cells curtail chronic viral infection. Nature. Nature Publishing Group; 2016;537:412–6.

213. Im SJ, Hashimoto M, Gerner MY, Lee J, Kissick HT, Burger MC, et al. Defining CD8+ T cells that provide the proliferative burst after PD-1 therapy. Nature. 2016;537:417.

214. Rh H, Re W, M G, Gj O, Cj Y, Se K. Pathology of incipient pancreatic cancer. Ann Oncol Off J Eur Soc Med Oncol [Internet]. Ann Oncol; 1999 [cited 2025 Aug 30];10 Suppl 4. Available from: https://pubmed.ncbi.nlm.nih.gov/10436775/

215. Pothula SP, Xu Z, Goldstein D, Biankin AV, Pirola RC, Wilson JS, et al. Hepatocyte growth factor inhibition: a novel therapeutic approach in pancreatic cancer. Br J Cancer. 2016;114:269–80.

216. Peng J, Sun B-F, Chen C-Y, Zhou J-Y, Chen Y-S, Chen H, et al. Single-cell RNA-seq highlights intra-tumoral heterogeneity and malignant progression in pancreatic ductal adenocarcinoma. Cell Res. 2019;29:725–38.

217. Kamphorst JJ, Nofal M, Commisso C, Hackett SR, Lu W, Grabocka E, et al. Human Pancreatic Cancer Tumors Are Nutrient Poor and Tumor Cells Actively Scavenge Extracellular Protein. Cancer Res. American Association for Cancer Research; 2015;75:544–53.

218. McDonald OG, Li X, Saunders T, Tryggvadottir R, Mentch SJ, Warmoes MO, et al. Large-scale epigenomic reprogramming during pancreatic cancer progression links anabolic glucose metabolism to distant metastasis. Nat Genet. 2017;49:367–76.

219. Rademaker G, Hernandez GA, Seo Y, Dahal S, Miller-Phillips L, Li AL, et al. PCSK9 drives sterol-dependent metastatic organ choice in pancreatic cancer. Nature. Nature Publishing Group; 2025;643:1381–90.

220. Halbrook CJ, Thurston G, Boyer S, Anaraki C, Jiménez JA, McCarthy A, et al. Differential integrated stress response and asparagine production drive symbiosis and therapy resistance of pancreatic adenocarcinoma cells. Nat Cancer. 2022;3:1386–403.

221. Clonal dominance defines metastatic dissemination in pancreatic cancer | Science Advances [Internet]. [cited 2025 Aug 30]. Available from: https://www.science.org/doi/10.1126/sciadv.add9342